The Journal of
Gemmology
2008 / Volume 31 / Nos. 3/4

The Gemmological Association of Great Britain

The Gemmological Association of Great Britain

27 Greville Street, London EC1N 8TN
T: +44 (0)20 7404 3334 **F:** +44 (0)20 7404 8843
E: information@gem-a.com **W:** www.gem-a.com

Registered Charity No. 1109555
Registered office: Palladium House, 1-4 Argyll Street, London W1F 7LD

President: Professor A. H. Rankin

Vice-Presidents: N. W. Deeks, R. A. Howie

Honorary Fellows: R. A. Howie, K. Nassau

Honorary Life Members: H. Bank, T.M.J. Davidson, D. J. Callaghan, E. A. Jobbins, J. I. Koivula, M.J. O'Donoghue, C. M. Ou Yang, I. Thomson, V. P. Watson, C. H. Winter

Chief Executive Officer: J. M. Ogden

Council: A. T. Collins – Chairman, S. Collins, J. Riley, E. Stern, J. F. Williams

Members' Audit Committee: A. J. Allnutt, P. Dwyer-Hickey, J. Greatwood, G. M. Green, B. Jackson, D. J. Lancaster

Branch Chairmen: Midlands – P. Phillips, North East – M. Houghton, North West – J. Riley, Scottish – B. Jackson, South East – V. Wetten, South West – R. M. Slater

The Journal of Gemmology

Editor: Dr R. R. Harding

Assistant Editors: M. J. O'Donoghue, P. G. Read

Associate Editors: Dr A. J. Allnutt (Chislehurst), Dr C. E. S. Arps (Leiden), G. Bosshart (Horgen), Prof. A. T. Collins (London), J. Finlayson (Stoke on Trent), Dr J. W. Harris (Glasgow), Prof. R. A. Howie (Derbyshire), E. A. Jobbins (Caterham), Dr J. M. Ogden (London), Prof. A. H. Rankin (Kingston upon Thames), Dr K. Schmetzer (Petershausen), Dr J. E. Shigley (Carlsbad), Prof. D. C. Smith (Paris), E. Stern (London), Prof. I. Sunagawa (Tokyo), Dr M. Superchi (Milan)

Production Editor: M. A Burland

The Editor is glad to consider original articles shedding new light on subjects of gemmological interest for publication in *The Journal of Gemmology*. A Guide to the preparation of typescripts for publication in *The Journal* is given on our website, or contact the Production Editor at the Gemmological Association of Great Britain.

Any opinions expressed in *The Journal of Gemmology* are understood to be the views of the contributors and not necessarily of the publishers.

©2008 Gemmological Association of Great Britain

A fancy reddish brown diamond with new optical absorption features

Taijin Lu, Tatsuya Odaki, Kazuyoshi Yasunaga and Hajime Uesugi

Abstract: Red or near-red natural diamonds are extremely rare, and the possible origins of their colour are unclear. A weak absorption band at 776 nm in the visible range and a clear absorption band at 6169 cm^{-1} in the infrared region were detected in a near-red diamond, which could be factors in understanding the possible origin of this colour in natural diamonds.

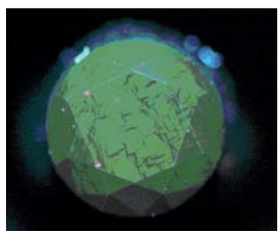

Keywords: diamond, spectroscopy, infrared, photoluminescence, UV-visible

Introduction

Although the popular image of diamond for centuries has been that of a colourless gem, it can be yellow, orange, blue, green, black, white, purple, pink and red, colours which are traditionally referred to as 'fancy' (see, e.g., Fritsch, 1998). Coloured diamonds contain impurities, such as nitrogen or boron, or structural defects, and are usually graded using a fancy-colours grading system (King *et al.*, 1994). In this system, the diamonds described as predominantly red are among the most intriguing and highly valued gems in the world, because of both the richness of their colour and their extreme rarity. As stated by the Gemological Institute of America (GIA), until 2002 only four fancy red diamonds from the public domain had been graded in the GIA Gem Laboratory (King and Shigley, 2003). The diamonds with near-red colours are usually graded using additional descriptive terms, such as fancy purple-pink, fancy reddish purple, etc. depending on the secondary hue, tone, and saturation. These fancy colour diamonds are also often well documented due to their high price and rarity (Kane, 1987). However, precisely because of this rarity, studies have been few and there is very little understanding of the possible origins of the red and near-red colours in natural diamonds. Recently, we have had an opportunity to examine a fancy reddish brown diamond, which is shown in *Figure 1*. Systematic non-destructive spectroscopic investigations under optimum measurement conditions have been carried out to record its optical absorption features and possibly relate them to the origin of its colour. UV-Visible-near infrared (UV-Vis-NIR) spectra were recorded with a Nihonfenko high-resolution spectrometer (Model Jasco V-670, 300 – 1000 nm, 0.5 nm resolution, deuterium-tungsten-halogen source) with our own designed optical fibre system which allows us to record the spectra at liquid nitrogen temperature with high resolution. Infrared absorption spectra were collected using both the Nihonfenko Jasco FT/IR-6100 and the FT/IR-660 plus Fourier-transform infrared (FTIR) spectrometers (6,000 – 400 cm^{-1}, and 11,000 – 7,000 cm^{-1}, 1 cm^{-1} resolution, up to 1024 scans, at room temperature). Raman and photoluminescence spectra were recorded using a Renishaw inVia Raman microscope (488 nm, 514.5 nm, and 632.8 nm laser sources, at liquid nitrogen temperature).

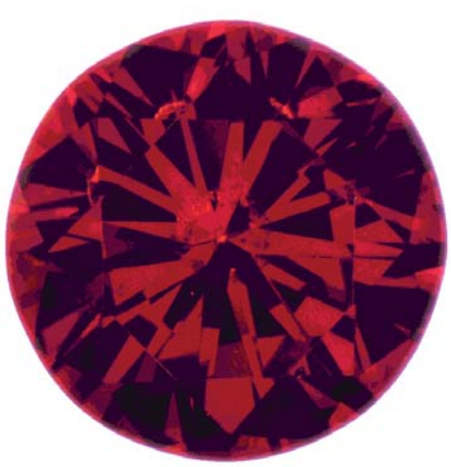

Figure 1: Fancy reddish brown diamond of 0.202 ct. Photo by H. Ito.

Results

The natural diamond of 0.202 ct, cut as a round brilliant, contains mineral inclusions easily visible in dark-field illumination under a gemmological microscope. After careful observation and comparison, the colour was graded as fancy reddish brown according to the GIA system, which is very close to red.

©2008 Gemmological Association of Great Britain

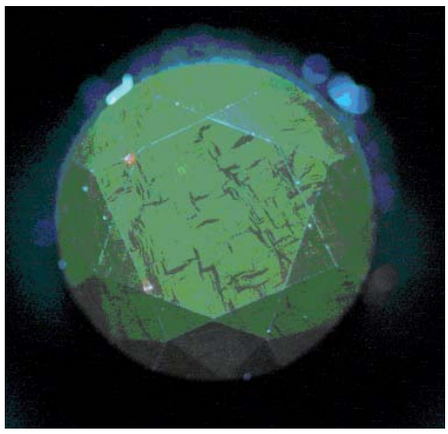

Figure 2: The reddish brown diamond showed green-yellow fluorescence when examined using the UV fluorescence imaging system of the DTC DiamondView. Growth features resembling script are visible in the image.

The stone was inert under both long-wave (365 nm) and short-wave (254 nm) UV lamps, but it displayed weak green-yellow fluorescence when examined in the DTC DiamondView imaging system *(Figure 2)*. A growth pattern consisting of short dark lines disposed at approximate right angles and resembling script is visible in the image. This probably represents agglutination of numerous tiny octahedral crystals in sub-parallel orientation at an early stage of the diamond's formation.

The UV-visible spectrum at room temperature is shown in *Figure 3(a)*. It shows complete absorption below 500 nm with a steep absorption curve to transmission near 700 nm. At liquid nitrogen temperature, a weak but clear absorption band at 776 nm was detected *(Figure 3b)*. Although a 776 nm band has been occasionally detected in photoluminescence spectra in natural blue diamond with red phosphorescence (Johnson and Moe, 2005), to the best of our knowledge, this is the first recorded observation of a band at this position in the UV-visible absorption spectrum of a natural diamond.

Details of the infrared absorption spectrum are shown in *Figure 4* and suggest that the diamond is mostly type Ib with minor IaA. The 1332, 1344, 1353, 1358, 1374 and 1387 cm^{-1} peaks are all nitrogen related (*Figure 4a,* and see Zaitsev, 2001). However, two weak absorption bands at 6169 cm^{-1} and 4702 cm^{-1} were detected in the 7000 – 4000 cm^{-1} range *(Figure 4b)*. The small 4702 cm^{-1} band has been reported by Fritsch *et al.* (1991), without attribution to its cause, but an extensive search of the literature has not yielded any mention of the 6169 cm^{-1} band which is clearly present in this diamond.

The Raman spectrum of the reddish brown diamond was recorded and contains the standard diamond peaks with no exceptional features. To further characterize the spectroscopic features of this diamond, photoluminescence (PL) spectra excited by an Ar-ion laser with both 488 nm and 514.5 nm wavelengths at liquid nitrogen temperature were recorded. A strong and broad emission band centred about 710 nm was detected. Sharp emission bands of 637 nm, 692 nm, 704 nm, 818 nm and 905 nm are superimposed on both sides of this broad band *(Figure 5)*. Under the Ar-ion laser, relatively strong red luminescence is visible even with the naked eye.

Discussion and summary

Pink to red (or purple) diamonds can be obtained from yellow to brown type Ib diamonds, whether natural or synthetic, when subjected to irradiation and annealing treatment (Collins, 1982). The colour is primarily due to a broad absorption band centred at 550 nm, and to the irradiation and annealing treatment-related absorption bands, such as GR1 (741 nm), N-V centres (575 nm, 637 nm), and the 595 nm band, which are usually detected using advanced spectroscopic techniques (Moses *et al.,* 1993). Since these absorption features are absent from the spectrum of the near-red diamond, its colour is probably natural. The weak 776 nm absorption band in the visible range and a clear 6169 cm^{-1} band in the infrared absorption spectrum are new absorption features in this diamond, but it must be stated that strongly coloured

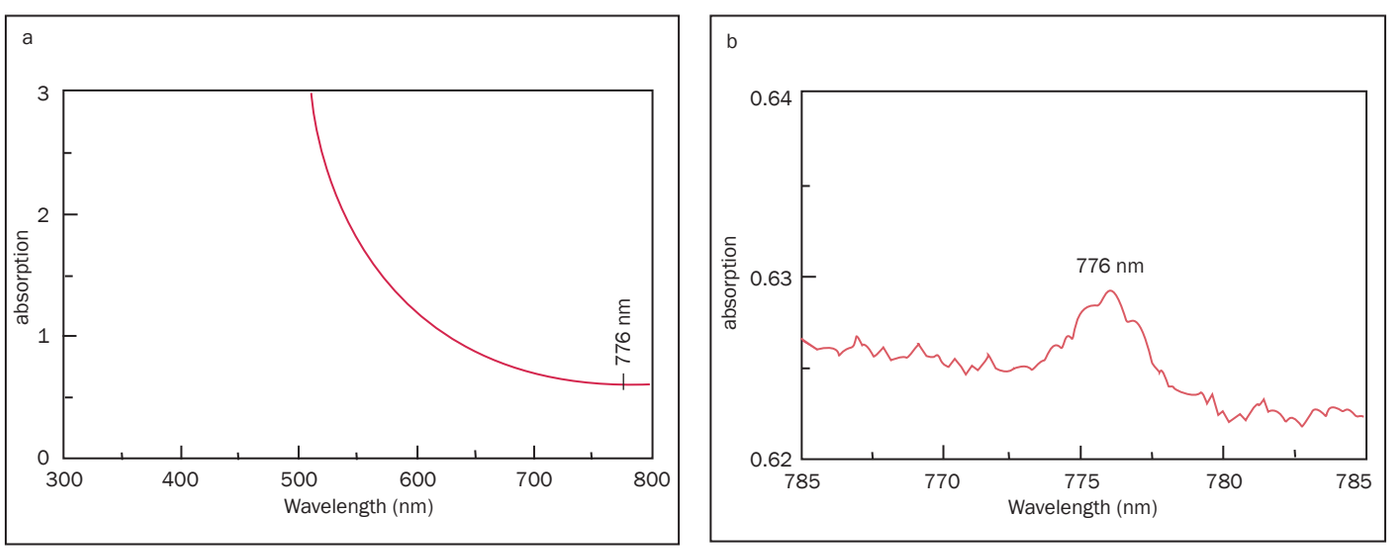

Figure 3: (a) Visible absorption spectrum of the reddish brown diamond at room temperature showing a steep absorption curve from 700 nm to complete absorption below about 500 nm. (b) A weak absorption band at 776 nm is present in the spectrum when the stone is cooled with liquid nitrogen.

natural diamonds often show previously undocumented spectroscopic features which may or may not turn out to have diagnostic value.

The infrared spectrum shows that the diamond is predominantly type Ib with absorption in the visible range caused by single nitrogen atoms in the diamond structure. However this absorption may be augmented by a band near 485 nm which occurs in diamonds showing a broad photoluminescence peak near 700 nm. Collins and Mohammed (1982) first drew attention to this band, although their diamonds exhibited yellow photoluminescence under long-wavelength UV whereas the reddish brown diamond was inert.

Although the cause of colour in this near-red diamond is not yet clear, the spectroscopic data could prove helpful when combined with data from similar stones in the future.

Acknowledgement

The authors thank Dr Ichiro Sunagawa, emeritus professor of Tohoku University and Yoshiko Doi, AGT Gem Laboratory and GIA Japan for their valuable comments and support.

References

Collins, A.T., 1982. Colour centres in diamond. *J. Gemmology,* **18,** 37-75

Collins, A.T. and Mohammed, K., 1982. Optical studies of vibronic bands in yellow luminescing natural diamonds. *J. Phys. C.,* **15,** 147-58

Fritsch E., 1998.The nature of colour in diamonds. In: G.E. Harlow (Ed.), *The Nature of Diamonds,* Cambridge University Press and American Museum of Natural History, New York, 1998, 23-47

Fritsch, E., Scarratt, K., and Collins, A.T., 1991. Optical properties of diamonds with an unusually high hydrogen content. In: *New Diamond Science and Technology – Proc. Second Int. Conf. on the New Diamond Sci. and Tech.*, R. Messier, J.T. Glass, J.E. Butler and R. Roy (Eds), 1991, Mater. Res. Soc., Pittsburgh, PA, 671-6

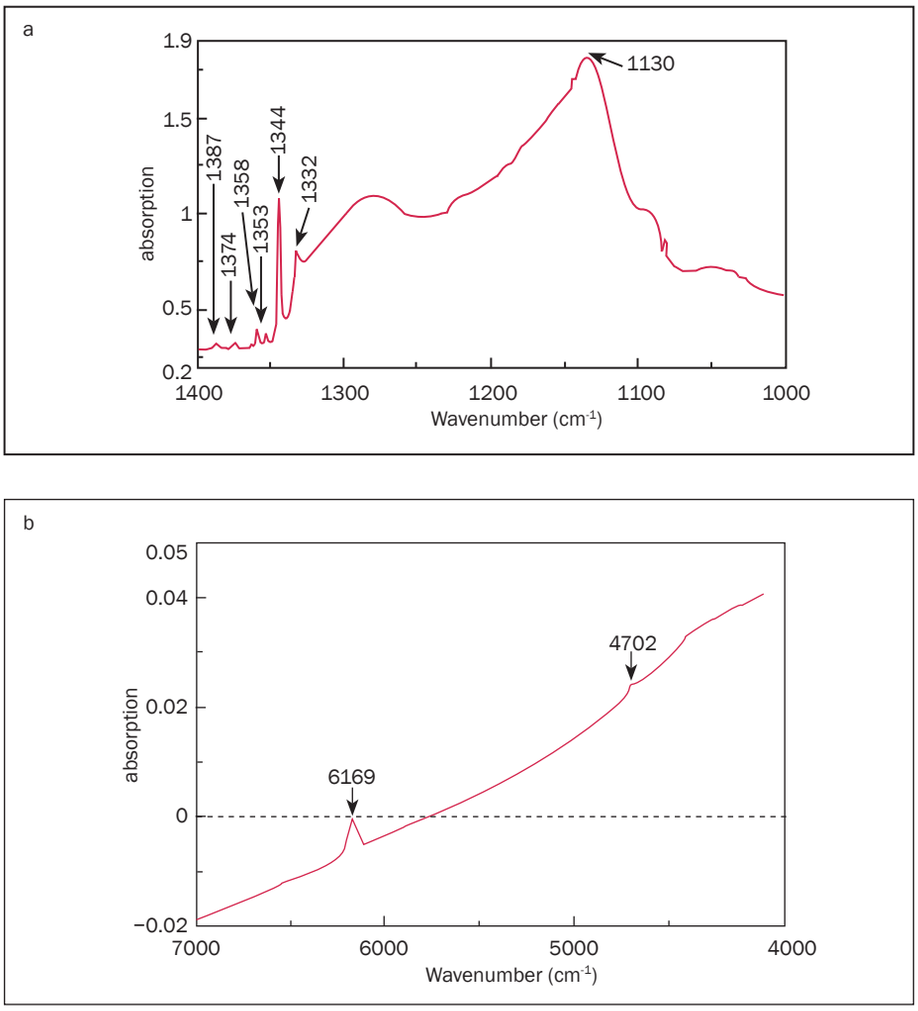

Figure 4: (a) The infrared absorption spectrum shows that the diamond is a type Ib with minor IaA. (b) There is a clear 6169 cm-1 absorption band and a small peak at 4702 cm-1 in the 7000–4000 cm-1 range.

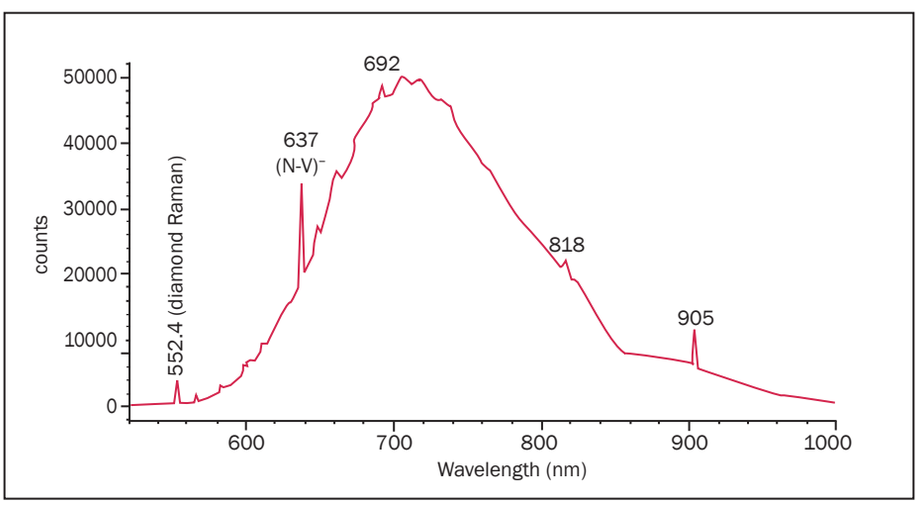

Figure 5: Photoluminescence spectrum of the reddish brown diamond showing a strong broad emission band centred around 710 nm. The spectrum is the result of excitation by an Ar-ion laser (514.5 nm) at liquid nitrogen temperature.

Johnson, P., and Moe, K.S., 2005. Strongly colored natural type IIb blue diamonds. *Gems & Gemology*, **40**, 258-9

Kane, R.E., 1987. Three notable fancy-color diamonds: purplish red, purple-pink, and reddish purple. *Gems & Gemology*, **23**, 90-5

King, J.M., Moses, T.M., Shigley, J.E., and Liu, Y., 1994. Color grading of colored diamonds in the GIA Gem Trade Laboratory. *Gems & Gemology,* **30**, 220-42

King, J.M., and Shigley, J.E., 2003. An important exhibition of seven rare gem diamonds. *Gems & Gemology,* **39**, 136-43

Moses, T.M., Reinitz, I., Fritsch, E., and Shigley, J.E., 1993. Two treated-color synthetic red diamonds seen in the trade. *Gems & Gemology,* **29**, 182-90

Zaitsev, A.M., 2001. *Optical Properties of Diamonds: A Data Handbook*. Springer -Verlag, Berlin, p.502

The Authors

Taijin Lu, Tatsuya Odaki, Kazuyoshi Yasunaga and Hajime Uesugi
AGT Gem Laboratory, Okachimachi CY Building, 5-15-14 Ueno, Taido-ku, Tokyo 110-0005, Japan
Tel: +81 3 3834 6586; Fax: +81 3 3834 6589; email: info@agt.jp

A place for CZ masters in diamond colour grading

Michael D. Cowing FGA

Abstract: Over the last 20 years and despite recommendations to the contrary, many gemmologists and appraisers have gravitated to the use of cubic zirconia (CZ) master stone sets to assist in the colour grading of diamonds. This investigation revisits with new insight, diamond grading technique and methodology. It addresses the judicious use of CZ master stone sets to augment diamond masters that are smaller in size and number. Study results support the use of accurately graded, carat-size CZs in reducing the subjectivity of colour grading when only incomplete (every other grade) diamond master sets of small (under 0.4 ct) sizes are available.

Keywords: colour grading, cubic zirconia, CZ, diamond

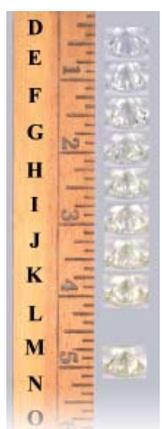

Introduction

This investigation explores historical guidance in the use of diamond master stones, and offers a rationale for augmenting master stone sets of smaller and fewer diamonds with a full set of carat size CZ masters. The question addressed is: Can the acknowledged subjectivity of diamond colour grading be reduced by supplementing an incomplete set of smaller diamond master stones with a complete set of larger CZ masters? Along with two gemmologist-appraiser colleagues, the author also conducted and reports on a study of the accuracy of eight ten-stone sets of CZ master stones, four from each of two main manufacturers of these sets.

Findings are reported of studies in five areas related to diamond colour grading:

1. The historical development by the Gemological Institute of America (GIA) of a colour grading standard beginning with the GIA colour grading 'yardstick'.
2. Industry and GIA teaching of methods and recommendations for colour grading using GIA Diamond Masters, which reduce the subjectivity of colour grading.
3. The pros and cons in the use of CZ master stones in diamond colour grading.
4. A study of grading environments involving a multiplicity of lighting types resulting in additional recommendations for colour grading using CZ or diamond master stones.
5. An evaluation of CZ master stone sets from two main manufacturers.

GIA's development of a colour grading system

Accurate colour grading of diamonds has been and remains one of the difficult challenges facing dealers, laboratories, gemmologists and appraisers. As diamond prices continue to rise, so does the necessity for accurate colour determination. Today, a single colour grade difference in, for example, a 2 ct, VS1, round brilliant can mean over a 20% change in its value. A mistake in grading can have this sort of large impact on appraised value. With amounts like this in the balance, it is incumbent upon the graders of diamond colour to be as accurate as possible despite the myriad of confounding factors that add an industry-acknowledged degree of subjectivity to colour grading.

It is helpful to examine how the Gemological Institute of America (GIA) has addressed and answered the need for accurate and consistent colour grading. In 1941 the GIA introduced "a method of grading diamond colours against a standard in the form of a definitely set and constant scale, as incorporated in the new GIA Colorimeter. This is the first time a colour-grading 'yardstick' has been established." "Thus, the problem of the relative colour of the grades seems to have been largely solved for the jeweller who has a series of key stones (GIA Masters) graded on the 'yardstick'" (Shipley and Liddicoat, 1941). *Figure 1* is a representation of that numerical 'yardstick' and its relation to the GIA letter grades and to the master diamond grades. The letter grades, which correspond to the numerical grade ranges of the 'yardstick', were introduced by GIA in 1953. The D-Z letter grading system has become the 'lingua franca' of colour grading in the United States and largely worldwide, and GIA graded, master diamond sets have become the standard reference tool for

©2008 Gemmological Association of Great Britain

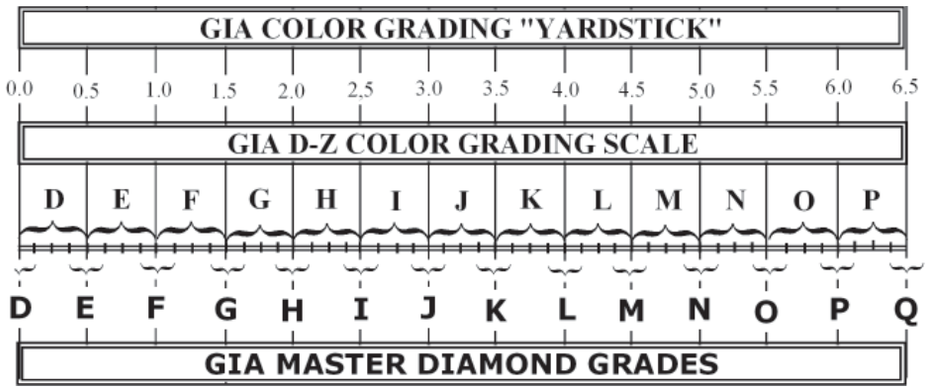

Figure 1: GIA 'yardstick', letter grades and GIA diamond master stone positions which define the letter grades.

diamond colour grading. The relationship between the letter grades, the numerical grades of the GIA 'yardstick', and the position and range of each master grade is shown in *Figure 1*. Notice the numerous brackets indicating the position and range of each grade relative to the GIA colour-grading 'yardstick'.

GIA master diamonds are graded with twice the accuracy of standard grading, so they in turn can be used for standard, whole-letter diamond grading. A master G, for example, is within a quarter grade range around the F/G border (1.5 ± 0.125), compared to the standard grade of G, which has a full grade range between the F/G border and the G/H border (1.5 to 1.999).

There is little to no argument with the view that a third carat or larger, complete set of GIA-graded master diamonds, like those shown in *Figure 2*, is the best tool for accurate colour grading. They are second-generation diamond master stones having been graded against the primary master stone set, which is often referred to as the 'master master' colour grading set at GIA (G. Roskin, pers. comm.)

In *Figure 2* is a complete diamond master stone set of nine, heavy-third carat, ideal cut, whole-grade master diamonds from E to L and N. Because of the expense of retaining diamonds of this size or larger for each colour grade, most small grading laboratories, gemmologist-appraisers and jewellers have purchased only a small number of quarter to third carat masters. Appraisers and laboratories certified by the American Gem Society (AGS) and the Accredited Gemmologist Association (AGA) are required to have at least five GIA-graded masters of a quarter carat or larger.

Prescription for accurate colour grading

A review of the guidelines for the use of GIA-graded diamond masters is important. These instructions help reduce subjectivity caused by the many variables that can affect colour grading. These guidelines are from the organizations, literature and grading manuals of GIA and AGS and from the experience of professional diamond graders.

1. Grading should be done in a lighting environment of diffuse, daylight-equivalent illumination free of coloured reflections from adjacent objects. This can be accomplished by using enclosures like those of the GIA DiamondLite and DiamondDock *(Figure 3)* or, as is often done, by using white-plastic diffusers over the light source and enclosing the diamond in a folded white card.
2. Clean the diamond to be graded and, if needed, also clean the master stones. Especially in the whiter colour grades, any dirt, particularly on the girdle, is liable to lower the apparent colour, possibly by as much as a grade or more.
3. To prevent distracting reflections and dispersion colours, use a dull, flat white background such as the several plastic trays from suppliers of gemmological equipment, the GIA DiamondLite or Diamond Dock trays or accordion-folded white paper or cardboard. A non-fluorescing background is prescribed, but observation of industry practice and personal experience indicates that either non-fluorescent material or common white paper containing a blue fluorescent dye work equally well, as long as they are flat white with no bluish tint under the illumination used in grading.

Figure 3: GIA Diamond Dock, photograph by Jonathan Weingarten

Figure 2: Complete set of GIA-graded diamond master stones from E through L and N.

A place for CZ masters in diamond colour grading

Figure 4: Foreign buyers area, trading floor of the Israel Diamond Exchange, courtesy Israel Diamond Exchange

4. The GIA's prescription for the grading illumination is daylight equivalent light. In past years, GIA recommended and used in their grading the daylight fluorescent tubes of their DiamondLite. In addition to the DiamondLite, the GIA Diamond Course (GIA, 1994) stated: "Filtered, cool white, balanced fluorescent light is best." The term 'cool white' is associated with northern daylight, as 'warm white' is with incandescent light. Because warm white is roughly every colour temperature from 2000 K to 4000/4500 K, the range of cool white is lighting above 4500 K to the 6500 K of the standard daylight (D65) fluorescent tubes (pers. comm., R. Geurts). (Note that in fluorescent lighting cool colour temperatures begin at the 4100 K of the 'cool white' fluorescent.)
Many gemmologists employ the small daylight fluorescent with white plastic diffuser attached to their GIA microscopes. Also in wide use by the trade is the eighteen-inch, daylight, 15-watt fluorescent tubes in a standard desk lamp. An example of their use can be seen in *Figure 4* which shows dealers on the trading floor of the Israel diamond exchange.
Notice that in spite of the available daylight from the large area of North facing windows, and ceiling mounted fluorescents, those examining diamonds are employing the lighting from standard desk lamps.
True daylight varies widely, but the 4200 K of a cool-white fluorescent to the 5500 K colour temperature of noon daylight, and up to the 6500 K of blue skylight are prescribed for diamond grading. Of this range of daylight colour temperatures, the 6500 K daylight fluorescent tube is a little too bluish-white for some, the author included, who find better colour discrimination under noon-daylight from a fluorescent tube in the 5000 K to 5500 K range. Examples are the 'full spectrum', tubes such as the Ott Light. Excellent colour discrimination can also be made in the 4200 K colour temperature of a cool white fluorescent. The principle is that the illumination, like a diamond's immediate surroundings, should be flat white without a blue or yellow tint. Additionally, all these fluorescent tubes and the ones in the GIA DiamondLite and DiamondDock emit a component of UV, which needs to be considered when grading diamonds that fluoresce from UV excitation, but that is a subject for another article.
5. Place the master stones table down with increasing colour left to right, as in *Figure 5,* in order to look into their pavilions in directions perpendicular to the pavilion facets or parallel to the girdle.
On the basis of the tone/saturation of its colour, place the diamond being graded between the master stones closest to it. If it fits just above a G master stone, for example, (which the GIA graded to be within a quarter grade of the F/G boundary), the colour grade is F. If it fits just below the G master, the colour grade is G. This procedure assumes a master stone for every grade. Many sets are incomplete, and where there are missing colour masters, visual interpolation of the grade between the surrounding master diamonds is necessary, or the more difficult extrapolation of the grade is necessary if the diamond is outside the colour range of the masters.

Figure 5: Six CZ masters and one diamond (colours E-K) in the tray of the Diamond Dock, photograph by Jonathan Weingarten.

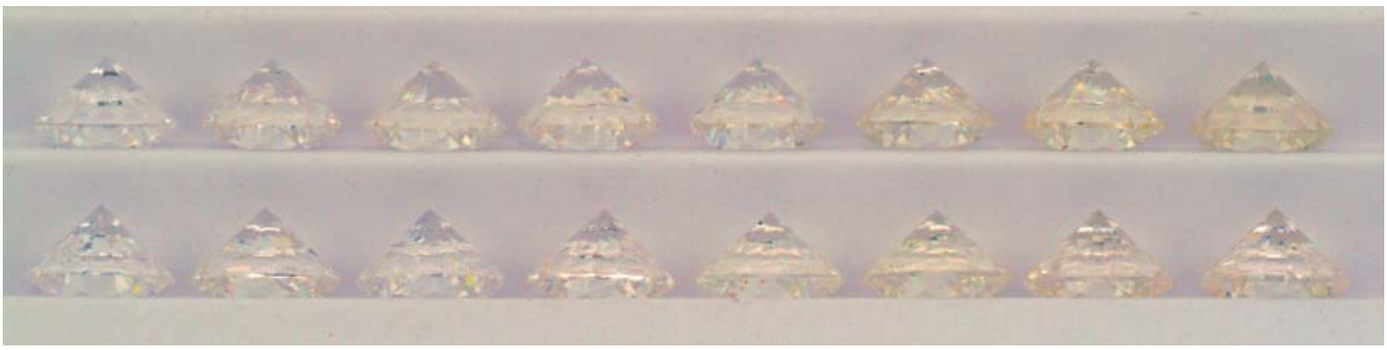

Figure 6: CZ master sets, colours E-L from manufacturer B (top row) and manufacturer A (bottom row).

6. To minimize confusion when comparing the unknown diamond's colour to the masters, these reference diamonds should be of similar well-made cut and proportions. They should be of Cape series, yellow hue, with no distracting inclusions, no more than faint fluorescence, and be similar in size with a minimum 0.25 ct weight. Master stones should not have thick and/or unpolished girdles, as these features can cause confusion. Unpolished girdles trap dirt and metal particles with handling, which can lower their perceived colour a grade or more.

This is the prescription for accurate colour grading using diamond masters. Attention to these instructions aids in reducing the subjectivity in diamond colour grading.

For and against CZ master stones for colour grading

With all the vigilance needed in the use of diamond colour master stones, what are the pros and cons in the use of CZs as masters?

A sidebar from GIA's Diamond Grading Course (GIA, 1994), titled "No CZ for D-Z" makes it clear that GIA writers and educators have advised against the use of CZs as master stones for colour grading. The reasons given are the different yellow hue, confusing reflections from CZ's greater dispersion, the difference in lustre, and the concern over CZ's colour stability. Any case made for the use of CZ masters has to address these concerns.

Large laboratories such as those of the GIA and the AGS have multiple sets of GIA-graded diamond master stones for colour grading. Small laboratories, such as the author's AGA Certified Gem Laboratory, and gemmologist- appraisers, who have obtained AGS's Independent Certified Gemmologist Appraiser (ICGA) designation, are required to grade with at least a five-diamond master set. However, many gemmologist-appraisers, the author included, feel it is necessary to use a complete set comprising each of the most important whole letter grades from E to L or lower.

A sample of 38 gemmologist-appraisers listing their colour grading equipment on the Internet revealed that 16 listed a combination of diamond and CZ master stones, seven listed only CZ, and 15 listed only diamond.

This small sample indicates that many gemmologist-appraisers have found a place for CZ in master stone sets. Many jewellers and others in the industry have employed CZ masters since they became available over 23 years ago. The appeal of CZ Masters is an economic one. Because of the poor economy of tying up large amounts of money in larger diamonds, most master stone sets consist of quarter to third carat sizes of four or more diamonds. Without a master diamond for each grade, visual interpolation or extrapolation is required, which increases the subjectivity of colour grading. In addition, disparity in size makes precise comparison of colour more difficult, and comparing the colour of a small quarter or third carat diamond master to a carat or greater size diamond requires considerable skill only obtained through practice and experience.

Both James Naughter GG FGA of A&A Gemological Laboratory (pers. comm.) and Howard Rubin GG of Gem Dialogue Systems (pers. comm.) relate that they can much more effectively arrive at a colour grade of a carat or greater size diamond using carat size CZ masters than by using the smaller and fewer stones of their diamond master sets. They and others find that a more accurate grade can be obtained with a 10 stone master set of carat size CZs than can be obtained with a small, incomplete set of diamond masters.

Al Gilbertson (pers. comm.), one of the two original AGS, ICGA appraisers with over thirty years experience, states that when on appraisal assignment outside the laboratory, he would take on the road with him a set of CZs that he had checked periodically for accuracy against his diamond master stone set. His diamond masters remained in his laboratory, while he risked only the loss of the relatively inexpensive CZ masters. He would compare his CZ masters once or twice a week against diamonds graded by GIA to develop familiarity and skill in their use. Gilbertson's point was not to shun the use of CZs, but to be practised in their use when the need arose. Periodic practice and checking of CZs raises proficiency in their use and would reveal any possible colour change.

The laboratory of David Atlas GG, President of D. Atlas & Co. Inc. (pers. comm.), employed several sets of CZ master stones in their colour grading and GIA-graded diamond master stones were used to check frequently for any colour change in the CZs.

Several diamond wholesale dealers known to the author use CZ master sets in their buying. The often-narrow margins in their wholesale transactions mean that

a one-grade mistake in colour grading can make the difference between profit and loss. Their success in the practical use of CZs in diamond buying and colour grading is testimony to the accuracy, and usefulness of their CZ masters.

For many, CZs have become a recognized and accepted tool in diamond colour grading. All these examples support the usefulness of CZ masters in the colour grading of diamonds.

Considerations specific to the use of CZ in colour grading

For those who currently use or who are contemplating using CZs for colour grading diamonds, there are a few factors to consider in addition to the guidelines listed for GIA diamond master stones.

Of foremost importance is having a CZ master stone set that is accurately graded against a full, reference GIA diamond master set. The CZs should correspond in tone and saturation and be close in hue to their diamond master set equivalents. The biggest problem is the accuracy and evenness of colour spacing of these master sets. After all, the GIA master diamonds are a 'second generation' having been graded against the 'master master primary set'. The CZ master sets are third generation stones incorporating possible accumulated (or cancelled) errors of two graders.

A revealing test of initial accuracy and evenness of spacing of a ten stone master set of either diamond or CZ is to mix them up, and by eye try to put them back in order of increasing colour. Assuming normal colour vision, if your placing results in the set being out of order, it is the set that is the problem.

In considering the hue differences between CZs used as masters and the yellow tints in type 1a, Cape series diamonds, these are small and not nearly as difficult as comparing the tone/saturation of a pale grey or pale brown diamond with the pale yellow, Cape series, master diamonds. The author and those interviewed for this article found little difficulty comparing the colour of yellow cape series diamonds to the yellow hue of CZ masters.

Addressing the concern for the colour stability of CZ, the experience of the author and of other owners and CZ-master manufacturers is that the type of CZ material used by the two main suppliers, one for over 22 years, has proved to be largely stable under normal care and use.

The differing absorption spectra of diamonds and CZ raises concern for possible colour shifts (called metameric failure) in different illumination environments. A way to avoid this possibility is by grading (and periodic checking and recalibrating against diamond masters) under lighting similar to illumination the manufacturer of the CZ set recommends and uses in his initial grading. Experiments by this investigator, grading in five different lighting environments, yielded the same colour grading determinations. This finding reduces the concern for possible colour shifts, as there was no apparent metameric failure. Relative to the diamond masters, no colour shifts of the CZs were observed.

Evaluation of CZ master stone sets

To provide a preliminary assessment of currently available CZ master stone sets, a number were obtained from several different vendors of gemmological equipment. All these suppliers carry CZ sets from either or both of two sources, designated A and B in this study. Purchased were eight, 10 stone sets, four from each manufacturer. The purpose was to evaluate the accuracy of the sets.

This investigator graded each set against a background of accordion-folded flat white paper with his complete diamond master set. To check for any possible colour shift in different lighting due to CZ's different absorption spectrum and varying small amounts of yellow fluorescence, the grading was done for each stone in five different lighting environments. These were a daylight fluorescent, a daylight fluorescent through a lexan plastic filter to remove UV, a cool white fluorescent, a 'full spectrum' fluorescent, and a white LED lamp.

Using all five lighting environments, the author found the same colour determination in each of these illuminations. This established that CZ's different absorption spectrum and varying amounts of fluorescence did not result in colour changes (metameric failure) large enough to cause additional error in colour grading.

Experimenting with these five different lighting environments resulted in the surprising finding that colour differences were more apparent and colour comparisons were more easily made in cool white and 'full spectrum' fluorescent lighting (colour temperatures from 4200 K to 5500 K). Colour differences of a grade or less were more difficult to see and evaluate in the slightly bluish-white daylight fluorescent and the LED lighting (colour temperatures 6500 K and above). This finding is interesting, because, on one hand, it is at odds with the widespread prescription for north daylight equivalent (6500 K) lighting (Bruton, 1978), while on the other hand, it supports GIA's Diamond Course (GIA, 1994) statement: "Filtered, cool white, balanced fluorescent light is best." The author suggests trying both to find a personal preference.

The B master sets contained the master stones D through L and N, while the A sets contained the stones E through N. The sets were evaluated as a 10 stone whole, and then re-scored for the more important eight grades E through L, shown in *Figure 6*, which both sets have in common.

The author graded all eight sets, and David Atlas and James Naughter graded four sets apiece, two from each manufacturer, and the results are given in *Table I*. It is important to acknowledge that the errors measured are a combination of errors in the manufacturers' gradings, differences between our three master stone sets, and any errors in grading by the three of us. The author had the advantage of a full set of diamond master colour grades, while James Naughter used a GIA and AGS graded five diamond master set, and David Atlas used a full set of CZs graded

A place for CZ masters in diamond colour grading

Table I: Results of grading by D. Atlas (DA), M. Cowing (MC) and J. Naughter (JN) of four A (A1-4) and four B (B1, 3, 5, 7) CZ master stone sets.

Set	Grader	D	E	F	G	H	I	J	K	L	M	N
A1	MC	-	Hi E	E/F	E	F/G	Hi I	Hi J	H/I	I(<J)	K	N
	DA	-	D	E	F	G	H	I	J	K	M	O/P
A2	MC	-	Hi D	D	E	F/G	F	H/I	Hi K	K	L	L/M
	JN	-	Hi D	D	Hi H	I	Hi J	K	Hi L	L	Lo L	M
A3	MC	-	D	Hi D	E	Hi F	Hi G	Hi I	K	Lo K	K	O
	DA	-	E	E	F	G	H/I	J	L/M	M	N	O/P
A4	MC	-	Hi D	Hi D	Hi F	Hi G	Hi G	K	K	Lo K	M	L/M
	JN	-	Hi D	Lo D	Lo E	Lo G	Hi H	J	K	Hi L	M	N/O
B1	MC	D	E	Hi F	G	Hi H	Hi I	Hi J	K	Hi L	-	N
	DA	D	E	F	F/G	H	I	J	K	L/M	-	O
B3	MC	D	E	E	F/G	G/H	H/I	Hi J	Hi K	Hi L	-	N
	DA	D	E	E	G	H	I	J	K	L/M	-	N/O
B5	MC	D	E	Hi F	Hi G	H	Hi I	Hi J	Hi K	K	-	M
	JN	Hi D	Hi E	Hi F	Hi G	Hi H	Hi I	Hi J	Hi K	Hi M	-	N
B7	MC	D	E	E/F	F/G	Hi H	Hi I	I	K	L	-	O
	JN	Hi D	Hi E	Lo E	F/G	Hi H	Hi I	Lo I	Lo K	M	-	N

against diamond masters and including a GIA H master diamond. On any given stone, our errors may increase or decrease the true manufacturer error adding uncertainty to this measure. However, the results, including the total average error in comparing the group of four sets from each manufacturer, do indicate a sufficiently accurate evaluation that shows the relative accuracy and consistency of the sets from each.

Two measures of error were used to evaluate the eight CZ master sets, the second being twice as demanding as the first. The first measure is normal colour grading, meaning the determination whether each CZ is within or at the top of its grade. This measure scores each CZ as either zero error if a stone is within or at the top of its stated grade or, if outside the grade, the number of grades it is off.

This first error measure, which determines how close the CZs were to their labelled grades, finds that the A sets have an average per stone error, over the most important eight grades, of 1.36 grades (scoring of author, MC) and 0.88 grades (scoring of David Atlas, DA and James Naughter, JN). In comparison, the B sets have an average per stone error of 0.09 grades (MC) and 0.13 grades (DA and JN).

The second and more critical error measure, which determines how close the CZs were to the diamond master stones they represent, finds that the A sets have an average per stone error over the most important 8 grades of 1.16 grades (MC) and 0.80 grades (DA and JN). In comparison, the B sets have an average per stone error of 0.19 grades (MC) and 0.38 grades (DA and JN).

On the basis of this survey therefore, the B sets are the more accurate. In addition to having higher accuracy, the B sets also have the more even spacing between the grades. Due to this even spacing, no two grades were too close and it was possible to scramble the B sets and, by eye, put them back in correct order.

Having said this, it is important to state that this survey was carried out on only a small sample of sets purchased in 2008,

Table II: Closeness of CZs to their labelled grades; errors measured in units and decimal points of one grade.

Set A					
Set	Grader	10 error ave.	Worst error in 10	8 error ave.	Worst error in 8
A1	MC	1.25	2.5	1.31	2.5
	DA	0.95	1.5	1	1
A2	MC	1.45	3	1.5	3
	JN	1	1	1	1
A3	MC	1.5	3	1.5	3
	DA	0.85	2	0.75	2
A4	MC	1.05	2	1.13	2
	JN	0.8	1.5	0.75	1.5
A#	MC	1.31	3	1.36	3
	DA & JN	0.9	2	0.88	2

Set B					
Set	Grader	10 error average	Worst error in 10	8 error average	Worst error in 8
B1	MC	0	0	0	0
	DA	0.1	1	0	0
B3	MC	0.1	1	0.13	1
	DA	0.1	1	0.13	1
B5	MC	0.2	1	0.13	1
	JN	0.1	1	0.13	1
B7	MC	0.2	1	0.13	1
	JN	0.2	1.	0.25	1
B#	MC	0.13	1	0.09	1
	DA & JN	0.13	1	0.13	1

N.B.: A# = average for all stones, or worst in all stones
B# = average for all stones, or worst in all stones.
DA denotes D. Atlas, MC denotes M. Cowing and JN denotes J. Naughter

Table III: Closeness of CZs to their equivalent diamond master stones; errors measured in units and decimal points of one grade.

A					
Set	Grader	10 error ave.	Worst error in 10	8 error ave.	Worst error in 8
A1	MC	1	2.5	1	2.5
	DA	0.65	2	0.5	0.5
A2	MC	1.05	2.5	1.13	2.5
	JN	1.2	1.5	1.25	1.5
A3	MC	1.28	2	1.23	2
	DA	0.95	2	0.75	2
A4	MC	1.18	2	1.29	2
	JN	0.71	1.5	0.7	1.2
A#	MC	1.13	2.5	1.16	2.5
	DA & JN	0.88	2	0.8	2

B					
Set	Grader	10 error average	Worst error in 10	8 error average	Worst error in 8
B1	MC	0.25	0.5	0.19	0.5
	DA	0.6	1.5	0.5	1
B3	MC	0.2	0.5	0.13	0.5
	DA	0.6	1	0.56	0.5
B5	MC	0.25	0.5	0.19	0.5
	JN	0.1	1	0.13	1
B7	MC	0.4	1.5	0.25	0.5
	JN	0.32	1.5	0.34	1.5
B#	MC	0.28	1.5	0.19	0.5
	DA & JN	0.41	1.5	0.38	1.5

N.B.: Symbols as in Table II.

whose dates of assembly are not known. It may be, for example, that the A and B sets were assembled at different times. The implications of this survey for sets in the future are not quantifiable by the author.

Conclusions

The main benefits of this study are in showing the practical use of accurately graded CZ master stone sets, and the factors and methodology in their proper use, demonstrating the importance of verifying the initial accuracy of the set, and making periodic checks against full, diamond master colour grading sets to ensure retention of that accuracy.

Interested gemmologist-appraisers are encouraged to explore for themselves why CZ masters have found a place in the colour grading of diamonds. This investigation finds that CZ masters have a contribution to make in reducing the subjectivity of diamond colour grading when, as is frequently the case, the available diamond masters are relatively small in number and/or size. The study findings and results also support the argument that an accurate and complete set of CZ masters can, by themselves, be effectively employed in diamond colour grading, if periodically checked for retention of that accuracy.

Acknowledgements

Thanks to the following individuals for their contributions, discussions, and suggestions: David Atlas, Al Gilbertson, Raymond Mason, James Naughter, Howard Rubin and Peter Yantzer, and special thanks to Richard Cartier for suggestions and assistance with organization and editing.

References

Bruton, E., 1978. *Diamonds*. 2nd edn. Chilton Book Co., Radnor, PA. 532 pp

Gemological Institute of America, 1994. *Diamonds – Diamond Grading, Assignment 10 – Grading Color*, 21 pp

Shipley, R.M., and Liddicoat, R.T. Jr., 1941. A solution to diamond color grading problems. *Gems & Gemology,* **3**(11), 162-8

The Author

Michael Cowing FGA
AGA Certified Gem Laboratory
email: michael@acagemlab.com

Gem-A Workshops

As the world's longest established gem educator, The Gemmological Association of Great Britain is the leading provider of the most up-to-date and comprehensive knowledge regarding gemstones and retail staff training. With highly qualified tutors, fully-equipped classrooms and a wide variety of teaching stones for students to examine, we provide all of the essentials for top-quality training. Our workshops are held from 10:00 am to 4:30 pm each day (unless otherwise stated) at our headquarters near Hatton Garden, one of London's finest jewellery quarters.

Diamond Buying Guide

If you are in the market to buy a diamond, we can help you. Whether it is the perfect ring for that special someone or a considered purchase for yourself, improving your knowledge about diamonds is essential for making the right purchase. Or maybe you just wish to improve your sales knowledge. Whether you are buying or selling, we will provide you with the practical information about the 4Cs: carat weight, clarity, colour and cut, which will enable you to make informed choices and give great diamond sales advice.

Dates: Monday 20 April and Tuesday 10 October 2009
Price: £80.00 + VAT*, Gem-A students £50.00 + VAT*

Introduction to Practical Gemmology

If you are new to the world of gemmology, or just want a fun hands-on day of learning how to test gemstones using the correct equipment, come along for an exciting day of gemstone testing. We will teach you the basic principles required for identification and will demonstrate how to use the equipment. You will then be able to try gem-testing yourself under the guidance of an experienced tutor, and will discover an exciting new world.

Dates: Monday 23 March and Tuesday 13 October 2009
Price: £80.00 + VAT*, Gem-A students £50.00 + VAT*

***Quote the special promotional code WKS09 when booking to receive £5 off the price of your workshop.**

Other upcoming workshops include:

Allure of Gems: Monday 9 March and Tuesday 29 September 2009

Three Day Advanced Diamond Grading: Wednesday, Thursday and Friday 22–24 April 2009

Bead Stringing for Jewellery and **Advanced Bead Stringing for Jewellery**: Dates to be announced.

For the latest information on Gem-A workshops and short courses go to www.gem-a.com/education/short-courses-and-workshops.aspx or contact us at information@gem-a.com or +44 (0) 20 7404 3334 if you would like to learn more about our workshops, or to book a place.

The geological context of gems in the Velasco Pegmatitic District, Argentina

Fernando Guillermo Sardi

Abstract: The Velasco Pegmatitic District is located in the Velasco range, La Rioja province, northwestern Argentina. The Velasco range is made up of several granitic units of different petrography, magmatic evolution and age among which are the Huaco and Sanagasta granites. The pegmatites in the Velasco district have a spatial and genetic relationship with these granites and belong to the rare-element class, beryl type, beryl-columbite-phosphate subtype. The pegmatites are usually zoned and the K-feldspar zone is generally the most important for gem-quality beryl. Heliodor and aquamarine varieties are present and these crystals can be cut to yield products of attractive beauty. Other beryl crystals with poor transparency can be utilized for cabochons or tumble polished. Rock-crystal and rose-quartz are also present in some pegmatites from the Velasco district.

Keywords: aquamarine, gemstone, heliodor, pegmatite, rock crystal, rose quartz, Velasco range

Introduction

The Velasco range is located in the central region of La Rioja province, northwestern Argentina *(Figure 1)*. It is the largest mountainous unit of the geological province of the Sierras Pampeanas, which is characterized by large volumes of crystalline rocks of several origins and ages.

Beryl-bearing pegmatites are found in the Huaco Granite (Toselli *et al.*, 2000) and in the Sanagasta Granite (Grosse and Sardi, 2005). For this reason, each granite is considered a lithological guide to possible gem occurrences (Sardi, 2005). Both granites have mainly porphyroid textures, without signs of deformation. Their outcrops occupy much of the central-north and central-east zones of the Velasco batholith *(Figure 2)*. The Huaco Granite covers 620 km² and the Sanagasta Granite 240 km² (Grosse and Sardi, 2005), and the Huaco Granite contains more Be-pegmatites than does the Sanagasta Granite.

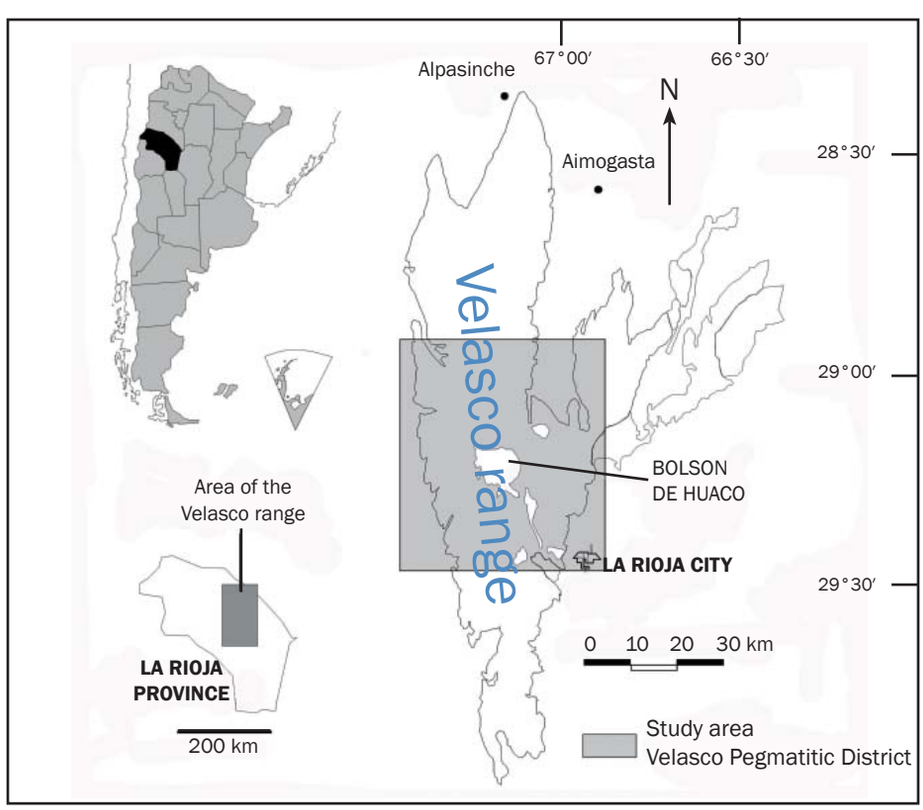

Figure 1: Location of the study area. On the right is the outline of the Velasco Range, and the indicated study area.

©2008 Gemmological Association of Great Britain

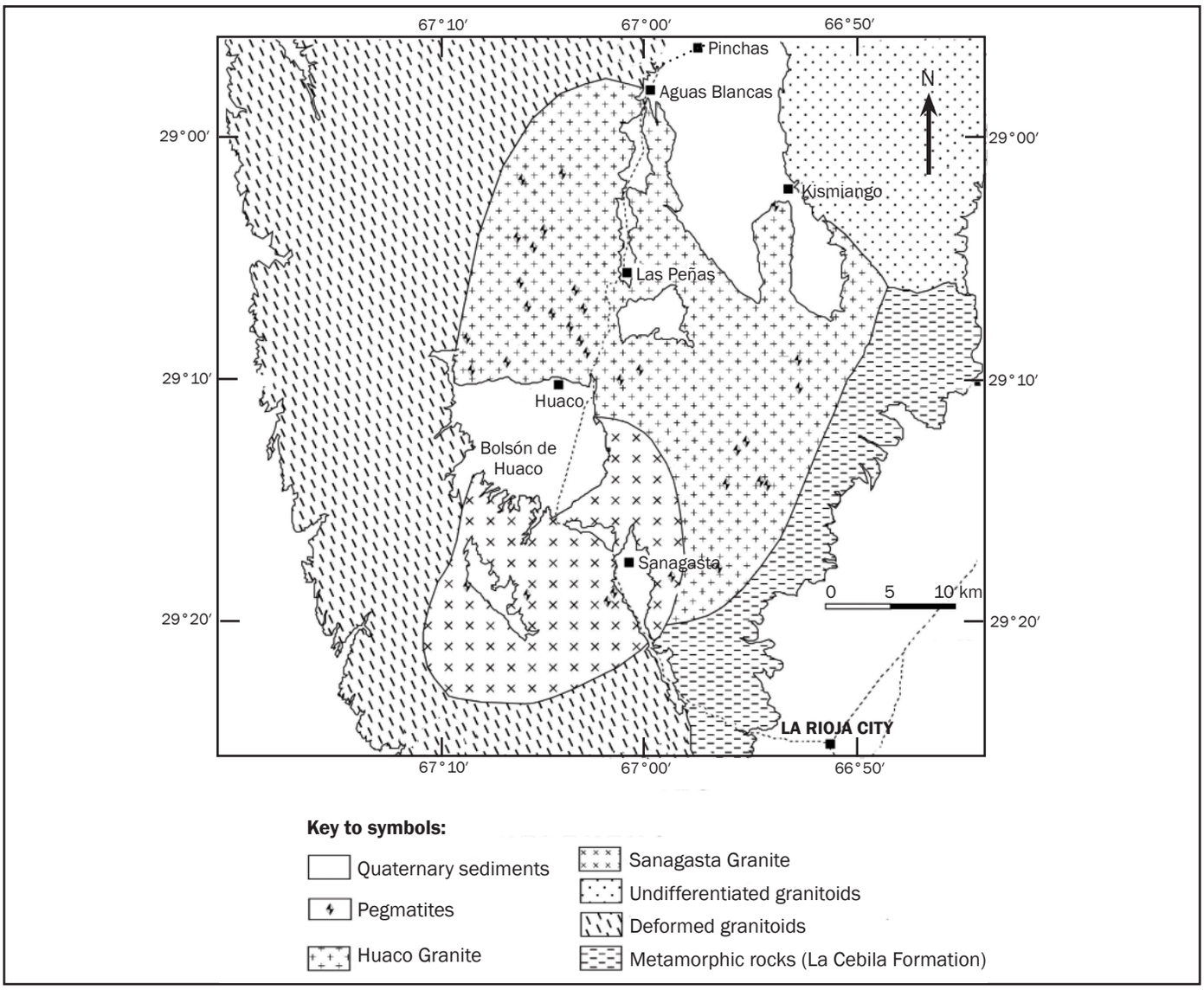

Figure 2: Simplified geological map of the Velasco Pegmatitic District. Modified from Sardi and Grosse (2005). Bolson de Huaco is an area which is a topographic depression covered with Quaternary sediments.

The pegmatites lie in the Velasco District of the Pampean Pegmatitic Province as defined by Galliski (1994). Herrera (1968), in a local classification, grouped the pegmatites from the Pampean Pegmatitic Province into four categories following a course of fractionation from 'type 1', barren pegmatites with oligoclase, to 'type 4', highly evolved with Li mineralization. In this case, the pegmatites from Velasco District correspond to the 'type 3' which is characterized, in general, by a simple zonal structure, by high diversity and abundance of accessory minerals, and by the appearance of a phase of substitution of potassium by sodium. Subsequently, they have been classified, according to Cerný (1991) as belonging to rare elements class; beryl type and beryl-columbite-phosphate subtype (Galliski, 1994; Sardi and Grosse, 2005).

The aim of this communication is to record some gem-quality minerals in the pegmatites. Most are beryl, and of lesser importance is quartz. Beryl is an accessory mineral in the Velasco pegmatites and has been extracted only sporadically and in an inconsistent manner during the last century. At the moment only gem-quality stones are being recovered. Mineralogical and gemmological studies of such deposits in the area are very scarce, and the data presented below are preliminary, and represent a beginning for more detailed research.

Geological setting

The Velasco range consists of a mixture of Palaeozoic granitic rocks of different origins and evolutions. Such rocks of I-type affiliation in the south and granitoids of S-type affiliation towards the centre and north of the range can clearly be distinguished (Toselli *et al.,* 2002, 2005; Bellos, 2005). In the south, the granitoids are granodioritic and tonalitic with hornblende and magnetite as accessory minerals, and per- and meta-aluminous tendencies in their compositions; while in the north, the rocks are shallow magmatic porphyroid granites with two micas, and with a per-aluminous character. The plutons in the centre and north of the

Velasco range comprise the Aimogasta Carboniferous Batholith (Toselli *et al.,* 2006) and they are intrusive into deformed orthogneisses of Ordovician age and also commonly into protomylonites and mylonites of Ordovician to Devonian age (Toselli *et al.,* 2006).

On the east flank of the Velasco range, the La Cebila Formation is represented by sporadic outcrops of meta-pelites and meta-psammites. These sediments are of Upper Precambrian – Lower Cambrian age (Aceñolaza *et al.,* 2000), and their metamorphic grade does not exceed greenschist facies. In the extreme north of the range, contact metamorphic rocks appear whose mineral association indicates nearby shallow-level granitic intrusions (Rossi *et al.,* 1997).

The Huaco (Toselli *et al.,* 2000) and Sanagasta (Grosse and Sardi, 2005) Granites make up the whole of the Aimogasta Carboniferous batholith. Petrographically, their main characteristic is a porphyroid texture with megacrysts of perthitic microcline, in some places making up to 50 % of the rock (Sardi *et al.,* 2002). These megacrysts are white in the Huaco and pink in the Sanagasta Granites. The Sanagasta granite's K-feldspar megacrysts are occasionally mantled by plagioclase generating a Rapakivi-like texture (Grosse and Sardi, 2005; Grosse *et al.,* 2008). Another difference is that the Sanagasta Granite has a higher biotite/muscovite ratio than the Huaco Granite. The matrix is essentially composed of quartz, microcline, plagioclase, biotite and muscovite. The geochemical studies made by Grosse *et al.* (2008) indicate the granites to be silica-rich, potassium-rich, ferroan and alkali-calcic to slightly calc-alkalic. U-Pb monazite age determinations on Huaco and Sanagasta Granites indicate Lower Carboniferous crystallization ages and the isotopic and geochemical studies indicate a mainly crustal source, possibly similar to the Ordovician peraluminous metagranitoids which are nearby (Grosse *et al.,* 2008).

Velasco District pegmatites

The Velasco District has numerous pegmatite bodies that are developed immediately north, east and south of Bolsón de Huaco (see explanation in the caption of *Figure 2*). The area of the Velasco Pegmatitic District is occupied by the Huaco and Sanagasta Granites and the Be-pegmatites have a spatial relation with them *(Figure 2)*. These bodies present more or less homogeneous characteristics as to their structures and mineral composition. According to Sardi *et al.* (2002), their contacts with the granitic host-rock are sharp.

The lengths of the pegmatites are no greater than 250 m and most consist of a marginal-external zone, an intermediate zone and core of quartz (Sardi, 2005). The marginal-external zone wraps around the coarse-grained minerals in the pegmatite. It is aplitic and/or equigranular fine- to medium-grained leucogranite and is composed of quartz, microcline, plagioclase, tourmaline, muscovite, biotite, apatite, and topaz (Sardi, 2005). The intermediate zone contains mainly quartz with microcline and/or plagioclase, with microcline being the more common; perthitic and graphic textures are also common. The accessory minerals in this zone are muscovite, scarce biotite, apatite, triplite, beryl and tourmaline (Sardi, 2005). Herrera (1971) and Ricci (1971) had already reported garnet, fluorite, columbite-tantalite and wolframite which can be added to this list. The core of the pegmatite is massive quartz, usually grey but some is pink. Here, the accessory minerals are very scarce: tourmaline, muscovite and beryl (Sardi, 2005).

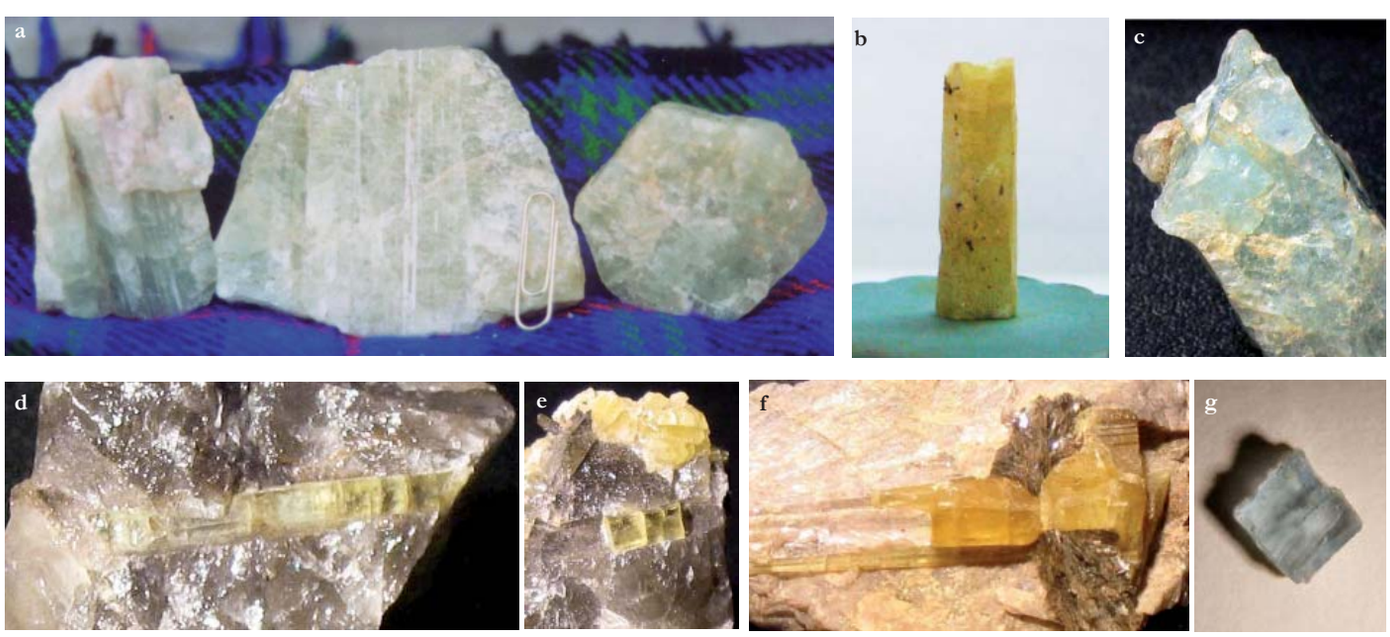

Figure 3: Beryl from the Velasco Pegmatitic District.
Milky beryl: (a) Green and pale green beryl; the left and centre fragments show striated faces, and in the one on the left a hexagonal contour is visible. Width of image 12.2 cm. (b) Idiomorphic yellow beryl. Width of image 3.2 cm. (c) Pale blue (turquoise colour) beryl – aquamarine. Width of image 0.6 cm.
Translucent and transparent beryl: (d and e) Heliodor varieties, associated with grey quartz. Width of images: 1.5 cm and 0.6 cm respectively); (f) Heliodor with feldspar and mica. Width of image: 1.7 cm. (g) Fragment of aquamarine. Width of image 1.8 cm.

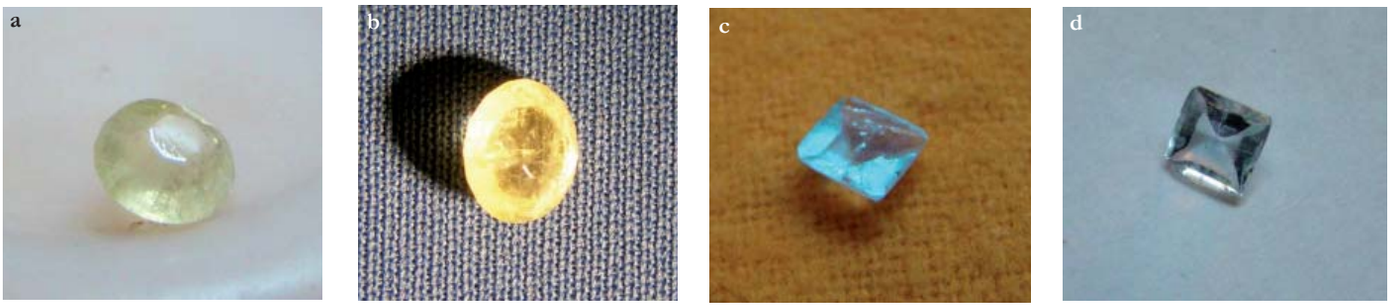

Figure 4: Faceted examples of heliodor and aquamarine. (a and b) Heliodor, 7 mm long, on different backgrounds and under different lights; weight 0.615 ct. (c and d) Aquamarine, 5 mm square, on different backgrounds and under different lights. Weight 1.279 ct.

Gemstones

Beryl

Beryl is generally concentrated in the intermediate zones associated with anhedral quartz, clusters of muscovite and K-feldspar (Sardi, 2005). Most beryls are green, yellow and pale blue *(Figures 3a, b and c)* but varieties of colourless beryl are very scarce and are associated mainly with quartz. The beryls are idiomorphic, and have vitreous lustre and conchoidal fracture. According to Sardi (2005), most are well-developed hexagonal prisms, some with vertically striated faces *(Figure 3a)*. The most common forms are first-order prisms and basal pinacoids, although some crystals appear wedge-shaped. The mineral size is variable. Transverse sections of the crystals measure up to 6 cm and the longest crystals are up to 12 cm. When the mineral is associated with muscovite, beryl is thin and long, but in association with grey quartz it is thicker. A poor cleavage can be present parallel to (0001). Only rarely does it have inclusions of other minerals such as tourmaline, quartz and muscovite.

The economic importance of beryl from the Velasco Pegmatitic District lies in its gem quality (Sardi, 2005). The yellow variety of beryl, heliodor, has total transparency, scarce fractures and is free of inclusions of other minerals *(Figures 3d, e and f);* pale green and pale blue aquamarine *(Figure 3g)* reach lengths of about 3 cm. The almost total absence of fractures in heliodor and aquamarine can permit their cutting and polishing to give beautiful and attractive stones *(Figures 4a, b, c and d)*. Some gem-quality crystals of beryl may be so embedded in quartz that it is difficult to extract them without fracturing; these may be more desirable and valuable for mineral collectors as heliodor or aquamarine in matrix. Goshenite is very scarce and small in size relative to heliodor, and thus is less important.

Non-gem-quality crystals of beryl are of greater size and range from translucent or semi-translucent to milky. They have only minor commercial value, and some may be cabochon cut or polished by tumbling. Gem-quality crystals are considered to have originated in the later stages of cooling and crystallization of the pegmatitic cavity and may be secondary or recrystallized.

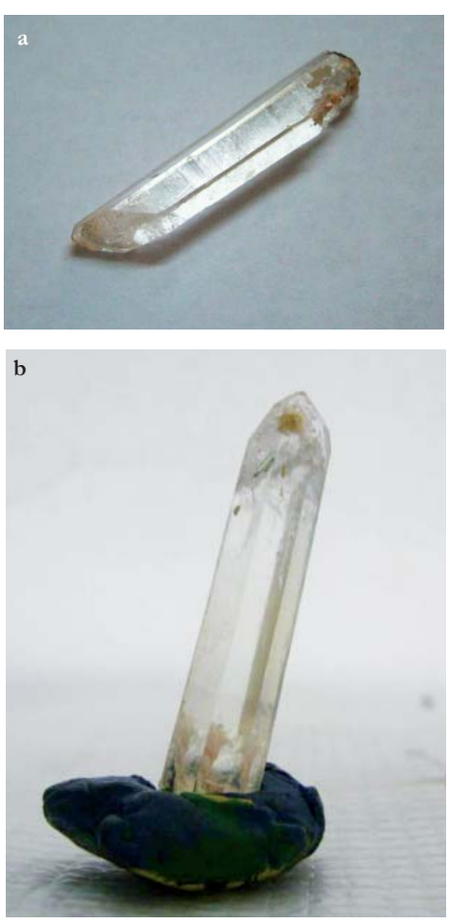

Figure 5: (a and b) Typical rock crystal, 42 mm long, on different backgrounds and under different lights; weight 4.2252 g; (c) A specimen of rose quartz, 96 mm high, with a rough top and polished sides.

Quartz

There is more than one generation of quartz in the pegmatites and the gem-quality quartz is considered to have been formed during the later pegmatitic (or hydrothermal) stage. The variety rock crystal has been found in the intermediate zone of the pegmatites in association with K-feldspar. It is colourless, entirely transparent, idiomorphic with hexagonal contours and without inclusions. Crystals reach 4.2 cm in length and 1 cm in width *(Figure 5a and b)*. Rose quartz has been

found in pegmatites in the Sanagasta Granite, generally forming part of the core-quartz of the pegmatites *(Figure 5c)*. It is coarsely crystalline and in some is very transparent and free of inclusions. The quartz gems are secondary in importance to the beryl.

Conclusions

At present, gem-quality beryl and quartz can be recovered from the pegmatites of the Velasco District (Argentina). Most of the gem beryl occurs in idiomorphic prisms of yellow, green or pale blue, in sizes up to 12 cm in length, and with different degrees of transparency. Some crystals of heliodor and aquamarine are large enough to have commercial value. The formation of the gems is attributed to crystallization in the late stages of pegmatitic evolution. Future studies, especially of a thermometric nature, could yield further insight into their origin. Gem-quality quartz in these pegmatites occurs as rock crystal and rose quartz.

Acknowledgements

The author thanks Dr Jorge Saadi (Consulting Geological, Córdoba province, Argentina) and Geol. Fernando Campos (Miguel Lillo Fundation, Tucumán province, Argentina) for advice on gemmological aspects of this work. The field-work and laboratory studies were carried out as part of the investigation projects of CIUNT (National University of Tucumán, Argentina) under the leadership of Dra. Juana Rossi. The photographs of the Figures 3, 4 and 5 were kindly provided by my friends Paul Grosse and Miguel Báez (National University of Tucumán, Argentina).

References

Aceñolaza, F., Miller, H., and Toselli, A., 2000. *Geología de la sierra de Velasco, provincia de La Rioja, Argentina*. 17 Geowissenschaftliches Lateinamerika-Kolloquium (LAK). CD-Proceedings, paper Nº 1, 6 pp. Institut für Geologie und Paläontologie der Universitat Stuttgart, Germany

Bellos, L., 2005. Geología y petrología del sector austral de la sierra de Velasco, al sur de los 29º 44' S, La Rioja, Argentina. *Serie de Correlación Geológica INSUGEO,* **19**, 261-78

Cerný, P., 1991. Rare-element granitic pegmatites. Part I: Anatomy and Internal evolution of pegmatite deposits. *Geoscience Canada*, **18**(2), 49-67

Galliski, M., 1994. La Provincia Pegmatítica Pampeana. I: Tipología y distribución de sus distritos económicos. *Asociación Geológica Argentina, Revista,* **49**(1-2), 99-112

Grosse, P., and Sardi, F., 2005. Geología de los granitos Huaco y Sanagasta, sector centro-oriental de la Sierra de Velasco, La Rioja. *Serie de Correlación Geológica INSUGEO,* **19**, 221-38

Grosse, P., Söllner, F., Báez, M., Toselli, A., Rossi, J., and De La Rosa, D., 2008. Lower Carboniferous post-orogenic granites in central-eastern Sierra de Velasco, Sierras Pampeanas, Argentina: U-Pb monazite geochronology, geochemistry and Sr-Nd isotopes. *International Journal of Earth Sciences* (in press)

Herrera, A., 1968. Geochemical evolution of Zoned Pegmatites of Argentina. *Economic Geology,* **63**(1), 13-29

Herrera, A., 1971. Pegmatitas de la sierra de Velasco y de la sierra Brava, provincia de La Rioja; estructura, mineralogía y genesis. *I Simposio Nacional de Geología Económica,* **I**, 245-58

Ricci, H. I., 1971. Geología y evaluación preliminar de las pegmatitas de la sierra de Velasco, Departamento Capital, Sanagasta y Castro Barros, La Rioja. Dirección Provincial de Minería de La Rioja. pp. 50. Unpublished.

Rossi, J. N., Toselli, A., Durand, F., Saravia, J., and Sardi, F., 1997. Significado geotectónico de corneanas piroxénicas en granitos de las Sierras de Paimán, Velasco y Famatina. Provincia de La Rioja. Argentina. *VIII Congreso Geológico Chileno,* **II**, 1498-501

Sardi, F., Toselli, A., and Rossi, J. N., 2002. Estudio geológico preliminar de las pegmatitas del Norte del Bolsón de Huaco, sierra de Velasco, La Rioja. *XV Congreso Geológico Argentino,* **II**, 33-4

Sardi, F. G., 2005. Petrografía y caracterización de la mena del distrito pegmatítico Velasco, La Rioja, Argentina. *XVI Congreso Geológico Argentino,* **V**, 231-8

Sardi, F. G., and Grosse, P., 2005. Consideraciones sobre la clasificación del distrito Velasco de la Provincia Pegmatítica Pampeana, Argentina. *XVI Congreso Geológico Argentino,* **V**, 239-42

Toselli, A., Rossi, J., Báez, M., Grosse, P., and Sardi, F., 2006. El Batolito Carbonífero Aimogasta, Sierra de Velasco, La Rioja, Argentina. *Serie de Correlación Geológica INSUGEO,* **21**, 137-54

Toselli, A., Rossi, J., Miller, H., Báez, M., Grosse, P., López, J., and Bellos, L., 2005. Las rocas graníticas y metamórficas de la Sierra de Velasco. *Serie de Correlación Geológic INSUGEO,* **19**, 211-20

Toselli, A., Rossi, J., Sardi, F., López, J., and Báez, M., 2000. *Caracterización petrográfica y geoquímica de granitoides de la sierra de Velasco, La Rioja, Argentina*. 17 Geowissenschaftliches Lateinamerika-Kolloquium (LAK), CD-Proceedings, paper Nº 81, pp. 6. Institut für Geologie und Paläontologie der Universitat Stuttgart. Germany

Toselli, A., Sial, A., and Rossi, J., 2002. Ordovician magmatism of the Sierras Pampeanas, Sistema de Famatina and Cordillera Oriental, NW of Argentina. *Serie de Correlación Geológica INSUGEO,* **16**, 313-26

The Author

Fernando Guillermo Sardi
INSUGEO-CONICET. Miguel Lillo 205, (4000) San Miguel de Tucumán, Argentina
fgsardi@csnat.unt.edu.ar

Gem-A's new

Open Distance Learning (ODL) Courses in Gemmology

Launched in 2008, Gem-A's new Foundation in Gemmology ODL Course is ideal for students who need the flexibility to work from home and the ability to plan their own schedule. You will learn about commercially important gem materials as well as a range of treated and imitation products.

The course includes distance tuition, a student web login, online tuition and assessed course work, examinations and student registration. It is essential that our students have internet access to complete the course. Students receive comprehensive and fully illustrated course notes, a gem reference guide, a gem testing kit and 20 study stones. UK ODL students receive three practical tutorials at Gem-A's London headquarters. Overseas students can either attend the UK tutorial sessions, or may arrange sessions with a Gem-A approved local provider.

Foundation Certificate in Gemmology

The Foundation course is assessed by course work and a final examination, with an emphasis throughout the course on the practical aspects of handling gem materials. Those who qualify are awarded the Foundation Certificate in Gemmology and are eligible to continue their studies with Gem-A's Diploma in Gemmology course.

Next start dates:

12 January 2009 – intensive 6 month programme
16 March 2009 – the 9 month programme

Course fees:

£1695 for UK students (to include the London practical workshop)
£1395 for overseas students

Full details of the ODL and other courses provided by Gem-A are given at www.gem-a.com/education.aspx or call +44 (0)20 7404 3334 for information

Gem-A Scottish Branch Conference 2009

Friday 1 May to Monday 4 May

The Queen's Hotel,
Perth, Scotland

This popular annual event attracts speakers and participants from many corners of the world. The well-balanced programme of lectures has something for anyone with an interest in gems.

Speakers will include:

KENNETH SCARRATT (KEYNOTE)
ALAN HODGKINSON
BRIAN JACKSON
JENNIFER SCARCE
DR HANCO ZWAAN

Sunday afternoon will be devoted to displays, demonstrations and workshops, and a field trip will be held on the Monday morning.

Social events are held each evening, including the Ceilidh (dinner/dance) on the Saturday.

For further information or to book contact Catriona McInnes on
0131 667 2199
email scotgem@blueyonder.co.uk

Magnetic susceptibility, a better approach to defining garnets

Dr D. B. Hoover FGA FGAA (Hon.), C. Williams FGA, B. Williams and C. Mitchell FGA

Abstract: Using a new, non-destructive method of gem testing, magnetic susceptibility, the authors show how the major end-member composition of any garnet may be confidently predicted by plotting RI against measured susceptibility. On this diagram, eight end-member garnets are plotted, so that any measured garnet can be placed in an appropriate ternary area. This method shows how previous methods of identifying garnets — by their colour, RI and spectrum — are insufficient to accurately identify chemistry in the garnet group. Furthermore, it can be done with inexpensive equipment available to most gemmologists.

Keywords: garnet, gem testing, magnetic susceptibility, refractive index, specific gravity, UV-Visible spectra

Spessartite garnet. Photo by R. Weldon.

Introduction

Most gemmologists classify garnets based on their colour, refractive index (RI) and absorption spectrum[1,2,3,4,5,6,7]. As new sources and new gem varieties of garnet are discovered, and as our information on garnet chemistry increases, problems with the present gemmological classification become more apparent[8]. The practising gemmologist needs a better means for characterization of garnets to avoid such problems. In this article, the authors will show how any gemmologist can closely infer the major end-members composition of a garnet — without expensive or high-tech equipment.

Two of the authors introduced a new method of gem testing — magnetic susceptibility — in a recent paper[9]. Due to the presence of transition metals in many garnets, the garnet group provides an interesting range of stones to which this method can be applied. Our research further confirmed that far more accurate garnet composition can be revealed in this way than was previously possible with only conventional gemmological testing equipment. Few non-destructive tests can give a better idea of the chemistry. When the RI is plotted against magnetic susceptibility, a more complete picture of a garnet's chemistry can be made. While this new characterization technique raises questions about the current nomenclature and classification of gem garnets, we will stick to the chemistry and leave nomenclature and classification to future debate.

Most modern gemmological texts identify six garnet end-member species; the pyralspite group — pyrope, almandine and spessartine; and the ugrandite group — grossular, andradite and uvarovite[8,10,11]. A garnet species in its theoretical pure form is referred to as an end-member, however they have not been found pure in nature. Natural garnets are always a mix of several end-members, typically with three to five species of significant quantity[12]. The mineralogist recognizes fifteen garnet end-members — some of which exist only in theory[12]. In this article we will consider eight of them, adding knorringite and goldmanite to the more familiar six *(Table I)*. The mineralogist names any of the mixed garnets by the name of the dominant end-member[12]. Thus, although a pyrope may contain less than 50% of the pyrope molecule, it can still be the dominant component when more than two end-members are present, which is commonly the case.

Due to the difficulty of getting sufficient compositional information quickly and easily, gemmology has generally followed a different nomenclature, opting to define nine varieties of garnets: pyrope, pyrope-almandine, almandine, almandine-spessartine, spessartine, spessartine-pyrope, grossular, grossular-andradite, and andradite[5,6,7]. Uvarovite is normally not included as it has limited gem significance. To date, gemmologists have not come to an agreement on what value of RI should mark the separation between

©2008 Gemmological Association of Great Britain

Table I: Properties and chemical formulae of the end-member garnets considered in this paper.

End-member	RI	SG (calc.)	Volume susceptibility (k) (calc.) × 10^{-4} SI	Chemistry
Pyrope	1.714	3.582	-0.225	$Mg_3Al_2Si_3O_{12}$
Almandine	1.829	4.315	40.7	$Fe_3Al_2Si_3O_{12}$
Spessartine	1.799	4.197	47.45---	$Mn_3Al_2Si_3O_{12}$
Grossular	1.734	3.594	-0.225	$Ca_3Al_2Si_3O_{12}$
Andradite	1.887	3.859	30.76	$Ca_3Fe_2Si_3O_{12}$
Uvarovite	1.865	3.850	12.9	$Ca_3Cr_2Si_3O_{12}$
Goldmanite	1.834	3.765	6.9	$Ca_3V_2Si_3O_{12}$
Knorringite	1.875	3.835	13.68	$Mg_3Cr_2Si_3O_{12}$

N.B. [12, 18]

these arbitrary boundaries in the garnet chemistry continuum[8]. Adding further to the confusion, gemmologists classify, mostly by colour, eight commonly-used trade names of these nine varieties; chrome pyrope, rhodolite, malaia, colour-change pyrope-spessartine, tsavorite, hessonite, topazolite, Mali and demantoid[5]. Note that these are their gemmological classes, not mineralogical classes. With trade names, it becomes yet more complicated, but no more accurate.

From our studies, we do not believe that gemmologists, relying only on RI, spectrum, and colour can reliably — or consistently — allocate the correct species or varietal name to a garnet being studied. Gemmological texts often imply, for example, that tsavorite, because it is coloured by vanadium and/or chromium, is allochromatic, when in fact it is a combination of garnet end-members that creates the colour. Very often there is a third (or even more) end-member present, that while less than 10% in quantity, can yet affect the RI and colour in such a way as to lead to a false conclusion by the traditional methods. Problems with the current state of affairs will become apparent later in this paper.

History

The mineralogical literature abounds with papers on the garnets[12]. Much of the information has limited relevance to gemmology in the classification and identification of gem garnets, as stones of gem quality comprise only a very small proportion of the whole, and gemmological identification methods must be non-destructive. In a series of articles on the garnets, Manson and Stockton [1,2,4] and Stockton and Manson[3,5] presented an in-depth study on 202 transparent, gem-quality garnets that is invaluable to gemmologists for presentation of the chemistry and physical properties of each of the studied garnets. In their final paper of the series[5] (p.215), they set the precedent for the garnet classifications currently in use.

Manson and Stockton obtained their accurate garnet chemistry analyses using microprobe equipment not available to the average gemmologist. It should be noted that while they measured the specific gravity (SG) of each gem, they do not use SG at all in characterizing gem garnets[5]. In fact, they state (p. 216): "Although we generally discourage the use of this property in gemmology, it nevertheless can provide some useful indications." We will see why they may have done this later on.

Mineralogists often use another method of quantitative measurement of garnet, — its unit cell length. This measurement of the length of one edge of the unit cell, from X-ray diffraction data, is not practical for the gemmologist. Sriramadas[13] has published eight ternary diagrams for the garnet group showing RIs and unit cell lengths on the triangles. Winchell[14] notes that ternary diagrams are mostly used to estimate composition from measured physical properties, but that generally there are too few properties to uniquely define the composition. Using the garnet group as an example, he shows how treating two physical properties as independent variables, one can plot the compositions, and yet another physical property on the same graph. In essence, one can put the information of the eight plots of Sriramadas, on one graph. Winchell[14] uses RI and cell length on the Y and X axes, and shows SG variation within each ternary diagram, which now becomes a general triangle. He recognizes, as others have, that SG is not a very reliable measurement for determining chemical composition.

The Manson and Stockton papers[1,2,3,4,5] note that virtually all gem garnets can be described by five end-members; namely, pyrope, almandine, spessartine, grossular, and andradite. Deer *et al.*[12] note that these five members usually make up more than 99% of any garnet's composition. This will be important in what follows. Stockton and Manson[5] also note that Cr^{+3}, V^{+3} and $Ti^{+3,+4}$, although important for colour in some garnets, can be treated as trace elements, and not as components of other end-member gem garnets, at least for this method of classification.

Johnson *et al.*[6] add another important contribution to gem garnet chemistry with a paper on the Mali grossular-andradite garnets. These gems are ugrandites with typical yellow-green stones averaging about 80% grossular, 18% andradite and 2% pyrope. It is important to note that these are typically strongly zoned; hence, their physical properties will vary as well as their colour across the zonation. In these Mali garnets, pyrope is typically 2 to 3% with almandine and spessartine much less. They noted that mineralogists may use physical properties such as unit cell length, RI and SG to determine garnet composition from end-member values, and tested how well their data served to match determined chemistry. They found that, for the Mali garnets, RI correlated well with the garnet chemistry, while there was poorer correlation with other physical properties, especially SG which was determined hydrostatically. It would be expected that since the Mali garnets are almost entirely grossular-andradite, only one property is needed to define the chemistry and RI would do this.

Adamo *et al.*[7] recently described correlations between physical properties and chemistry for 17 gem-quality garnets in both the ugrandite and pyralspite groups, and also examined IR spectral features to see what they may contribute to classification of the garnets. They concluded that IR spectra, in particular, permit discrimination between the pyralspite and ugrandite series. Their data generally agree with what was found by Manson and Stockton[1,2,3,4,5]. Three hessonites contained from 84.5 to 92.75% grossular with andradite the other major component at 5 to 14%. Pyralspite members were under 2.1%. The two tsavorites measured showed about 90% grossular, and 4% goldmanite (vanadium garnet). Of ten pyralspites measured, grossular contents ranged from 0 to 6.15%, the andradite component was generally under 1% but in one sample was 8.3%. Uvarovite reached 1.7% in a chrome-pyrope, and goldmanite 3.65% in a colour-change pyrope-spessartine. The chromium content of a garnet may be expressed as either uvarovite or knorringite, but since knorringite is stable only at very high pressures (greater than 70-100kbar)[12], the chrome in most gem garnets is probably better considered as part of the uvarovite end member. An important exception may be in some gem chrome pyrope.

Adamo *et al.*[7] used the same garnet nomenclature as Stockton and Manson[5] but added the variety grossular-andradite, based on the work of Johnson *et al.*[6]

It was in 1933 that Winchell divided the garnet group into two series composed each of three major garnet species — the ugrandite series (uvarovite, grossular, andradite), and the pyralspite series (pyrope, almandine, spessartine). These two mineralogical series do not appear to be as well known to gemmologists as they should be. Although complete solid solution between natural members of each series was believed possible, there appeared to be a compositional gap between them. Modern studies on the garnets have shown there to be more miscibility between the various garnet end-members than previously thought but the two series do show structural differences and most gem garnets appear to fall within or close to one series or the other.

Table II: Some paramagnetic ions, their valencies, effective magnetic moments, and the square of the moment, which is proportional to the magnetic attraction.

Ion	Magnetic moment (experimental)	Magnetic moment squared (relative attraction)
Transition elements:		
Fe^{3+}, Mn^{2+}	5.9	34.8
Fe^{2+}	5.4	29.2
Mn^{3+}, Cr^{2+}	4.9	24.0
Co^{2+}	4.8	23.0
Cr^{3+}, V^{2+}	3.8	14.4
Ni^{2+}	3.2	10.2
V^{3+}	2.8	7.84
Cu^{2+}	1.9	3.61
Ti^{3+}, V^{4+}	1.8	3.24
Rare-earth elements:		
Dysprosium Dy^{3+}	10.6	112.
Holmium Ho^{3+}	10.4	108.
Erbium Er^{3+}, terbium Tb^{3+}	9.5	90.
Gadolinium Gd^{3+}	8.0	64.
Thulium Tm^{3+}	7.3	53.
Ytterbium Yb^{3+}	4.5	20.
Neodymium Nd^{3+}, praseodymium Pr^{3+}	3.5	12.2
Europium Eu^{3+}	3.4	11.6
Cerium Ce^{3+}	2.4	5.7
Samarium Sm^{3+}	1.5	2.2

Magnetic measurements

Modern understanding of magnetism shows that it arises from the motion of electrons in atoms in the same way that an electrical current in a wire produces a magnetic field about the wire. Within the atom, electrons move in orbits about the nucleus and also spin. Both of these motions produce very small magnetic dipole fields, so the electrons act as very small permanent magnets within the atom. The magnetic property of any material is the resultant of the contributions of all of its atoms and how this reacts to an applied magnetic field. More on this complex subject can be obtained from Kittel[15], college physics texts, or the Internet.

We will be primarily concerned with magnetic susceptibility per unit volume, k, a bulk property of all materials, that can be directly measured. These materials can be classified in three distinct groups according to the sign and value of their magnetic susceptibility.

The orbiting electrons about an atom of any material, when in the presence of an applied field, will precess, presenting a weak opposing magnetic field. Precession is the wobble that a toy top makes when the spin axis is not in line with the vertical direction. If no other magnetic effects are present, these materials will be weakly repelled by a magnet, and k will be negative. Such materials are called diamagnetic. Most gems are diamagnetic.

In some atoms and molecules there is a net magnetization generally related to electron spin, but which in bulk is zero due to thermal motion of the atoms. However, when a field is applied they

can become oriented to give a small net positive susceptibility, overcoming the negative value due to diamagnetism. Such materials are called paramagnetic. The elements contributing to this type of magnetism, that are relevant to gemmology, are the transition and rare-earth elements. These elements, while best known for their colour causing properties, whether as major or trace components in many gems, also have paramagnetic properties.

As shown in *Table II,* the manganese- and iron-bearing gems will have the greatest paramagnetic susceptibilities, as the rare-earth content of most gems is small. Thus, magnetic testing will indicate the presence or quantity of these elements, just as absorption spectra show their presence by the absorption of light. Paramagnetic gems are of the most interest in gem characterization and identification by means of susceptibility measurements. The table shows the square of the measured effective ion moment, because this is directly proportional to susceptibility.

Ferromagnetic materials have much larger absolute susceptibilities than diamagnetic or paramagnetic materials due to a natural alignment of magnetic moments of the individual atoms. They are further distinguished by being made up of small individual magnetic domains in which the magnetization may not be the same as a neighbour. To the gemmologist, ferromagnetic minerals, such as magnetite, are of interest where they may be present as inclusions, but are generally of less importance than paramagnetic minerals.

In the past, non-laboratory gemmologists have had only two truly quantitative, physical tests available by which to characterize gemstones. These are refractive index (RI and related birefringence) and SG. Unfortunately, RI and SG are not very independent variables, as many years ago Gladstone and Dale (quoted in Larsen and Berman[16]) showed that the ratio of RI to SG is approximately a constant, (RI-1)/SG=k. Because of the Gladstone-Dale relationship, and the fact that accurate measurement of SG is generally difficult, mineralogists and gemmologists often marginalize the use of SG for characterization of their materials. This is clearly one of the reasons that Stockton and Manson[5] didn't make use of SG in their work.

Figure 1: Apparatus used to measure magnetic susceptibility in this study.

By having a new, independent, quantitative physical property by which to characterize gems, the gemmologist now has much greater scope to characterize gemstones than before. Not only can we measure a gem's susceptibility, but we can also calculate what its susceptibility should be from its chemistry when known; or, with certain assumptions, calculate the quantity of a transition metal in a gemstone as shown by Hoover and Williams[9].

Making magnetic susceptibility measurements

The basic theory behind susceptibility measurements has been described in a previous article[9], where the magnetic attraction (pull) between a very small Neodymium-iron-boron (NdFeB – or NIB) magnet and the flat table of a cut gem was measured on an electronic scale. If the NIB magnet pole face is smaller in diameter than the gem's table, then the pull is a direct measure of the gem's susceptibility. We have used cylindrical magnets of ¼, 3/16, 1/8 and 1/16 inch diameters by ½ inch long. These N42 grade NIB magnets are available from K&J Magnetics Inc. (www.kjmagnetics.com). These are inexpensive, but very strong. We recommend following the manufacturers warnings regarding use. For the best precision, the largest magnet that fits within the stone's table should be used. For all measurements shown in this paper we used a 1/8 inch magnet, which allowed measurements on stones of one carat or larger. In order to convert this pull

Magnetic susceptibility, a better approach to defining garnets

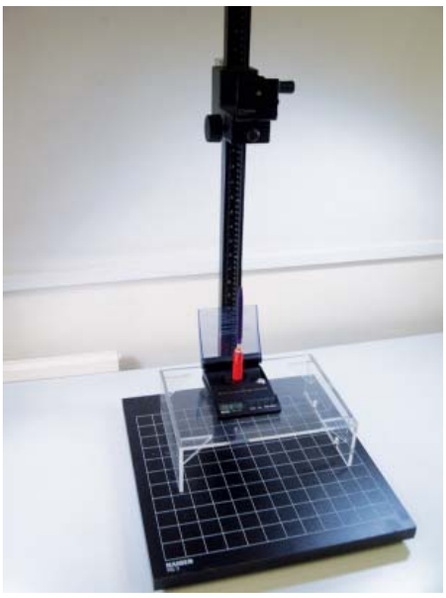

Figure 2 (above): An early prototype using a photo stand. While less precise than later set-ups, this arrangement proved useful for experimenting with the technique.

into a measure of the gem's susceptibility one need only measure a material of known and consistent susceptibility — a standard. A standard can be any paramagnetic material in which the paramagnetic element that causes the magnetic susceptibility is equally distributed and in consistent quantity. For our testing purposes, we used cobalt chloride ($CoCl_2.6H_2O$) with a pull of 0.855 ct (measured with one of our 1/8 inch (3.12 mm) magnets) and susceptibility of 9.87 × 10^{-4} SI units. The equation below shows the relationship to determine an unknown susceptibility from pull measurements.

Equation 1

k = C × Pull

where Pull = measured pull of the test stone and

$$C = \frac{k \text{ (of standard)}}{\text{Pull (of standard)}}$$

As an example, a 3.10 ct pyralspite has a pull of 1.135 ct with the 1/8 inch magnet. Its susceptibility, k =[9.87×10^{-4}SI /.855 ct] ×1.135 ct = 11.54×10^{-4} SI/ct × 1.135 ct = 13.10×10^{-4}SI.

The concept is very simple, but the measurement must be done with care and it takes some practice to become consistent. The equipment is shown in *Figures 1, 2* and *3*. The authors

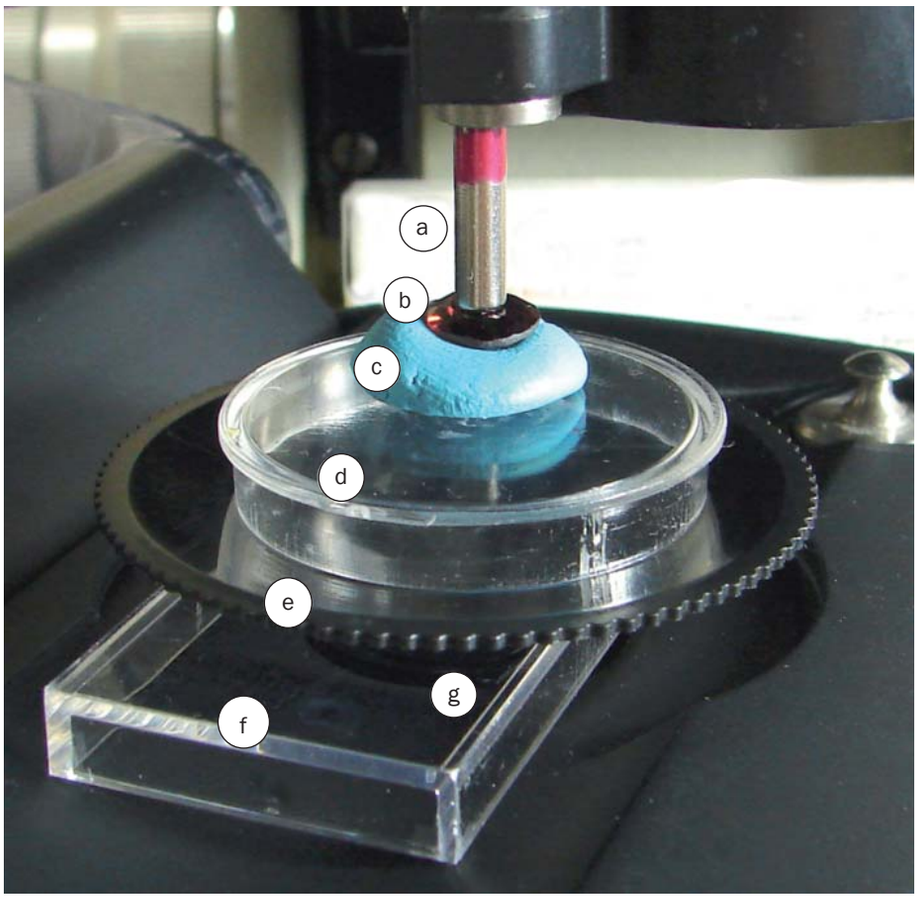

Figure 3 (right): Close-up of magnet and stone interface on scale. a) cylindrical NIB magnet; b) stone under test; c) Blu Tack ring support to hold the stone; d) non-magnetic stone support; e) scale measuring cup; f) bridge support – to avoid pressure on the scale while the stone table is made parallel to the magnet face; g) scale's active surface (underneath the bridge).

are continuing to investigate ways to improve the apparatus and technique, but believe that their present method is quite adequate for garnet characterization.

The current apparatus is a surplus biological microscope stand containing a fine focus mechanism, and an x-y translation stage for centring the gem table with the magnet face. In place of the microscope optics is a plastic fitting with a steel bolt at its centre, to which a cylindrical magnet of whatever size needed may be placed. This holds the magnet in a fixed, stable, and rigid position. The fine focus knob raises and lowers the microscope stage by micrometres, with a macro knob for larger adjustments.

For measuring the force of the magnetic attraction, a small digital scale was placed on the microscope stage. We used a GemOro PCT50 scale, but any similar scale that measures to 0.005 ct should work. The gem is placed on a non-magnetic pedestal, table up, and held in place with Blu Tack, then placed within the scale's measuring cup. A number of precautions need to be observed in order to obtain accurate and reproducible measurements. First, the magnet and gem table must be absolutely clean and free of all grease, dirt and dust. An antistatic brush will help prevent static electricity from affecting measurements, as well as aid in the removal of charged dust, especially in cold climates. One needs to regularly check the magnet pole surface, as these very strong magnets tend to acquire minute specks of magnetic particles, which must be removed before measuring.

Once these precautions are satisfied, it is critical to make the magnet pole surface and the gem's table exactly parallel. This is done by placing the gem within a bit of Blu Tack so that it is held in place along the girdle. A rigid bridge consisting of a 1/8 inch plastic sheet measuring 1 by 2 inches

Magnetic susceptibility, a better approach to defining garnets

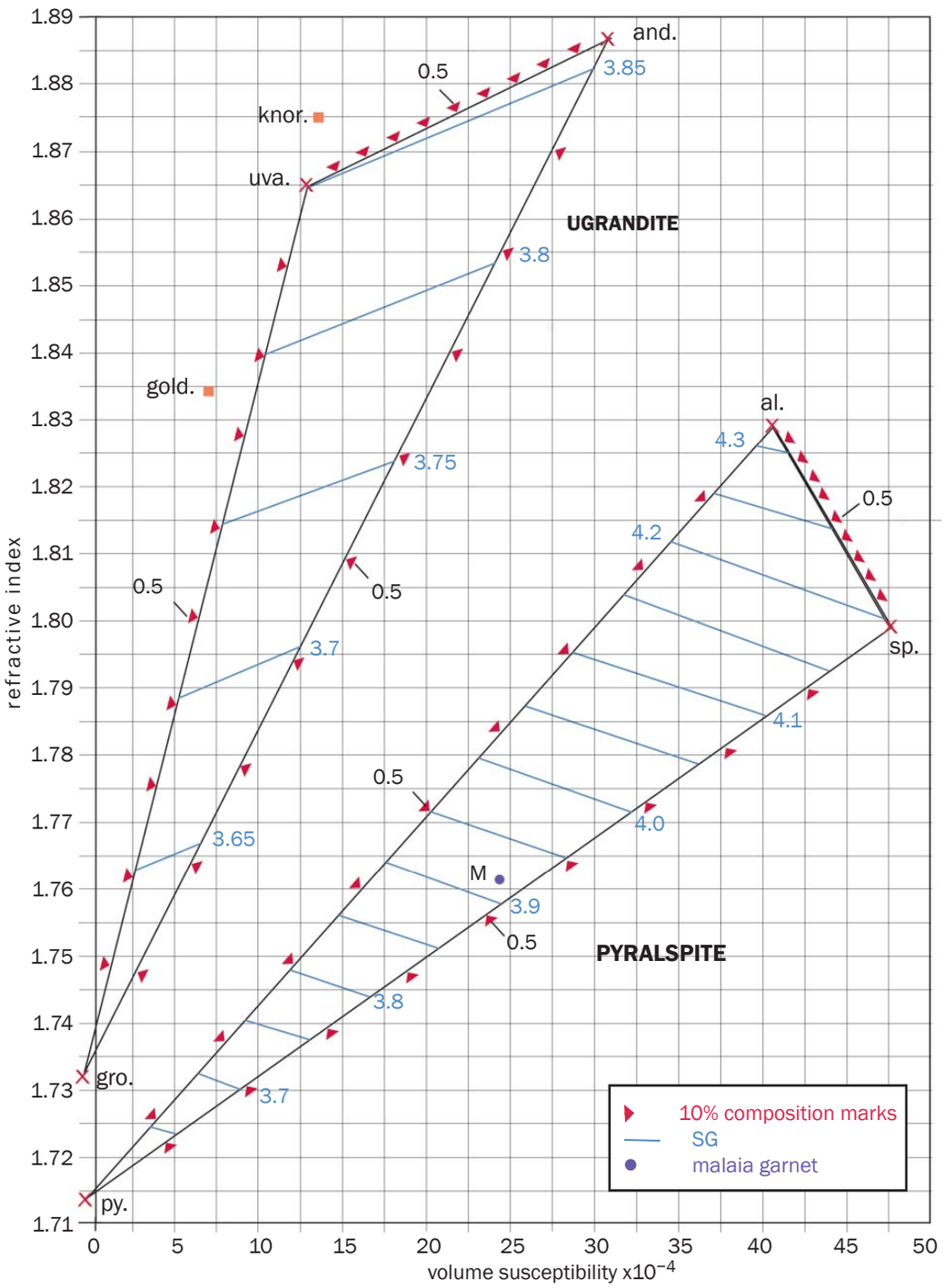

Figure 4: Plot of RI versus magnetic susceptibility for the garnet end-members pyrope, almandine, spessartine, grossular, andradite, uvarovite, goldmanite and knorringite. The pyralspite and ugrandite ternary triangles are shown with 10% triangles (red) shown along sides, and SG variations (blue) within each ternary. The purple data point (M) in the middle of the pyralspite ternary is that of a malaia garnet we measured.

is placed above the scale's recessed active surface and the measuring cup placed on this bridge. This then permits the magnet and gem table to be brought in contact and pressure put on the interface, so as to push the gem into the Blu Tack and align the two surfaces exactly parallel. With the bridge in place, the magnet is separated a millimetre or less from the gem table, and the surfaces viewed from two directions, at about 90 degrees difference, to be sure that they are parallel. Once the surfaces are parallel, the microscope stage is lowered, the bridge removed, and the measuring cup placed back on the scale. Again, check that the table and magnet face are parallel. In practice, we have had little problem in parallelism after the bridge is removed if care is taken. Next, the magnet and gem are separated by several centimetres, and the scale is turned on and tared. Then the microscope stage is gradually brought up to meet the magnet, and the maximum attraction measured. A magnetic attraction will show as a negative reading. Upon contact of the magnet with the gem, the scale reading will go in a positive direction. The maximum negative reading is the 'pull'. This number is then converted to k, using the formula (1).

A diamagnetic gem will give a very small positive measurement, due to the 'push' or repulsion of the stone by the magnet. For a 1/8-inch magnet, this will typically be about 0.02 ct.

As more individuals try their hand at such measurements there undoubtedly will be better methods developed for their implementation. At present, this method gives the best results for us.

Results

A ternary diagram, sometimes called a triangular plot, is a simple graphical tool to show chemical compositions in a three-component system. The diagram is an equilateral triangle where 100% of a component is plotted at each triangle point. Zero percent of that component would be at the opposite side and the centre point of the triangle would represent 33.3% of each. They are often used to determine garnet composition, and have been described and used in the papers by Manson and Stockton[1,2,3,4,5]. The pyralspite and ugrandite groups are examples, but if other garnet end-members are important in a garnet, additional diagrams are needed. For the five principal garnet end-members, grossular, andradite, pyrope, almandine and spessartine, ten ternary diagrams would be required to cover all possibilities for three major components[14]. Where four components are involved it becomes a bit more complex, but details can be found in Hutchison[17] (p.374 *et seq.*).

Because many physical properties of minerals have been shown to be approximately linear functions of the proportions of their components, the ternary diagrams can also show the variation of a physical property (P) with chemistry within the triangle[14,17], summarized in the following equation:

Equation 2

$P=\Sigma\ p_i m_i = p_1 m_1 + p_2 m_2 + p_3 m_3 \ldots$

where p_i = the property of the ith end-member such as RI, and m_i = the mole percent of that end-member in the composition.

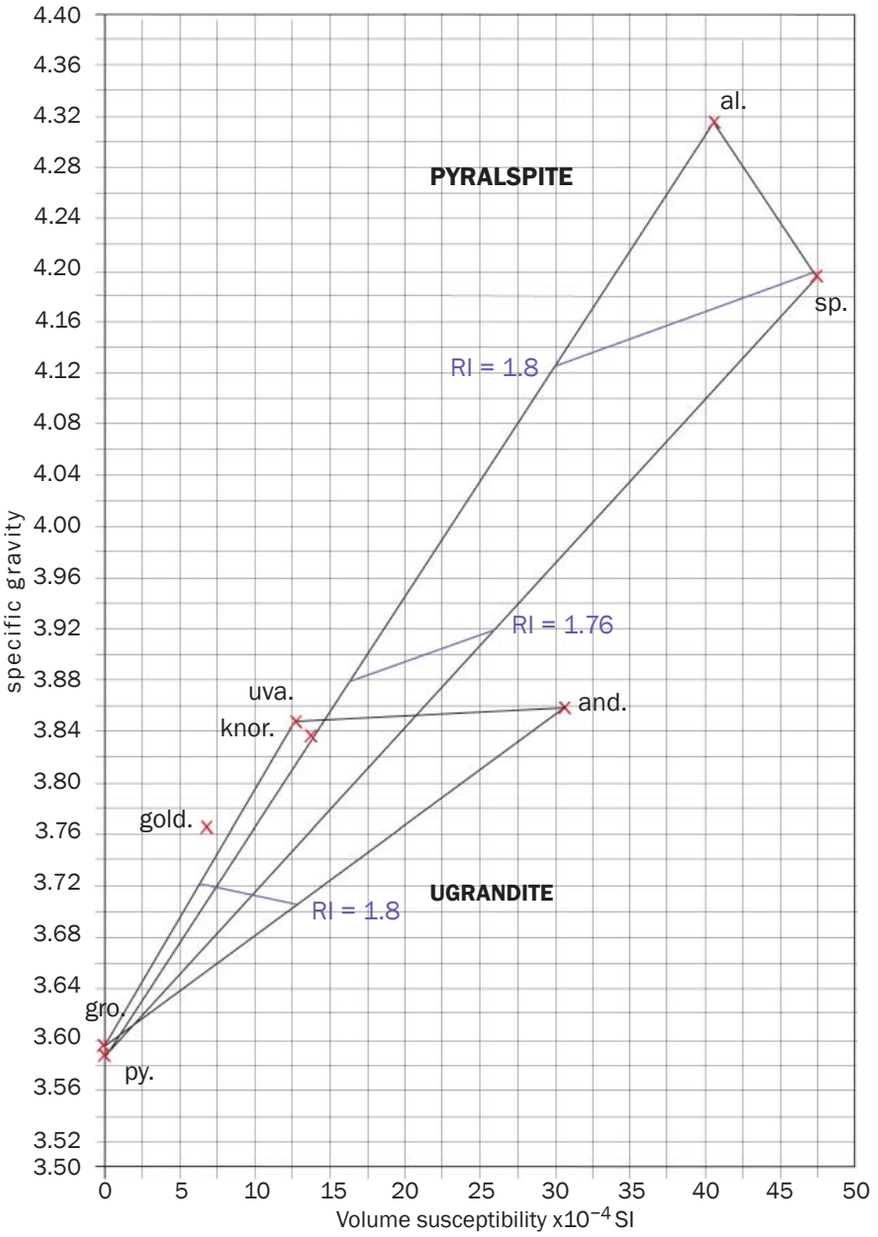

Figure 5: Plot of SG versus magnetic susceptibility for the garnet end-members pyrope, almandine, spessartine, grossular, andradite, uvarovite, goldmanite and knorringite. The pyralspite and ugrandite ternary triangles are shown with reddish purple lines indicating lines of constant RI.

Because we wish to distinguish between the various garnets, the statement by Deer *et al.*[12] (p.497) on the subject is worth reviewing: "Within the garnet group the various species are best distinguished by their RIs, SGs and cell edges in conjunction, if possible, with partial chemical data, e.g. for FeO or MnO. The entry of even small amounts of the uvarovite molecule to the ugrandite series imparts an emerald-green colour in hand specimen; chrome-pyrope is usually reddish but some show a green hue."

Because most gemmologists are not normally able to measure the cell edge dimension of a garnet, we will substitute the value of magnetic susceptibility for this, and plot RI against magnetic susceptibility. This provides information on the FeO and MnO that Winchell[14] called for.

Proposed new garnet characterization technique

In order to effectively use the plot in *Figures 4* and *5*, one needs to understand how the values of each end-member garnet are shown. The gemmological properties of RI and SG, for the eight

Magnetic susceptibility, a better approach to defining garnets

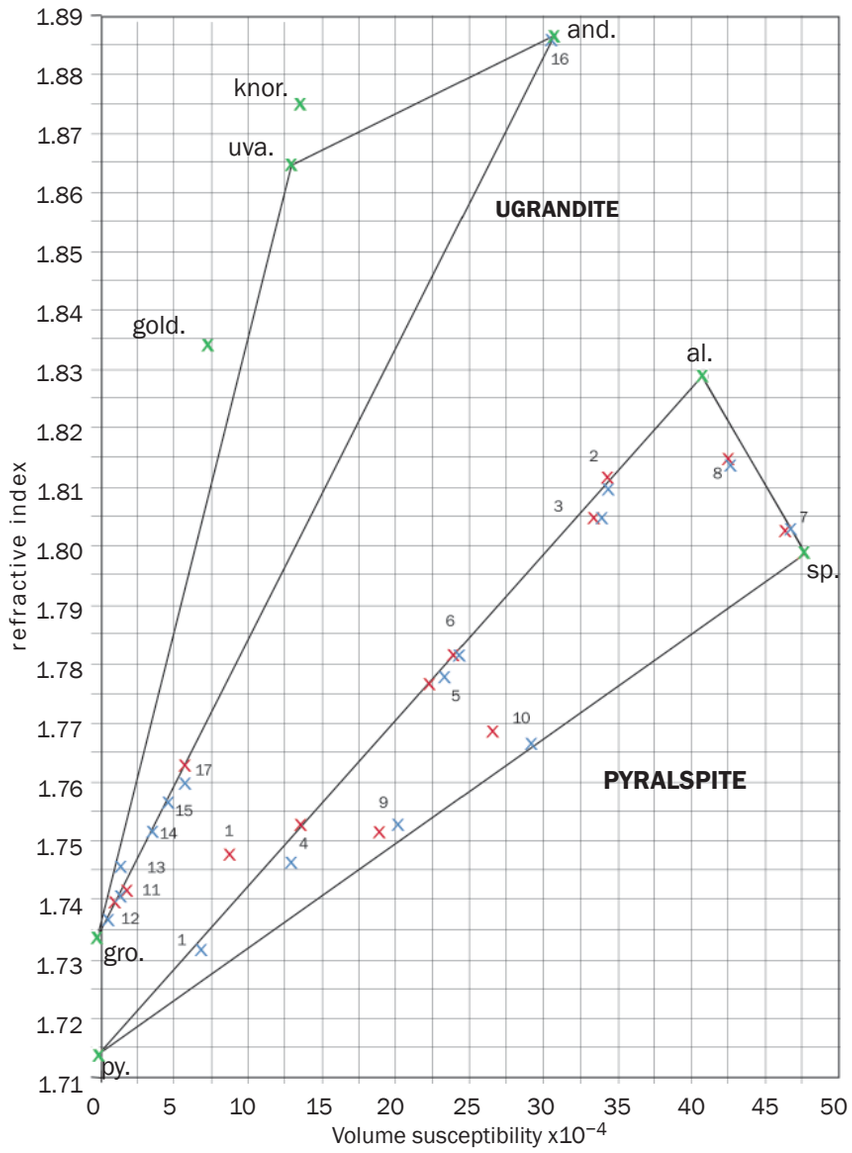

Figure 6: Plot of RI versus magnetic susceptibility for the garnet end-member data of Adamo et al.[7] *Red crosses are calculated for all end-members found, blue crosses are for the three main end-members of each series.*

end-member garnets we will consider, are taken from the mineralogical literature[12,18]. The values for their magnetic susceptibilities have been calculated based on 'ideal chemistry' as shown in *Table I* and mean measured moments from *Table II* by use of the Langevin equation[15].

Figure 4 illustrates the basic plot used, with RI on the Y-axis and magnetic susceptibility (k) on the X-axis. Of the eight principal garnet end-members plotted, the commonest six are joined to demonstrate the ternary diagrams. These are the pyralspite and ugrandite triangles (which are no longer equilateral) with the end-member abbreviations shown at each corner. Small red triangles along each side mark 10% intervals, with the 50% position labelled (0.5). Blue lines and numbers mark SG values, assuming only pyralspite or ugrandite components are present.

As can be seen in *Figure 4*, if one has a pyralspite garnet with no other garnet components, then it must plot within the pyralspite triangle, but if a measured garnet is within the triangle, how does one determine what its pyralspite composition is? Consider a malaia garnet that we measured with an RI of 1.762, and susceptibility of 24.1 × 10^{-4}SI. This is plotted in *Figure 4* as a purple spot (M). From its position in the triangle, it is apparent that this garnet is a pyrope-spessartine-almandine. First, one prints the illustration to a piece of paper so that lines can be drawn and measured. Additionally, this is available for downloading from one of the author's websites (www.stonegrouplabs.com go to 'Articles and Papers', then 'Garnet Chart'). The scale of the printout is irrelevant. From each apex of the pyralspite ternary, draw lines through the data point (the purple dot). Next, measure the length of the line between the pyrope apex to the opposite base, and the length between this base and the data point. When we did this, the measurements were 163 mm and 77.5 mm. The ratio 77.5/163 = 47.5 is the proportion of pyrope in the garnet. Doing this for the other components, we find 42% spessartine, and 11% almandine. These total 100.5% when added, showing minor graphical measurement error, but still a far more accurate idea of the components than would otherwise be known. This malaia garnet would be described as approximately $Py_{47}Sp_{42}Al_{11}$. The precision of all measurements is important to accurately define the chemistry. Based on our repeat measurements we estimate that RI should be within +/- .001 and susceptibility about +/- 1 × 10^{-4} SI. Thus, the error bars are of similar magnitude on the graphs for the scales used, suggesting that each property measurement contributes to a similar error in chemistry.

Note that it only requires values of RI and k to be able to specify the three pyralspite components. A value of the SG, if accurate, would be able to confirm the composition, or if accurate and not in agreement would indicate the presence of one or more additional end-members.

With this understanding, it should be clear that if we take the malaia garnet and add a little andradite, but keep the pyralspite components balanced, the data point would move up in RI, with very little change in susceptibility. Adding a little grossular would pull the point down and to the left. In this figure, for clarity we have shown only the two principal garnet ternary diagrams, but clearly one could draw in all the others. Other results presented below from pyropes and almandines plot within the grossular-

pyrope-almandine triangle, indicating that these garnets most likely contain a measurable grossular component.

These can be computed in a similar manner to pyralspites or ugrandites, by closing the lines for the relevant triangle — grossular, pyrope and almandine.

We want to emphasize that the only change that we are making to long-used mineralogical techniques[14] is the substitution of magnetic susceptibility for unit cell length.

Another way to present the RI, SG, and k data is shown in *Figure 5*, which has SG on the Y-axis and magnetic susceptibility on the X-axis, giving additional insights into property variations. *Figure 5* shows that there is an overlap between the pyralspite and ugrandite groups below an SG of 3.86. The violet lines in each group mark lines of constant RI. The diagram clearly shows there is complete separation between the two groups for indices above 1.80. This is particularly important for the identification of garnets whose RI is above 1.80, where most gemmologists cannot obtain measurements. Thus, SG can be substituted for RI using this new technique. As *Figure 5* shows, andradite, almandine and spessartine can be distinguished on the SG-susceptibility chart at the higher RIs.

Using *Figure 4* as the basic diagram and by taking published compositions from the literature, we can now calculate what their RIs, magnetic susceptibilities and SGs should be. This can be done using as many end-member components as we have values for. However, in using such chemical data, one needs to be aware of the problems of calculating end-member molecules from chemical analyses as noted by Deer *et al.*[12] Conversely, we can estimate what the compositions could be, based on the measured values of the properties, for each three-component system if we have two properties, or for four-component systems if we have values of RI, susceptibility and SG. In many cases, there will be more than one combination of end-members that can fit a given physical property set. It is up to the gemmologist to choose which possibility is most probable. We believe this new technique for indirect determination of garnet chemistry, permitting better characterization of the garnet group, is a major step forward in gemmology.

Table III: Comparison of measured and calculated properties of selected garnets from Adamo et al., *2007.*

Specimen number	Property	Measured	Calculated on basis of		Composition
			All end members	Three main end members	
1	RI	1.741	1.748	1.732	$Py_{75}Al_{14}Sp_{0.7}An_{8.3}Uv_{1.7}$
	SG	3.68	3.719	3.704	
	Susc. #		8.79	6.69	
2	RI	>1.79	1.812	1.81	$Py_{15}Al_{81}Sp_{1.1}An_{2.3}$
	SG	4.19	4.190	4.196	
	Susc. #		34.20	34.27	
7	RI	>1.79	1.803	1.803	$Py_{.04}Al_{12}Sp_{87}Gr_{0.4}An_{0.6}$
	SG	4.13	4.207	4.212	
	Susc. #		46.34	46.62	
10	RI	1.775	1.769	1.767	$Py_{34}Al_{1.1}Sp_{54}Gr_{5.4}Uv_{1.0}Go_{3.6}$
	SG	4.00	3.935	3.963	
	Susc. #		26.53	29.11	
11	RI	1.738	1.742	1.741	$Uv_{.05}Gr_{93}An_{5.1}Py_{1.4}Sp_{0.7}$
	SG	3.59	3.612	3.607	
	Susc. #		1.70	1.35	
12	RI	1.741	1.740	1.737	$Uv_{1.1}Gr_{91}An_{.05}Py_{2.1}Sp_{1.5}Go_{3.7}$
	S.G	3.62	3.612	3.600	
	Susc.		0.94	0.45	
16	RI	>1.79	1.886	1.886	$An_{99.2}Py_{0.7}Al_{0.06}Sp_{0.04}$
	SG	3.88	3.857	3.857	
	Susc.		30.55	30.56	
17	RI	1.766	1.763	1.760	$Uv_{0.1}Gr_{78}An_{19}Py_{2.8}Sp_{0.2}$
	S.G	3.66	3.645	3.680	
	Susc.		5.76	5.68	

NB: Calculation based on equation (2)
Magnetic susceptibility all × 10^{-4} SI

Determination of properties from chemistry

As an example of using compositions to determine properties, we have plotted on *Figure 6* RI and susceptibility data calculated for the pyrope and ugrandite garnets of Adamo *et al.*[7] using equation (2). Values in red are derived using all the end-member compositions given by Adamo *et al.*, while those in blue are for only the three main components of either the pyralspite or ugrandite subgroups, and normalized to 100%, much as Manson and Stockton[5] have done. The numbers on each data point correspond to those of Adamo *et al.*[7] The end-member garnets *(Table I)* are indicated by green crosses and labelled. The pairs of red and blue crosses, generally, are fairly close. In *Table III* is a selection comparing these calculated values against measured values given by Adamo *et al.* The analyses of the ten pyralspites showed seven end-members present, but no individual specimen with all seven. Four to six end-members were found between these pyralspites, with half needing only

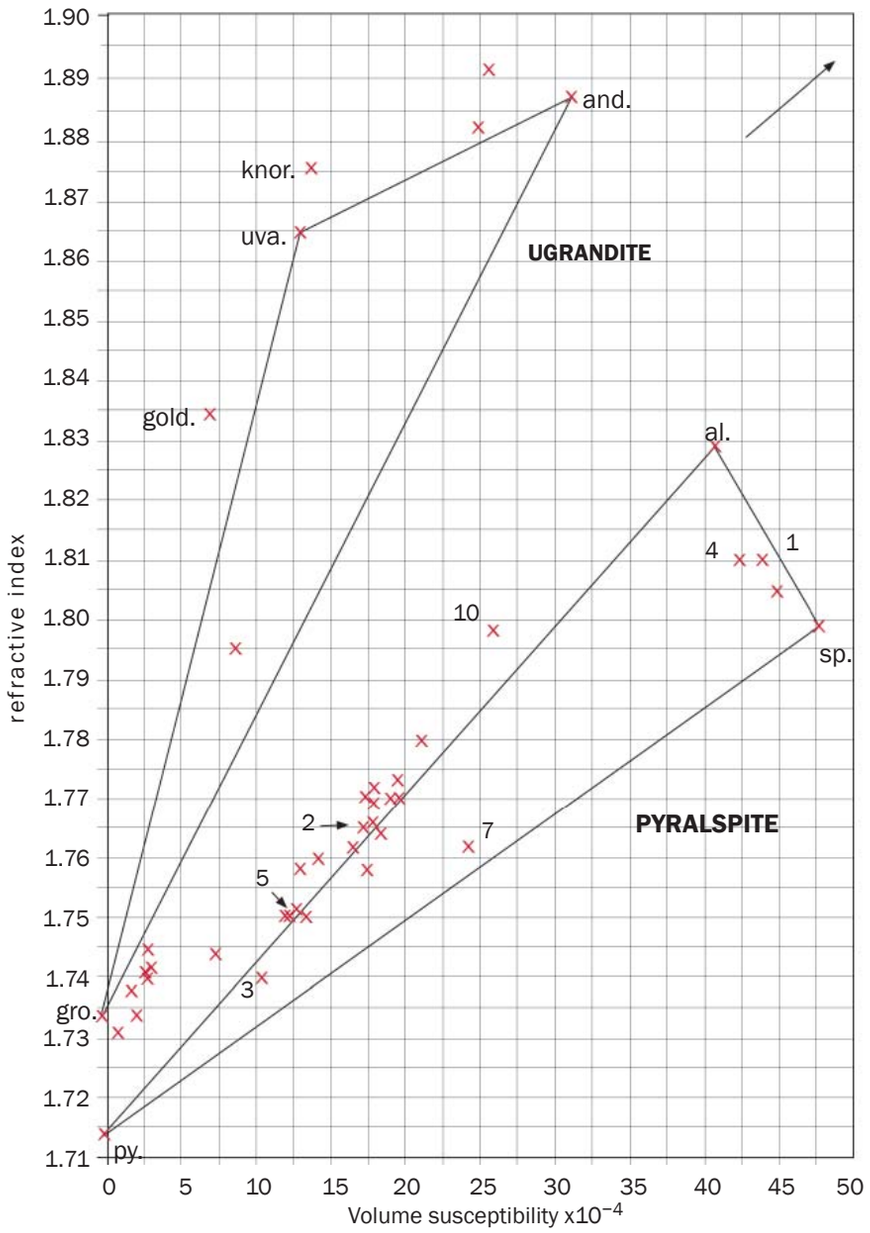

Figure 7: Plot of RI versus magnetic susceptibility for a series of garnets measured by the authors. The pyralspite and ugrandite ternary triangles are shown.

four end-members to describe them. Grossular and andradite were the largest non-pyralspite components found. The chrome pyrope, specimen 1 of Adamo's list *(Figure 6)*, shows the greatest divergence between values based on the pyralspite component (blue cross within the pyralspite ternary diagram) versus complete chemistry. This stone had 8.3% andradite, and 1.7% uvarovite mixed with pyrope, almandine and spessartine components. The shift in graph position is toward the uvarovite-andradite positions, as would be expected. The other specimens in this series, 2–10, had 2.3%, 1.6%, 4.01%, 5.04%, 1.25%, 0.98%, 0.8%, 6.1%, and 10% non-pyralspite components respectively.

In the ugrandite group specimens (*Table III* and *Figure 6*), the data show the grossular garnets stretched out on the grossular-andradite join up to about 20% andradite (specimen 17). This is a similar pattern to that found by Manson and Stockton[2]. Some of the red crosses do not show because of overlap with the blue ones. In *Table III* the measured and calculated property values of a selection of the ugrandites can be compared. One andradite (16) is essentially pure and this is typical, as most natural andradites are compositionally close to the end-member[12].

The distribution of points in *Figure 6* shows that for these gem garnets, measurements of the RI and susceptibility correlate with the chemical composition rather well, remembering that the red crosses represent the practical measurements. Chrome pyrope, the garnet with the widest spread between red and blue values (specimen 1), shows that it can't be well characterized as a pure pyralspite and that some additional component needs to be considered, such as andradite or uvarovite.

The data of Adamo *et al.,* although far fewer in number, illustrate what Manson and Stockton[1,2,4,] and Stockton and Manson[3,5] found: in general, gem andradite and grossular fall close to their respective end-members in the ugrandite ternary diagram; gem almandine and pyrope fall along the pyrope-almandine line with little spessartine present; and similarly for the almandine-spessartine group. The malaia (specimen 9) and colour-change (specimen 10) pyralspite garnets are mainly spessartine-pyrope with minor almandine. These values, we believe, are well correlated, including those for SG.

Estimation of chemistry from properties

For gemmologists, the most practical and quick means of determining the composition of a garnet is through magnetic susceptibility. We have measured the RI and susceptibility of 39 gem garnets from worldwide sources and the results are given in *Table IV* and *Figure 7*. Grossulars plot close to the end-member, as do the andradites. In the pyralspite group, most almandine-pyropes show little evidence of a spessartine component, and the almandine-spessartines show little pyrope. It is only the malaia garnets that have a strong mix of all three end-members. In *Figure 7* the RIs of stones below 1.79 were measured with a conventional, critical angle refractometer. Those with RI over 1.79 were measured with a deviation angle refractometer, built by one of the authors (D.H.), making use of a laser pointer light source. The accuracy of this device is estimated at +/-

Absorption spectra and chemistry

A thorough investigation of the use of absorption spectra to determine garnet species would require another paper; so to indicate the diagnostic limitations of this method, only a few features of the pyralspite series will be discussed. In the pyralspite garnets, it is the Mg^{2+}, Mn^{2+} and Fe^{2+} contents that determine the species. This gives us three choices when looking at a pyralspite spectrum, if, for the moment, trace elements are neglected, there is either an Fe^{2+} spectrum, a Mn^{2+} spectrum, or both. Stockton and Manson[5] rely on the presence of the 410 and 430 nm Mn lines to indicate if any Mn is present. Rossman[19] (p.218) notes: "Only the sharp 410 nm band is seen in the spectrum of many minerals with minor amounts of Mn^{2+} in the presence of greater quantities of Fe^{2+}." This raises the question of whether Mn lines in many garnets can be identified with the hand spectroscope, as these weak lines are commonly hidden in the obscurity of the blue end of the spectrum. Pearson[20] also discusses the poor sensitivity at each end of the visible spectrum of the human eye and its limitations for identification of absorption lines in the blue to violet when using a hand spectroscope.

Figures 8a and *8b* show pairs of similar spectra from garnets we have measured (specimens 1, 2 and 3, 4) in *Figure 7*. These transmission spectra were run on an Ocean Optics S2000 Spectrophotometer. The classic almandine absorption lines at about 505, 526 and 576 nm are present in all.

In *Figure 8a* the spectra of specimens 1 (spessartine) and 2 (pyrope) appear nearly identical. In the region between 400 and 500 nm, note that the 410 and 430 nm absorption lines used by gemmologists to identify Mn^{2+} (5) are not present. This was confirmed with the hand spectroscope, where only a cut-off at approximately 440 nm was observed. The 575 line was most apparent, the 505 was relatively strong,

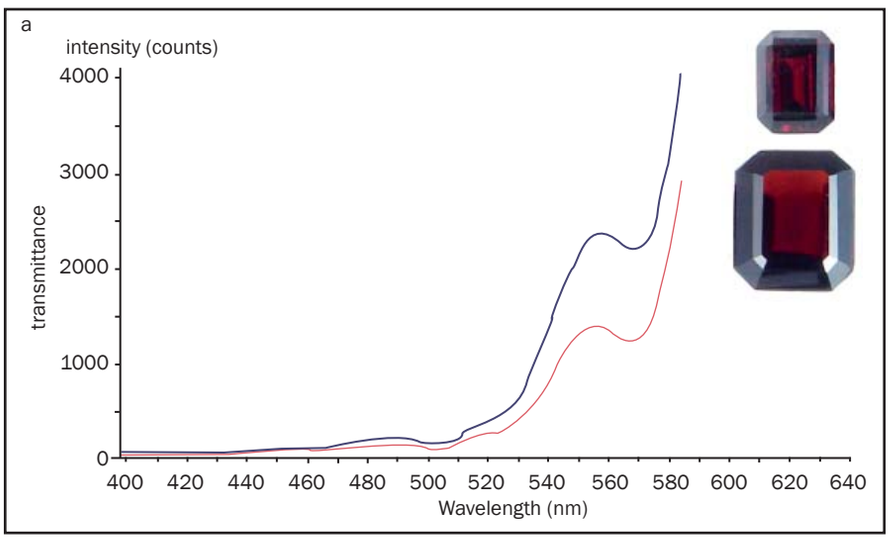

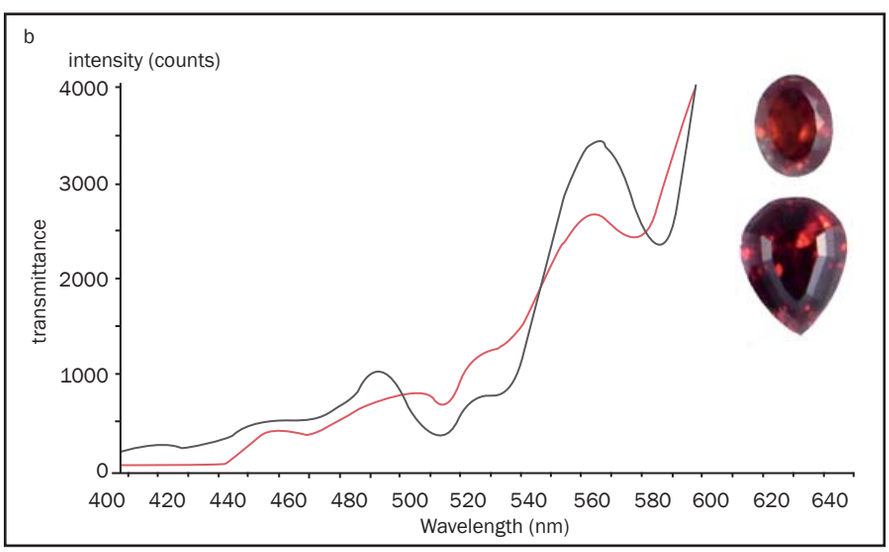

Figures 8a and b: Graphs of transmission spectra for the four pictured garnets, showing similarities between pyrope and spessartine spectra. a) Red line is a 2.24 ct spessartine (no. 1); black line is a 4.19 ct pyrope (no. 2); b) Red line is a 1.61 ct oval spessartine (no. 4); black line is a 4.73 ct pyrope (no. 3).

and the 526 line could be seen by only one of the authors. No characteristic manganese lines could be seen.

In *Figure 8b* there are some small differences in spectra of specimens 3 (pyrope) and 4 (spessartine), especially a shift in the two troughs (absorptions) near 575 nm between the two spectra. The almandine lines are clearly prominent. The cut-off in the blue is near 430 nm, with no evidence of manganese lines at either 410 or 430 nm. There is also a weak absorption near 460 nm, but this is not recognized as a strong Mn line. There are no Mn lines visible with the hand spectroscope. With the hand spectroscope, the authors observed only iron lines at 510 and 575, with a cut-off at approximately 430 for the 1.61 ct oval (red curve). The 526 line seen in *8b* could not be distinguished with the hand spectroscope. For the 4.74 ct pear shape, two authors observed a cut-off at 400 and 430 nm, strong lines at 575 nm, a good line at 505 nm, and a weak line at 526 nm. In each of these sets, one stone is near the almandine-spessartine boundary with little pyrope, and the other primarily pyrope *(Figure 7)*. Yet all stones have very similar colours.

Table IV: Magnetic susceptibility and other properties of the garnets measured in this study.

No.	Species or variety	Weight ct.	Locality	Colour	RI	k × 10^{-4}
1	spessartine	2.24	?	deep red	1.810	43.8
5	pyrope	3.42	Mozambique?	red	1.751	12.5
7	malaia	2.78	E. Africa	orange	1.762	24.1
10	almandine	2.57	India	deep red	1.798	25.8
14	tsavorite	2.54	E. Africa	medium bright green	1.731	0.69
15	demantoid	1.25	Russia	green	1.892	25.5
24	hessonite	3.73	Sri Lanka?	orange	1.741	2.54
25	'uvarovite'	17.97	Cab, S. Africa	fine deep green	1.795	8.53
28	rhodolite	1.55	Tocantins, Brazil	purple	1.77	17.2
29	rhodolite	7.75	unknown	purple-red	1.773	19.3

0.004 and because the laser wavelength is 680 nm, the RI values were corrected for dispersion.

From the data given in *Figure 7*, it is apparent that these garnets can easily be separated into pyralspite or ugrandite groups based on RI and susceptibility values. If there is any question, SG should assist, due to the large density gradient between the two groups (*Figures 4* and *5*). Of greater importance is the power this gives us in identifying the chemistry of a particular gem within the pyralspite or ugrandite groups. As an example, look at the garnet labelled 5 in *Figure 7*. This 3.42 ct stone is on the almandine-pyrope line, so can be specified as approximately $Py_{68}Al_{32}$ with an RI of 1.751 and susceptibility of 12.5 × 10^{-4}SI. Of course, a mix of other different garnet end-members could be devised to give the same physical properties, but this is the simplest. This stone was sold as a Mozambique spessartine many years ago, but our data indicate clearly that it is predominantly pyrope. In colour, it is close to the other three adjacent pyropes.

The malaia garnet labelled 7 is an example where three end-members are present (see also M in *Figure 4*). It is approximately $Py_{47}Sp_{42}Al_{11}$, compared to the malaia measured by Adamo *et al.*[7] (no. 9 in *Figure 6*), which was $Py_{52.7}Sp_{33.6}Al_{7.5}Gr_{6.1}$. The garnet labelled 10 was purchased as an Indian almandine, but it falls above the almandine-grossular join, so must have some andradite or chrome garnet component. A clue to its probable composition is provided by Deer *et al.*[12] in the composition of one Indian garnet from Madras, which is $Al_{61.4}Py_{30.8}An_{5.9}Sp_{1.4}Gr_{0.5}$. This composition gives a calculated RI of 1.796 and susceptibility of 27.4 × 10^{-4}, remarkably close to that of the measured Indian almandine (1.798, 25.8). If one calculates the composition from its position in the pyrope-almandine andradite ternary diagram, one obtains a composition of $Al_{62}Py_{30}An_{8}$. This, we believe, is a good example of what can be done with this new technique.

Discussion

By plotting pairs of RI and susceptibility values for garnets as shown in *Figure 4* and following, one can directly define a garnet's chemistry based on the composition of any three selected end-member molecules. Because it has been found that 99% of most garnet compositions can be described by a combination of the five common garnet end-members[5,12], the probable compositions of any tested garnet are quite restricted.

Additionally, by plotting RI and magnetic susceptibility, the pyralspite and ugrandite series' ternary triangles are quite separate and do not overlap[12,14]. Clearly, a stone lying in the pyralspite ternary area will have a limited amount of any ugrandite component that could be present in order to fit measured physical properties.

The measurements of 39 stones plotted in *Figure 7* reveal variations in gem garnet chemistry that were not obvious from previous gemmological work[5,6,7,10]. Looking at the pyrope to almandines near the line (join) between the pyrope and almandine end-members, it is clear that most of these have some measurable component from the ugrandite series garnets. This is evident by their plotting at higher RI values than the line along the join. If one looks at garnet chemistry given for example in Deer *et al.*[12] for pyrope, chrome-pyrope, and almandine, most analyses show a significant ugrandite component (or knorringite, in some stones) with one of these being the second largest component. This had been reported by Rouse[10], but not emphasized. Our data show that this is rather common in gem garnets, and needs to be considered when discussing variations in garnet properties.

Further research and testing of this new method is called for in order to confirm results from this method with measured chemistry on more stones. The current method is good for identifying the chemistry in terms of three end-members. To combine SG measurements with the current information will increase its complexity, but could more accurately define the chemistry in terms of four end-members. For example, grossular and spessartine components in a stone can balance each other out, hiding evidence of both, as has been observed in some rhodolites.

The authors have presented a means for quantitatively measuring the magnetic susceptibility of cut gemstones as an aid in characterizing their end-member chemistry. In fact, any rough material need only have one polished surface to enable testing by this method. The simplicity of the method makes it ideal for field-testing new finds of garnet.

It is recognized that trade and varietal names of garnet will continue to be used for commercial purposes. However, for gemmological purposes, we believe it would be better to describe the actual end-member chemistry of a garnet derived using this new method. The technique overcomes the present RI and SG limitations as garnet identification methods. Further, it will allow new varieties to be easily defined in the garnet continuum with less confusion about their composition.

Acknowledgements

The authors would like to thank colleagues in the trade, too numerous to name, for frank discussions of garnet characterization, identification and nomenclature. Particular thanks go to Sylvia Gumpesberger for her persistence in pushing us to examine, in a quantitative sense, what magnetic measurements might do to advance the science of gemmology. We wish to thank Grant Pearson for in-depth discussion of eye-visible gem spectra. We are also indebted to the late Professor N. Haralyi whose early magnetic work first caught our attention, and finally, our appreciation to an anonymous reviewer whose suggestions considerably improved the paper.

References

1. Manson, D.V., and Stockton, C.M., 1981. Gem garnets in the red-to-violet color range. *Gems & Gemology,* **17**(4), 191-204
2. Manson, D.V., and Stockton, C.M., 1982. Gem-quality grossular garnets. *Gems & Gemology*, **18**(4), 204-13
3. Stockton, C.M., and Manson, D.V., 1982. Gem garnets: the orange to red-orange color range. International Gemological Symposium Proceedings, Gemological Institute of America, Santa Monica, CA
4. Manson, D.V., and Stockton, C.M., 1984. Pyrope-spessartine garnets with unusual color behaviour. *Gems & Gemology,* **20**(4), 200-7
5. Stockton, C.M., and Manson, D.V., 1985. A proposed new classification for gem-quality garnets. *Gems & Gemology,* **21**(4), 205-18
6. Johnson, M.L., Boehm, E., Krupp, H., Zang, J.W., and Kammerling, R.C., 1995. Gem-quality grossular-andradite: a new garnet from Mali. *Gems & Gemology*, **31**(3), 52-67
7. Adamo, I., Pavese, A., Prosperi, L., Diella, V., and Ajò, D., 2007. Gem-quality garnets: correlations between gemmological properties, chemical composition and infrared spectroscopy. *Journal of Gemmology,* **30**(5/6), 307-19
8. Rouse, J.D., 1986. *Garnet*. Butterworths & Co., London, 134 pp
9. Hoover, D.B., and Williams, B., 2007. Magnetic susceptibility for gemstone discrimination. *Australian Gemmologist,* **23**(4), 146-59
10. Rouse, J.D., 1994. The Garnets. In: Webster, R., revised by Read, P.G., *Gems, their sources, descriptions and identification,* 5th edn. Butterworth-Heineman, Oxford, 191-206
11. Arem, J., 1987, *Color encyclopedia of gemstones*. 2nd edn. Van Nostrand, New York, 248 pp
12. Deer, W.A., Howie, R.A., and Zussman, J., 1982. *Rock-Forming Minerals. V.1A 2nd edn, Orthosilicates*. Longman, London, 919 pp
13. Sriramadas, A., 1957. Diagrams for the correlation of unit cell edges and refractive indices with the chemical composition of garnets. *American Mineralogist,* **42**(3/4), 294-8
14. Winchell, H., 1958. The composition and physical properties of garnet. *American Mineralogist,* **42**(5/6), 595-600
15. Kittel, C., 1956. *Introduction to solid state physics*. 2nd edn. J. Wiley, New York, 617 pp
16. Larsen, E.S., and Berman, H., 1934. The microscopic determination of the non-opaque minerals. *U.S. Geological Survey Bulletin 848,* 2nd edn, 266 p
17. Hutchison, C.S., 1974. *Laboratory handbook of petrographic techniques*. J. Wiley & Sons, New York, 527 pp
18. Meagher, E.P., 1982. Silicate garnets. In: Ribbe, P.H. (Ed.), *Reviews in Mineralogy, 5, Orthosilicates,* 2nd edn., 25-66. Min. Soc. America, Washington DC
19. Rossman, G.R., 1988. Optical spectroscopy. In: Hawthorne, F.C. (Ed.), *Reviews in Mineralogy, 18, Spectroscopic methods in mineralogy and geology,* 207-54. Min. Soc. America, Washington DC
20. Pearson, G., 2003. Spectra of gem materials. *Australian Gemmologist,* **21**(12), 478-85

The Author

D. B. Hoover
Stone Group Labs, Springfield, Missouri, USA. e-mail dbhoover@aol.com
C. Williams
Bear Essentials, Jefferson City, Missouri, USA. email cara@stonegrouplabs.com
B. Williams
Bear Essentials and Stone Group labs, Jefferson City, Missouri, USA. email bear@stonegrouplabs.com
C. Mitchell
Gem-A, London. email claire.mitchell@gem-a.com

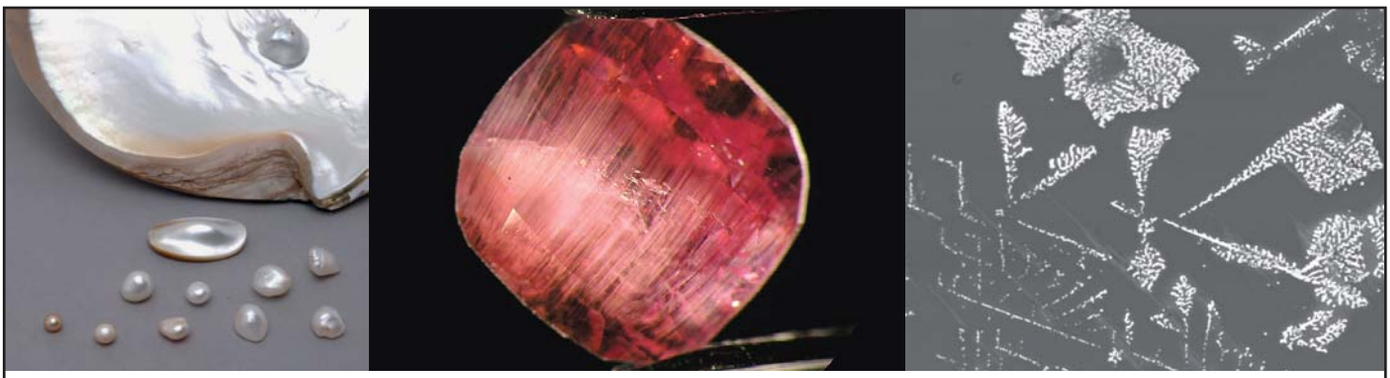

2009 EUROPEAN GEMMOLOGICAL SYMPOSIUM

Organized by the Swiss Gemmological Society SGG/SSG

Friday 5 June to Sunday 7 June 2009

Berne, Switzerland

The Swiss Gemmological Society is proud to invite all interested gemmologists to the 2009 European Gemmological Symposium.

Programme: Speakers will present a range of topics on diamonds, coloured stones, pearls and the jewellery trade, highlighting both the history of gemmology and state-of-the-art gemmological research.

Keynote Speakers: *Sir Gabi Tolkowsky and Martin Rapaport*

Further speakers include: *Maggie Campbell Pedersen, Laurent Cartier, Jean-Pierre Chalain, Dr Eric Erel, Thomas Hainschwang, Vera Hammer, Prof. Dr Henry A. Hänni, Michael Hügi, Dr Michael S. Krzemnicki, Helen Molesworth, Andy Müller, Dr Daniel Nyfeler, Dr Jack Ogden, Vincent Pardieu and Roland Schlüssel*

Poster session: Details given at www.gemmologie.ch or email EGS.2009@gmail.com. Contributions welcome.

Additional events (participation optional):

- Welcome cocktail on the evening of Thursday 4 June and Symposium Dinner on Friday 5 June.
- A visit of the mineral collection of the Natural History Museum in Berne during the afternoon of Friday 5 June.
- An excursion to the famous crystal cave at Grimsel in the Swiss Alps on Sunday 7 June.

EGS
European Gemmological Symposium

To book: For details on the pricing, registration and how to book a hotel in Berne, please visit www.gemmologie.ch.

Gem-A Conference 2009

Saturday 17 and Sunday 18 October

The Hilton London Kensington

Pencil it in ...

The refraction of light by garnet depends on both composition and structure

David K. Teertstra

Abstract: The index of refraction *(n)*, used to identify minerals, depends on both composition and crystal structure. The method of optical analysis implies that a photon refracts by local interaction with individual ions. The index *n* is calculated exactly using a dependence of the specific refractivity of ions on the inter-ionic distances and angles of the crystal, and is influenced by bonds to surrounding ions up to half-a-unit-cell distant.

Keywords: crystal chemistry, crystal structure, garnet, index of refraction, optics, photon

Introduction

This paper deals with controversial aspects of light and its refraction in gems and minerals, and proposes a model to deal with them. In this model, for convenience, the particles have been called photons but it should be understood that these particles have some postulated properties that differ from those of the conventional photon of quantum theory. The photon is a probe of the crystal structure. The energy of the photon is constant; the photon remains intact and the wavelength is not reduced. The ions of each element have a specific electric structure and a characteristic contribution to the net index of refraction of the material. Accounting for the crystal structure, this new method of optical analysis also gives an accurate measure of composition.

What a gem looks like depends on its interaction with light, determined mainly by the processes of reflection, refraction and absorption. The optical properties of gems are essential to their identification. Measurements of refraction can be diagnostic, mainly because the index of refraction depends upon the composition and structure. Each measured index of refraction relates to a specific structure and state of cation order (Teertstra 2005, 2006). For a given structure-type (garnet is considered here, see *Table I*), a change of composition directly relates to a change in the optics, whereas for a fixed composition, polymorphs of minerals can be distinguished optically (e.g. kyanite, sillimanite, andalusite). That said, the relation between optical properties and composition has been precise only for pure binary or ternary series, as a theory relating optical properties to both composition and crystal structure is entirely absent.

A general theory, relating each compositional and structural state (as expressed by the structural formula of the mineral, e.g. $Mg_3Al_2Si_3O_{12}$ for pyrope) to the specific physical properties, has remained elusive. To make progress, one must understand both light and crystallography. Historically, for example, the evidence for X-rays as a high-energy form of light rather than a new type of particle was simultaneous with the evidence for the structure of minerals as ordered three-dimensional arrays of

Table I: Physical properties (n, a, D) of end-member silicate garnets.

Species	formula	n	a (nm)	$D_{calc.}$
Pyr – pyrope	$Mg_3Al_2Si_3O_{12}$	1.714	1.1459	3.5591
Alm – almandine	$Fe_3Al_2Si_3O_{12}$	1.830	1.1526	4.3184
Sps – spessartine	$Mn_3Al_2Si_3O_{12}$	1.800	1.1621	4.1902
Grs – grossular	$Ca_3Al_2Si_3O_{12}$	1.734	1.1851	3.5952
And – andradite	$Ca_3Fe^{+3}{}_2Si_3O_{12}$	1.889	1.2058	3.8507
Uvr – uvarovite	$Ca_3Cr_2Si_3O_{12}$	1.865	1.1996	3.8514
Gld – goldmanite	$Ca_3V_2Si_3O_{12}$	1.834	1.2070	3.7651

NB: *n* is refractive index; *a* is the unit cell edge; *D* is the density calculated from the unit cell.

©2008 Gemmological Association of Great Britain

atoms. From the equations of Bragg and Laue, and by using the scattering factors of ions, both the structure and composition of a crystal can be determined. In thin-sheet diffraction, light is reflected only at specific angles if the wavelength of light is similar to the distance between planar layers of atoms. However, the same information can be determined using the refraction data of a group of minerals, but using the refractivity factors of ions.

Although the photoelectric effect (now a subset of the theory of atomic absorption, in which an atomic-electric transition from a low-energy orbital to a high-energy orbital accompanies the absorption of a photon by an individual atom) indicated to Einstein that light is a local particle of similar size to an electron, the only model of light currently available results from the plane-wave solution to the Maxwell equations for electricity and magnetism. The model of light as an electromagnetic wave requires the energy to be spread out along the wavelength as well as across the wavefront, in conflict with the physical evidence for a finite local particle of light. In the theory presented here, for example, each ion has a specific refractivity and the net index of refraction is explained only if light consists of photons that interact locally with each ion.

The wave theory of light requires a homogeneous (or average) index of refraction for materials, but the mineralogical data indicate that the index of refraction (n) increases as the density (D) increases, so $n \propto D$, or $n = KD$. Such changes of n and D are due to substitutional exchange mechanisms such as Mg <–> Fe that are common to many minerals. By considering that each ion in a dielectric crystal has a characteristic optical refractivity (by virtue of the number of and density of electrons), a characteristic radius (by virtue of the atomic-electric structure) and a characteristic atomic weight (by virtue of the number of protons and neutrons), the net values of n and D calculated as a simple sum of the ionic properties agrees rather well with measurement (see Mandarino 2007 for calculation of n from oxides).

The equation for ions in crystals is $n/D = \Sigma(k_i d_i)$, where k_i is the molar ionic refractivity and d_i is the fractional density (the weight of a number of ions i of atomic weight AW per unit-cell volume V is also the ion weight fraction). For a single ion, the refractivity is $s_i = k_i AW/An$, in nm^3, where An is Avogadro's number. The index of refraction is then a sum of the partial contributions of the refraction of each ion, with $n = \Sigma|n_i| = A_N\Sigma(s_i'|d_i|/AW)$. This modified Gladstone-Dale equation (Gladstone and Dale, 1864; Teertstra, 2005) is offensive to wave theorists who insist that light does not interact with individual atoms, but the fact remains that the wave theory is complex and difficult to use and produces distinctly inaccurate values of n (e.g. Rocquefelte *et al.,* 2004, 2006). And although the theory of light as an electromagnetic wave has had over a century of development, not a single worker in physics has been able to relate the optical properties of crystals to the structure using the theory. Also a modified theory of light may be required, as a working model of the photon does not currently exist.

From the wave theory of light to a proposed local photon

Early workers in optics such as Isaac Newton and Albert Einstein considered that the interactions of light with matter were best explained if light consists of a stream of local particles. However, as the interference patterns of light and of water waves appear similar, and as phenomena such as refraction are described by trigonometric functions, the earliest mathematical descriptions are of light as a sinusoidal wave. The relations between electricity and magnetism derived in 1864 by James Maxwell generated not only a simple formula for the speed of light, but also allowed a description of light as a plane-polarized electromagnetic wave. This wave contains a negative electric component that alternates further along in space with a positive electric component, while magnetic flux occurs perpendicular to the electric plane. As light can be described as an electromagnetic wave (Iksander, 1992), it must be acted on by the electric force to effect refraction, but this idea seems to be absent from physics.

For wave refraction, it is required that the wavelength of light is reduced on entering a denser medium (e.g. yellow light in air is effectively blue in water), but such a reduction of wavelength is non-observable and physically indeterminate. For a reduced wavelength, the quantum equation for energy ($E = hc/\lambda$ where h is Planck's constant, c is the speed of light and λ is wavelength) predicts an increased energy, but this is also indeterminate. The wave theory assumes that light may be redirected (reflected or refracted) at no energetic cost, so explanations for thermodynamics or for the motion of free ions toward a light source (e.g. ion trapping by lasers) are absent. There are also no fundamental explanations for diffraction or for atomic absorption or emission by single atoms. The current situation in physics is that separate sets of equations exist for waves and for particles, and the wave-like and particle-like aspects of light are considered complementary. The overall consensus is that one cannot use light to gather information about objects that are smaller than the wavelength of light, but a glance at the results in *Table II* indicates radii of refraction that are similar to atomic radii.

The main problem tackled here is that the wave theory of light has only poor relations to the refractive properties of materials. Although it was known to Maxwell that each pure material (e.g. diamond, sulphur) has a specific index of refraction (commonly determined using yellow light), and that index of refraction of a solution depends on the index of refraction of the end-member components (e.g. water and alcohol), functional electromagnetic equations could only be found by assuming an average index of refraction for materials. In wave theory, a uniform wave-front cannot be maintained if each ion has a unique index of refraction. If light is refracted by each ion, light must consist of particles.

From the wave theory of light, transmission through a gem occurs as the electric component of light induces an oscillation in the electrons of the material. Much of the refraction is thus attributed to the loosely-held valence electrons of the anions, as these are the most polarizable. However, calculations of index of refraction based on polarizability (in nm^3; e.g. the Lorentz-Lorenz equation; Jaffe 1988, Eggleton 1991, Iksander 1992) are poor because cations are also major contributors to the index of refraction.

The theory of electromagnetism also lacks connections to mass. It is known, however, that charge is maintained by reduction of rest mass when particles of opposite charge form electric bonds. The mass of hydrogen is less that the mass of the electron and proton alone (this is the binding energy $E = mc^2$), as mass is consumed to maintain charges of -1 for the electron and +1 for the proton. Applying such ideas to light, and requiring local mechanisms of propagation (by rejecting the mysterious process of action at a distance required for waves), a local decline in the electromagnetic energy of a photon requires an exchange with mass (*Figure 1*). For a local photon, the electromagnetic energy of a packet of light oscillates with mass, if the total energy is constrained to a finite region of space. Mass is zero for maximum electromagnetic energy and vice-versa, so the photon has wave properties only on trace over time. This reduction of symmetry from a plane wave requires an electric-charge monopole, alternating over time from positive to negative, with polar loops of dipole magnetic flux that are perpendicular to the electric-charge monopole *(Figure 1)*.

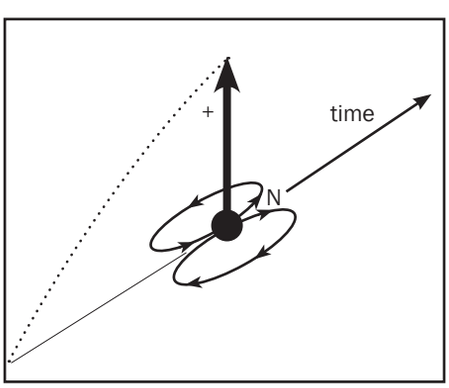

Figure 1. A model of a local photon. Over one-quarter of the wavelength, the electric-charge monopole increases from zero to a maximum value, in phase with dipole magnetic flux. The electromagnetic energy is conserved by exchange with transient mass; the mass is zero when the electric-charge monopole is at a maximum. The photon maintains constant speed and momentum and exhibits a sin2θ wave on trace over time.

Refraction occurs as this local photon is acted on by the electric charge about each ion. Refraction thus occurs by serial displacement of the photon about each ion in the crystal structure as the photon takes a roller-coaster ride through the gem. The index of refraction is due to an increased path length rather than a reduced wavelength. In this analysis, no new laws of physics are required although new principles are introduced, and a simple equation for photon refraction then indicates the composition and structure of the material.

A relation between optics, composition and crystal structure

From atomic theory, ions form from neutral elements by the gain or loss of electrons. The elements Mg and O react to form an ionic bond with Mg^{2+} and O^{2-} ions in an MgO molecule, as both ions gain an electric structure like that of an inert gas. The two positive charges of Mg^{2+} can be considered to extend with spherical symmetry from the surface of an inert-gas core of electrons (Ne). The two valence electrons of O^{2-} are held in orbital paths by the positive charge of the nuclear protons, but are also attracted to the Mg^{2+} cation.

In liquids and solids, the cations attract coordination polyhedra of anions and vice-versa. However, as ions of like charge repel one another, paths through the structure of a dielectric solid consist of alternating cations and anions. The regular grid-like arrangement of cations in crystals relates to near-equal forces of repulsion between cations, but the valence electrons of O^{2-} glue the structure together.

In the present theory of refraction, a single ion of Mg^{2+} can do work on a passing photon to change its direction. As the ion presents a spherical distribution of charge to a photon that is incoming from any direction, the characteristic refractivity of this free ion ($s_i = k_i AW/An$ in nm^3) is considered to represent the refractive volume of the ion.

The electric force F on a charge near the ion varies with distance d in proportion to $1/d^2$, but Coulomb's law (of $F \propto 1/d^2$) lacks subtlety. The ions Mg^{2+} and Fe^{2+} in MgO and FeO are considered identical because d is measured from the centre of charge (effectively the nucleus), but these ions have differences in electric structure that shield the charge of the nucleus to different degree. The ions differ in refractivity. The working solution used here is to consider refractivity due to ionic charge as Coulomb-like, with the s_i of an ion affecting other ions in proportion to $1/d^2$.

For the equation $n/D = \Sigma(k_i d_i)$ applied to a simple binary series such as (Mg,Fe)O, by knowing *n, D* and d_i from analysis, it is easy to find relative values of molar refractivity k_i for Mg^{2+}, Fe^{2+} and O^{2-} that exactly return the measured values of *n* and *D*. However, these values of k_i generate inexact values of *n* and *D* in other polymorphs of (Mg,Fe)O, probably due to differences in the structure-type (Eggleton, 1991).

One may also find relative values of k_i for Mg^{2+}, Fe^{2+}, Mn^{2+} and Ca^{2+} in garnet that give minimal differences between calculated and measured values of *n* and *D* for all samples in the quaternary space of the $(Mg,Fe,Mn,Ca)_3 Al_2Si_3O_{12}$ solid solution, but these k_i values give inexact results when applied to the broader $(Mg,Fe,Mn,Ca)_3 (Al,Fe^{3+},V,Cr)_2Si_3O_{12}$ solid solution, again probably due to differences in structure.

Workers in mineral optics have sought constant values for the molar refractivity of oxides (Mandarino, 2007), suggesting a characteristic electric structure for ions or molecules, but a general relation between optics, composition and structure must also account for birefringence. The effective refractivity of an ion has been shown to vary depending on the general structure-type (Eggleton, 1991) and on variation within a specific structure (Teertstra, 2005).

Table II: Values of refractivity (s_i), cut-off distance (dc), radius of refraction (R) and radius (r) of free ions.

Ion	s_i (nm^3)	dc (nm)	R (nm)	r (nm)	R/r
Mg^{2+}	0.02158	0.38	0.174	0.089	1.9
Fe^{2+}	0.03130	0.42	0.196	0.091	2.2
Mn^{2+}	0.03200	0.43	0.197	0.098	2.0
Ca^{2+}	0.03436	0.43	0.202	0.112	1.8
Al^{3+}	0.00168	0.30	0.074	0.053	1.4
Fe^{3+}	0.02680	0.58	0.186	0.065	2.9
V^{3+}	0.02170	0.60	0.173	0.064	2.7
Cr^{3+}	0.02130	0.64	0.172	0.062	2.8
Si^{4+}	0.01400	0.50	0.150	0.026	5.8
O^{2-}	0.02500	0.50	0.181	0.140	1.3

The structure factor

The idea of photon refraction by individual ions naturally arises because the volume of refraction of an ion is similar to the ionic volume (Shannon and Prewitt, 1969). Also of interest, *Table II* indicates that the refractivity of a free ion is a function of charge and radius.

The present theory uses visible-light refraction data and compares this to the X-ray data for thin-sheet diffraction. The density calculated from X-ray diffraction measurements is $D = \Sigma(a_i AW)/VAn$, where a number of atoms a of type i and atomic weight AW (g/mol) occupy the unit-cell volume V (nm^3). From single-crystal structure refinement, the composition is determined by the scattering factors of the ions, and also by the inter-ionic distances if the scattering factors are similar (e.g. <Al-O> and <Si-O> distances in nm for Al-Si solid solution at a site). The density calculated by refraction, $D = n/\Sigma(k_i d_i)$, where $d_i = a_i AW/V = w_i$ (the ion weight fraction), must agree with the density calculated by diffraction; that is, the value k_i is a refractive factor analogous to the ionic X-ray scattering factor.

The refractivity of ions is explained entirely by classical electrostatic theory, as the charge of each ion acts on the photon by the Coulomb force. If the refractivity is proportional to the electric force, it must fall off as $1/d^2$. With the inter-ionic distances di known from the crystal structure (Novak and Gibbs, 1971), values for the ionic refractivity can proxy for the electric force. With reference to *Figures 2* and *3*, the explanation is as follows.

If the refractivity of a free (unbound) single ion of Mg^{2+} is, say, $s_i(Mg^{2+}) = 2$, and say $s_i(O^{2-}) = 6$, then the net refractivity of the MgO molecule will increase as the inter-ionic distance (di) decreases (once the ions are close enough to bond). This requires di < dc, where dc is a cut-off distance beyond which the refractivity of one ion does not measurably affect the refractivity of a distant neighbour. The inter-ionic distances di are taken from the structure data of Novak and Gibbs (1971), but one must iterate to find the dc values for each ion.

The ion O^{2-} places charge at Mg^{2+} a distance di away, and this increases the refractivity of Mg by $s_i'(Mg^{2+}) = s_i(Mg^{2+}) + s_i(O^{2-})(dc - di)^2$. A high estimated s_i of O^{2-} means that it places sufficient charge at Mg^{2+} to increase the refractivity of Mg^{2+} from 2 to an effective value of, say, $s_i'(Mg^{2+}) = 2.6$, but with a low refractivity of Mg^{2+}, the effective refractivity s_i' of O^{2-} in the Mg-O bond may be only 6.02. Now if a second ion of Mg bonds to the MgO molecule, it will further increase the effective refractivity of O^{2-} but will decrease the effective refractivity of Mg^{2+} (due to repulsion). But if the bond is stable, n (Mg-O-Mg) > n (Mg-O).

Now suppose that Fe partly substitutes into the Mg site. A fractional site

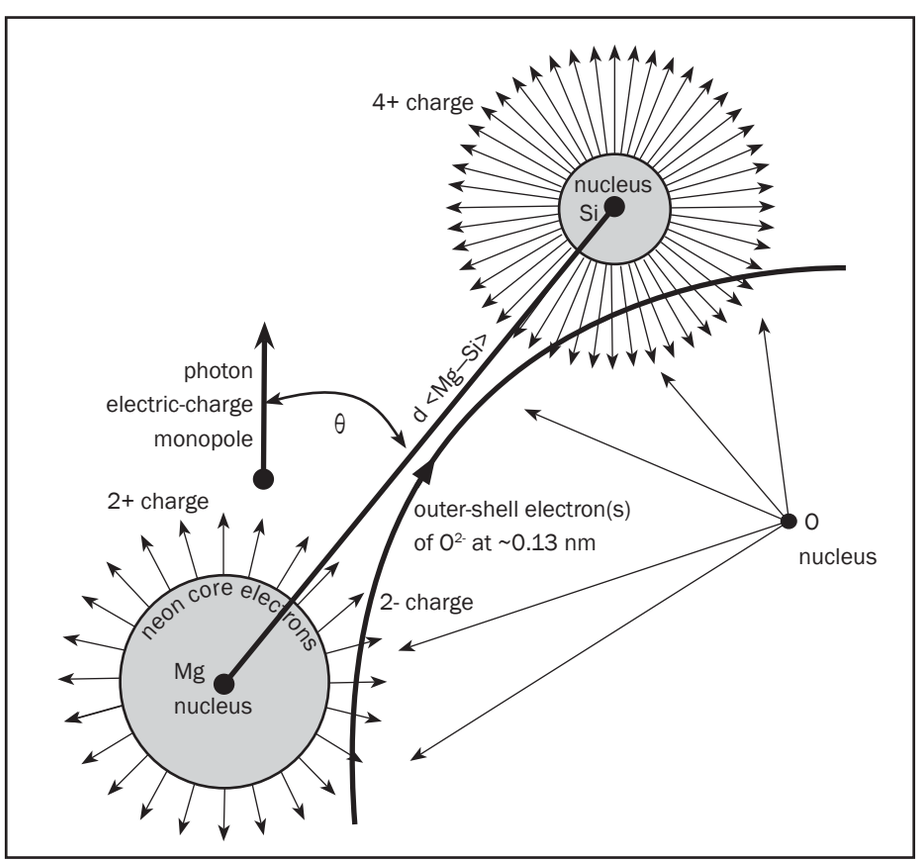

Figure 2. A generalized model of the relations between the polarization of light, the refractivity and identity of ions, and inter-ionic distances and angles. The model is applicable to aperiodic molecules, liquids and solids, and crystals. The force on a photon near an ion depends on the distances and angles to surrounding ions.

The refraction of light by garnet depends on both composition and structure

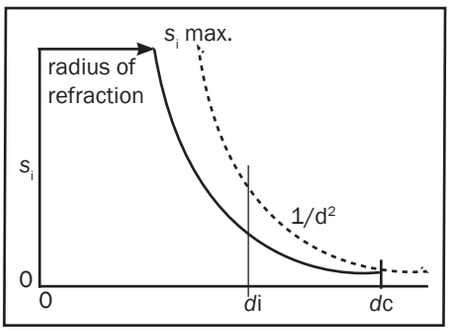

Figure 3. Ion refractivity s_i vs. cut-off distance dc. If a photon refracts at a specific level of energy at a radial distance from the nucleus, the charge beyond that radius of refraction falls off by $1/d^2$. An ion contributes a fraction of its refractivity s_i to a neighbour at di, also falling off as $1/d^2$. Beyond the cut-off distance dc, the ion does not contribute to the refractivity of a neighbour. Increasing the cut-off distance (from solid curve to dashed curve) is equivalent to increasing the radius of refraction; more charge is placed at di and the refractivity of the neighbouring ion is increased.

occupancy (*f*) is needed to account for the solid solution, such that Mg + Fe = 1 for full occupancy of the site. For example, the site may contain 20% Fe, giving *f*(Mg) = 0.8 and *f*(Fe) = 0.2 for the formula $(Mg_{0.8}Fe_{0.2})O$.

Experimentally, the electric vector of the photon is given a known direction by passing the light through a polarizing filter such as Polaroid. Attempts to describe the refraction of light through a crystal by reference to a plane wave of light were unsuccessful. If a local photon is considered, a single value for the refractivity of an ion occurs if the refraction of a photon is dominated by that ion over the time when the photon is near the ion. The refractivity is changed to minor degree by charge placed at the ion by surrounding ions. This additional force on the photon is at a maximum value for ions above and below the electric-charge monopole of the photon, and is zero for ions perpendicular to the proposed monopole. For garnet, it is convenient to calculate the angle θ by considering polarized light refracting along an a axis. The sum is taken for all ions in a sphere surrounding the site of interest; it is not with reference to a plane of polarization exhibited by a wave of light.

The general structure-factor for refraction is $C = \Sigma[\cos\theta\, f s_i(dc - di)^2]$, where *f* is the fractional site occupancy of ion i (accounting for solid solution), θ is the angle between an ion and the electric monopole of the photon (in this case parallel to the a axis of garnet), dc is the cut-off radius beyond which the refractivity of one ion does not affect the refractivity of another ion, and di is the inter-ionic distance. Knowing *n, D* and the inter-ionic distances for each composition, and calculating cosθ from the structure, there are only two variables for each ion, s_i and dc (*Table II*). However, these two variables are constrained to fall off as $1/d^2$ from free to bound cations and must explain the *n* and *D* values of all members of the solid solution. The system is thus highly constrained and strongly convergent on specific values of s_i and dc.

Note that the structure factor for refraction is different from the structure factor for diffraction. The physical phenomenon affecting refraction is the identity of an ion that is (for a time) dominating the local refraction of a photon; one must also account for the distance and angle to all ions surrounding this ion that alter its refractivity. By contrast, diffraction results from the sheet arrangement of ions in a crystal, and the specific identity of ions in a plane only influences the intensity of reflection. Any structure proposed to explain the refraction data need not be periodic (i.e. crystalline), thus allowing the photon as a probe of aperiodic materials including molecules, glass or liquids.

Table III: Site structure factors for end-member species of garnet.

Species	C_X	C_Y	C_Z
pyrope	0.00792	0.00877	0.01041
almandine	0.00757	0.00808	0.00938
spessartine	0.00732	0.00769	0.00891
grossular	0.00677	0.00592	0.00828
andradite	0.00373	0.00649	0.00535
goldmanite	0.00443	0.00654	0.00615
uvarovite	0.00296	0.00576	0.00453

With reference to the structural formula $X_3Y_2Z_3O_{12}$ of the anhydrous isotropic species of garnet, a photon undergoing local refraction about an ion in the X-site has a degree of refraction that is dominated by the X-cation, but the refractivity is influenced by all the surrounding ions (mainly by the nearest ions of oxygen, but also by the more distant X-, Y- and Z-site cations). The X-site contains large divalent cations in a distorted cube of coordinating oxygen anions. The Y-site contains trivalent cations in octahedral coordination, and the Z-site contains tetravalent cations in tetrahedral coordination. Each oxygen ion is coordinated by one Z-cation, one Y-cation and two X-cations (Novak and Gibbs, 1971).

For example, the structure factor for the X-site is the sum $C_X = C_{XO} - C_{XX} - C_{XY} - C_{XZ}$. For pyrope, $Mg_3Al_2Si_3O_{12}$, this is $C_X = \Sigma[\cos\theta\, f s_i(O^{2-})(dc - di)^2] - \Sigma[\cos\theta\, f s_i(Mg^{2+})(dc - di)^2] - \Sigma[\cos\theta\, f s_i(Al^{3+})(dc -$

Table IV: Values of molar refractivity (k_i) of ions in end-member silicate garnets.

Species	Mg^{2+}	Fe^{2+}	Mn^{2+}	Ca^{2+}	Al^{3+}	Fe^{3+}	V^{3+}	Cr^{3+}	Si^{4+}	O^{2-}
pyrope	0.7310	0.4223	0.4376	0.6349	0.2332	0.3511	0.3359	0.3220	0.5234	0.4383
almandine	0.7223	0.4181	0.4338	0.6298	0.2185	0.3535	0.3386	0.3229	0.5001	0.4529
spessartine	0.7156	0.4156	0.4310	0.6256	0.2092	0.3541	0.3359	0.3212	0.4904	0.4636
grossular	0.6980	0.4106	0.4259	0.6196	0.1687	0.3439	0.3218	0.3091	0.4790	0.4860
andradite	0.6205	0.3772	0.3916	0.5726	0.1816	0.3503	0.3282	0.3159	0.4250	0.5494
goldmanite	0.6180	0.3758	0.3905	0.5712	0.1863	0.3529	0.3309	0.3183	0.4231	0.5443
uvarovite	0.5890	0.3634	0.3779	0.5536	0.1653	0.3425	0.3199	0.3073	0.3930	0.5766

$di)^2$] -Σ[cosθ $fs_i(Si^{4+})(dc - di)^2$]. If $s_i(Mg^{2+})$ = 0.02158 and C_X = 0.00792 (*Table III*), the effective refractivity s_i' of Mg^{2+} in the X-site is 0.02950 nm^3 and $k_i(XMg^{2+})$ is 0.7310 cm^3/g (*Table IV*). The substitution of another X-cation for Mg increases the size of the unit cell and increases the <X-X>, <X-Y>, <X-Z> and <X-O> distances and the effective refractivity of Mg^{2+} decreases. With the refractivity contribution of an ion constrained to fall off as $s_i(dc - di)^2$, only the specific values of s_i and dc will return the measured values of *n* of *Table I*. The calculated values of *n* are not reported because the equation is sufficiently accurate to match the measured values of *n* for all species of garnet in the $(Mg,Fe,Mn,Ca)_3(Al,Fe^{3+},V,Cr)_2Si_3O_{12}$ solid solution.

The molar values of refractivity reported in the matrix of *Table IV* include the structure factors. From the structural formula and relative to end-member pyrope, the calculated unit-cell edge is *a* = 1.1459 + 0.0130667 Ca + 0.005400 Mn + 0.0022333 $^{X}Fe^{2+}$ + 0.010350 $^{Y}Fe^{3+}$ + 0.010950 V + 0.007250 Cr nm, and *V* = a^3. For pyrope, the ionic weight fractions (or fractional densities) calculated from the formula $Mg_3Al_2Si_3O_{12}$ are 0.1809 Mg, 0.1339 Al, 0.2090 Si and 0.4762 O, Σ1. With eight formula units in the unit cell volume, the formula weight is 403.127 g/mol and the density is 3.5591 g/cm^3. The calculated index of refraction is *n* = *D*[(0.1809)(0.7310) + (0.1339)(0.2332) + (0.2090)(0.5234) + (0.4762)(0.4383)] = 1.714. For minor to trace quantities of Mn, Ca, $^{X}Fe^{2+}$, $^{Y}Fe^{3+}$, V and Cr, one may use the k_i values for these ions in pyrope.

The k_i values of the ions vary depending on the identity of and the distance to the surrounding ions. From pyrope to almandine, for example, there is a linear change in $k(Mg^{2+})$; this is (0.7223-0.7310)/3 per $^{X}Fe^{2+}$, and this is an additional (0.7223-0.6180)/2 per V for a hypothetical ferroan goldmanite. From the structural formula and relative to end-member pyrope, the calculated molar refractivity of Mg is $k(Mg^{2+})$ = 0.7310 - 0.011000 Ca + 0.0051333 Mn + 0.002900 $^{X}Fe^{2+}$ + 0.055250 $^{Y}Fe^{3+}$ + 0.056500 V + 0.007100 Cr. The other k_i values may be calculated in a similar manner.

Accounting for changes in density, the resultant of the k_i matrix is an easy-to-use formula: *n* = 1.714 + 0.0066667 Ca + 0.0286667 Mn + 0.0386667 $^{X}Fe^{2+}$ + 0.077500 $^{Y}Fe^{3+}$ + 0.05000 V + 0.065500 Cr. This formula was used to verify the values of n used in *Table I* (Teertstra, 2006) in that a linear best fit is attained between calculated and measured values of *n* for numerous compositions of garnet reported in the literature.

Practical implications

The optical properties of materials are essential to their identification. Each proposed structural formula implies a specific state of cation order and definite physical properties for gems and minerals. Using the values of s_i and dc in *Table I*, the physical properties of any proposed ionic structure may predicted (e.g. spinel, olivine, pyroxene, glass). The method of optical analysis is sensitive to light elements that cannot be analyzed by electron microprobe. Once values for the refractivity of ions are known, given a composition, the method can also be used to predict the structure.

If the index of refraction and the density or the unit-cell-volume are measured, the values of k_i may be used to determine the structural formula and hence the composition of a garnet sample. Convergence on the correct formula occurs as differences across the equality $n/\Sigma(k_i d_i) = \Sigma(a_i AW)/V An$ are minimized.

If the composition is measured along with *n*, and the formula shows ΣX>3 and ΣY<2, then a recalculation of $^{Y}Fe^{3+}$ from $^{X}Fe^{2+}$ may be verified by an improved agreement between calculated and measured values of *n*. The index of refraction is sensitive to the valence of an ion and to the order of cations in the structure.

References

Eggleton, R.A., 1991. Gladstone-Dale constants for the major elements in silicates: Coordination number, polarizability and the Lorentz-Lorenz relation. *Can. Mineral.,* **29**, 525-32

Gladstone, J.H., and Dale, T.P., 1864. Researches on the refraction, dispersion and sensitiveness of liquids. *Phil. Trans. Royal Soc. London,* **153**, 317-43

Iksander, M.F., 1992. *Electromagnetic Fields and Waves.* Prentice-Hall, Englewood Cliffs, New Jersey

Jaffe, H.W., 1988. *Crystal Chemistry and Refractivity.* Cambridge University Press, Cambridge

Mandarino, J.A., 2007. The Gladstone-Dale compatibility of minerals and its use in selecting mineral species for further study. *Can. Mineral.*, **45**, 1307-24

Novak, G.A., and Gibbs, G.V., 1971. The crystal chemistry of the silicate garnets. *Am. Mineral.,* **56,** 791-825

Rocquefelte, X., Goubin, F., Koo, H.-J., Whangbo, M.-H., and Jobic, S., 2004. Investigation of the origin of the empirical relationship between refractive index and density on the basis of first principles calculations for the refractive indices of various TiO_2 phases. *Inorg. Chem.,* **43,** 2246-51

Rocquefelte, X., Jobic, S., and Whangbo, M.-H., 2006. On the volume-dependence of the index of refraction from the viewpoint of the complex dielectric function and the Kramers-Kronig relation. *J. Phys. Chem.,* **110**, 2511-14

Shannon, R.D., and Prewitt, C.T., 1969. Effective ionic radii in oxides and fluorides. *Acta Crystallogr.,* **25B**, 928-9

Teertstra, D.K., 2005. The optical analysis of minerals. *Can. Mineral.,* **43**, 543-52

Teertstra, D.K., 2006. Index-of-refraction and unit-cell constraints on cation valence and order in garnet. *Can. Mineral.,* **44**, 341-6

The Author

David K. Teertstra

Euclid Geometrics, 509.5 Morningside Drive, Albuquerque, New Mexico, 87108, U.S.A.
email: en369@freenet.carleton.ca

Ornamental variscite: A new gemstone resource from Western Australia

Margot Willing, Susan Stöcklmayer and Dr Martin Wells

Abstract: Variscite ($AlPO_4.2H_2O$) is an uncommon bluish-green mineral that has been used as an ornamental gemstone since the Neolithic Age. A new location of variscite has recently been investigated on Woodlands Station, Western Australia. The variscite from here occurs in a variety of aggregated habits within fine-grained Proterozoic siltstones and breccias. Rock surfaces have been found encrusted with microcrystals of variscite and wardite. Within the host rocks, associated minerals include metavariscite, crandallite, jarosite, quartz and grains of native gold. The gemmological properties of the Woodlands variscite are: RI range of 1.570 to 1.582, and SG from 2.49 to 2.55, and these are within the ranges of variscite from other world sources. X-ray diffraction analysis confirms the variscite to be of the 'Meßbach-type' in association with metavariscite, a dimorph of variscite. Using visible reflectance spectroscopy, trivalent chromium was verified as the main chromophore responsible for the colour. Minor vanadium is also present, probably in mixed oxidation states of +3 and +4.

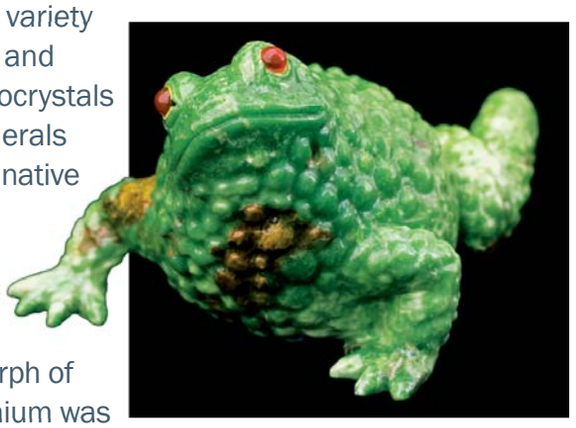

Keywords: Gold inclusions, 'Meßbach-type' variscite, metavariscite, trivalent chromium, Woodlands Station, Western Australia

Introduction

Ornamental variscite is bluish green in colour, fine grained and massive in habit. Its colour ranges from white, through light brown and bluish-green to yellowish-green. When used together with its matrix minerals and associated relict host rock, the resulting reticulated patterns are reminiscent of the variations in colour and textures shown by turquoise-in-matrix. Variscite has characteristics common with turquoise, the best-known ornamental phosphate gem mineral. They are recorded together in some worldwide localities and the mining history of both minerals dates to the Neolithic Age.

Variscite, a hydrated aluminium phosphate ($AlPO_4.2H_2O$), was first described in 1837, from a source in Germany where it occurred at Meßbach quarry, Altmannsgrün, near Plauen, Vogtland, formerly Variscia (Dana, 1892). This find was not a source of ornamental grade material. In Querre's words: "Lacroix, the famous French geologist, determined in 1896 the formula of variscite, official name of this mineral [$AlPO_4.2H_2O$]" (Querre *et al.,* 2007). Variscite also occurs as microcrystals that are recorded as colourless, green or red. The rare ferroan red variety occurs as encrustations on hematite at Iron Monarch quarry, Iron Knob in South Australia and at Boa Vista mine in Minas Gerais, Brazil (http://www.mindat.org/). Variscite forms at low temperature as a secondary mineral commonly associated with other hydrated minerals particularly its dimorph — metavariscite. It is found as veins and nodular encrustations within and on a variety of rock types. It may occur as a replacement mineral having developed *in situ* from phosphate-bearing fluids in association with fine-grained and clay-bearing aluminous rocks. It is also reported having formed at ambient temperature with other phosphate minerals within soils and on various substrates including serpentinite derived by chemical action from bird guano (Simpson, 1952).

History of early exploitation (4500–3000 BC) of variscite from the Iberian Peninsula is reported from recent archaeological work (Arribas *et al.,* 1970, Harrison *et al.,* 2001; Camprubi *et al.,* 2003; Dominguez-Bella, 2004), where evidence at some sites

©2008 Gemmological Association of Great Britain

Figure 1a: Variscite seahorse on quartz base, height 20 cm. Carved by Robert Jüchem, Idar-Oberstein, Germany.
Figures 1b and 1c: Gold mounted pendant (30 mm diameter) and gold-mounted cufflinks (17 mm square), fashioned by Murray Thompson, Goldsmith, Brett Barker.

indicates workings continued to be mined into the Middle Ages. Variscite jewellery in the form of beads, necklaces and pendants is recorded from numerous Neolithic sites in Spain and Portugal, from burial sites in France (Forde, 1930) and, more recently, from rare Roman (AD 43–410) sites in England (Middleton, 2007).

Most of the ornamental variscite used in modern times for lapidary and jewellery purposes has originated from finds in the U.S.A., notably Utah. Deposits from here, first discovered in 1893, have been worked sporadically into the mid-twentieth century (Larsen, 1942; Dickerson, 1971). Clay Canyon in the Oquirrh Mountains, Fairfield County, Utah, has been the largest producer (Thomssen, 1991) with other occurrences including the Little Green Monster, and Utahlite Hill, Box Elder County and Amatrice Hill, Tooele County (Doelling, 1980). The state of Nevada has also been a source for gem variscite, with the Verde Web variscite mine in Lander County (Novak, 1982) being one recorded producer.

Variscite of blue green colour and translucent quality suited for ornamental purposes *(Figure 1)* is being mined from a new location at Woodlands Station in remote Western Australia (WA). Recent research has established that elemental gold occurs as inclusions within this variscite (Hancock, 2008). Although variscite is recorded from other locations within WA it has only been mined previously from Milgun Station, south east of this new find.

In this paper, the authors describe the properties of this new ornamental variscite, its geological occurrence and associated minerals.

Terminology

Minerals

Metavariscite: monoclinic; dimorph of variscite.

Strengite: orthorhombic; Fe $PO_4.2H_2O$, forms an isomorphous series with variscite; Fe^{3+} replacing Al^{3+}.

Variscite: orthorhombic; a member of a mineral series that includes arsenates and phosphates with the general formula $AXO_4.2H_2O$, where A = aluminium (Al^{3+}), iron (Fe^{3+}), chromium (Cr^{3+}) or indium (In^{3+}) and X may be arsenic (As) or phosphorus (P). Two polymorphic varieties of variscite exist: 'Meßbach' (VM) and 'Lucin' (VL) types, closely related, differing only in unit cell dimensions. Both terms are derived from their localities in Meßbach, Vogtland, Germany and Lucin (Utah, U.S.A.); see Clark (1993).

Historical mining and uses of variscite

Early to Middle Stone Age (c. 4500–2500 BC)

Exploitation of variscite as an ornamental material dates to prehistory. It was desirable, favoured for its intense green and blue-green colour. It was also of value as shown by the efforts made by Neolithic peoples to mine, fashion and trade it over hundreds of kilometres through parts of Europe. Recent archaeological work, notably at Can Tintorer in the Gavà Neolithic Mining Complex, about 20 km SW of Barcelona in NE Spain shows the early and deliberate exploitation and mining of variscite from 4000 BC over a period of 300-400 years (Harrison *et al.,* 2001). Veinlets and seams of variscite were worked from host rock slates via underground passages and galleries covering hundreds of metres, to depths of 40 m (Camprubi *et al.,* 2003). Beads and other items *(Figure 2a)* were fashioned in settlements nearby and exchanged across Spain and into the Pyrenees, distances up to 550 km.

Figure 2a: Variscite collar necklace found in a burial site inside the Neolithic mines of Gavà, Spain.

At Palazuelo de las Cuevas, Zamora, west of Can Tintorer, the mining of variscite also dates to the fourth millennium BC and beads from these two areas do not overlap in their trading. Variscite from here was also exploited in the later Roman period (Dominguez–Bella, 2004) and into the Middle Ages (Arribas, 1970). Similar mining and bead trading is known in parts of Portugal, where hundreds of beads have been discovered (Meireles, 1987).

Beads and pendants of variscite of various sorts and styles are also known and described from the Carnac region of

Figure 2b: Variscite pendant and beads from burial sites in Mané-er-Hroëk, Brittany, France (4500-4000 BC). British Museum collection, with permission.

north-western France, notably Neolithic tombs at Lannec-er Ro'h and Mané-er-Hroek, Morbihan, Brittany (Forde, 1930; Cassen, 1998). Recent trace element analyses of green beads and pendants from these burial sites indicate that the original source of the variscite is from the Iberian Peninsula (Querre *et al.,* 2007). An item of this collection, housed in the British Museum is a pendant fashioned from one piece of variscite and measuring 45 mm x 29.5 mm *(Figure 2b)*. The collection of ten beads displays various qualities of variscite, but overall the colours are intense, the beads well polished, the shapes varying between ovoid, discoidal and cylindrical with two showing several sets of bevels or facets, and all unornamented. The largest has a length of 21 mm. All are drilled through for suspending with large diameter holes, from 2 to 4 mm. These worked variscite articles have previously been described under the terms 'Callais' and 'Callainite' (Bauer, 1904), and it is possible that other archaeological finds of green ornamental materials may include variscite that has not yet been verified mineralogically.

The Roman Period (AD 43–410)

Rare finds of variscite beads and jewellery are also known from the Roman era, and some examples from Britain are listed in *Table I*. In contrast to the large numbers of beads dated from the Stone Age period, those attributed to the Roman era are uncommon.

These rare archaeological finds demonstrate the importance and high esteem associated with owning variscite jewellery. The source of the variscite found in these Roman deposits has not been established with certainty.

Table I: Variscite artefacts found at archaeological sites in Britain; all Roman Period (AD 43-410).

Variscite artefacts	Archaeological sites	Reference
Fragment of a ring shank; carved in criss-cross design with serpents' head finial*	Gadebridge Park, Hemel Hempstead	Neal, D.S. (1974)
3 x beads; octagonal cross-sections	Balkerne Lane, Colchester	Crummy, N. (1983)
1 x bead; octagonal cross section	Tanner Row, York	Hooley, D. (1988)
1 x bead; faceted cuboid	Rougier Street, York	Hooley, D. (1988) Unpublished Ref. in Middleton *et al.* (2007)
7 x cylindrical green beads; mounted on an incomplete gold necklace	Grange Farm, Gillingham, Kent	Middleton *et al.* (2007)

** The first record of variscite identified from an archaeological site in Britain*

Common misnomers

- *Amatrice or amatrix:* a trade name, a coined term to describe variscite together with matrix material; also referred to as American matrix and variscite-quartz. Amatrice commonly includes wardite within its occurrence as concretionary masses.
- *Callais, callainite:* obsolete mineral names, originally terms describing turquoise and attributed to Pliny. These terms also have described non-specific green ornamental materials from ancient grave sites in Brittany. Both turquoise and variscite have been so described in archaeological studies and early mineral reference works.
- *Lucinite:* a trade name for variscite from near Lucin, Utah.
- *Utahlite:* a trade name for compact variscite nodules from Stransbury Mountains of Tooele County, Utah.
- *Variquoise:* a trade name describing combined variscite and turquoise rock
- *Verde web variscite:* a trade name for light blue and light green variscite with included black 'spider web' pattern matrix, from Lander County, Nevada. For more on variscite names, see Dietrich (2008).

Variscite from Western Australia

Variscite from the new occurrence in Western Australia was first shown in 2006 at the Arizona Mineral and Fossil Show in Tucson (Laurs *et al.,* 2007). The material is comparable to the highest quality that has been exploited worldwide with an intense bluish-green colour and translucent quality. Some of the material occurs with textural characteristics that make sculptural *objets d'art* attractive and recognizably different to variscite from elsewhere. The new deposit outcrops sporadically over a distance of several kilometres and has potential to be an important source of gem- and carving-quality material. Until these recent new finds, the only previous mining of variscite in Western Australia was on Milgun Station, located 67 km southeast of the 'Woodlands' deposit.

During a period from the early 1980s until 2001 several mining companies were active in the general area searching for gold and various base metals. Variscite was recorded in drill samples from several locations on Woodlands Station during this time. This historical information was later followed up and more recent detailed prospecting has established several areas where variscite occurs. The variscite described in this paper is from the first new discovery that was made in 2004.

Located within the 1:250 000 Western Australian Geological and Topographical map series Sheet SG 50 -3 (Mt Egerton), it is situated on Woodlands Station *(Figure 3)* within the Shire of Meekatharra, approximately 1000 km north of Perth and 95 km east south east of Mount Augustus. The most direct access is off the Mt Augustus/Woodlands road that intersects the Great Northern Highway a few kilometres north of Meekatharra.

Figure 3: Woodlands Station variscite deposit, Western Australia; view northwards from the mine site. Foreground shows mined ore.

Geological setting

All the new occurrences of variscite on Woodlands Station, as well as those from sources on Milgun Station, occur within sedimentary rocks that form part of the Mesoproterozoic Bangemall Supergroup, dated at 1000–1600 Ma. The most recent occurrences are from argillaceous sediments and silicified breccias of the upper Kiangi Creek Formation, part of the middle Edmund Group. The Kiangi Creek Formation comprises predominantly terrigenous sediments, especially arenites, and fine-grained brown and grey shales, and silt-, mud- and claystones, with minor horizons of cherts and dolomites including a stromatolite horizon. The original sediments were accumulated on a marine shelf, with restricted current circulation under hypersaline conditions (Muhling and Brakel, 1985).

Variscite occurs as conformable seams within brown siltstones and as cross-cutting veins and irregular zones within brecciated chert and silicified siltstone horizons. Quartz veining is commonly associated with variscite where the host rocks are brecciated.

Field occurrences

Occurrences of stratabound variscite have been traced in the host rocks along strike for approximately one kilometre and zones containing nodular and veinlet forms of variscite have been found over a larger area. The horizon containing the variscite veins varies between approximately 400 and 900 mm in thickness (D. Vaughan, pers. comm., 2008). Individual stratabound variscite seams range from a maximum width of ~55 mm to more common widths of <20 mm; seams also interconnect with one another via narrower veins *(Figure 4)*. In some veins variscite has a markedly fibrous nature occurring in cross-fibre orientation to the general bedding of the host rocks. Elsewhere, the host rocks have been brecciated and cross-cutting veins of variscite both traverse and enclose angular rock fragments. Veins may be less than 1 mm wide and connect with irregularly shaped zones several centimetres across; however only one open-cut has so far been progressed and all the material described is from this site. The open-cut is ~30-40 m in length and has been mined only during short periods in the wintertime, so far yielding several tonnes of material. At other times, the quarry site is temporarily covered with spoils material, and the variscite, as described here, was collected from loose samples at the ore heap, augmented with selected specimens donated by the mine owners.

Figure 4: At the mine site. Specimen boulder showing variscite veining.

Nature of the variscite

The variscite is varied in its nature and colour; that exploited for decorative and gemmological purposes is microcrystalline, intense green in colour and commonly microfibrous in habit. There is wide variation in occurrences of this fine grained variscite; from the seams already described that are fairly regular in width, to contorted and 'ptygma'-like veins with folds that pinch and swell *(Figure 5a)*. In other specimens variscite occurs as globular and botryoidal aggregations and, unusually, in tapered pod-like aggregations *(Figure 5b)*. Rare encrustations of microcrystals of colourless variscite *(Figure 5c)* and wardite *(Figure 5d)* were identified on rock surfaces and in fillings of small cavities.

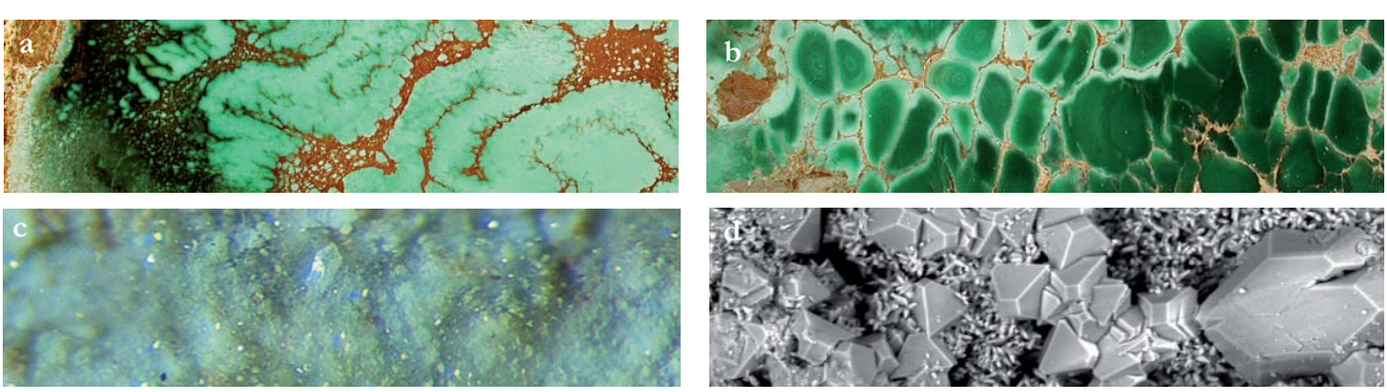

Figure 5: (a) Blue-green variscite-in-matrix showing 'ptygma'-like veining.
(b) Vein of pod-form variscite with brown rock matrix. Seam thickness ~35 mm.
(c) Rock surface — encrustations of secondary minerals; dominantly colourless variscite crystals. Centre: crystal of variscite (0.5 mm).
(d) SEM image showing wardite crystals as an encrustation on siltstone.

Material and methods

Samples of gem-quality variscite were cut using a 0.35 mm diameter diamond wire saw, and sections of four specimens V1, 4–6 are shown in *Figure 6a*. Standard gemmological methods were used on a selection of fashioned cabochons and carvings *(Figure 6b)* to determine refractive index (RI), specific gravity (SG) and luminescence. The absorption spectrum was captured with a digital camera attached to a monocular microscope which housed a diffraction grating spectroscope. Internal features were examined through a binocular microscope with oblique illumination.

Petrographic thin sections were prepared to view the relationship between country rock and the variscite mineralization through a standard petrological microscope. Further mineral identification work was assisted by RI oil-immersion techniques on grain crushes. Due to the very fine-grained nature of the minerals it was necessary to confirm all identification work with scanning electron microscope (SEM) and X-ray diffraction (XRD) techniques.

The XRD data were collected using a Philips X'Pert XRD fitted with a Cu tube (1.54056Å), automatic divergence slits, and diffracted beam graphite monochromator with the following settings: 2-theta range = 5–65°, step size = 0.03°, step time = 2s, divergence slit = 1 mm (fixed), receiving slit = 0.8 mm.

The Debye Scherrer X-ray powder (XRD) camera method was used to identify crystals occurring on rock surfaces.

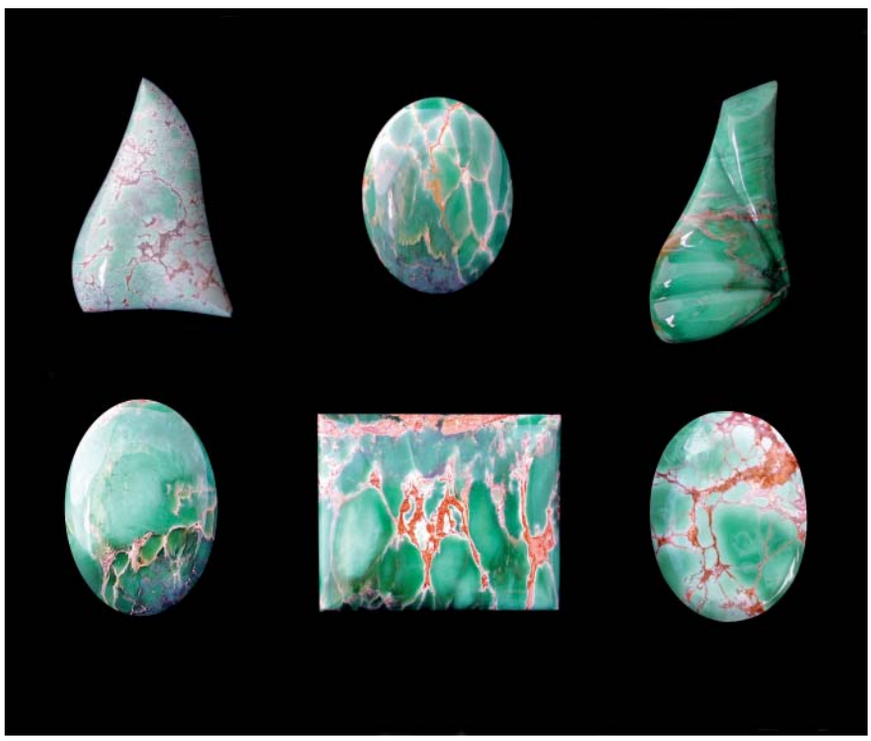

Figure 6b: A composite image of a selection of gem-quality 'Woodlands' variscite cabochons and carvings. Specimens top left and top right carved by Dalan Hargrave; oval and rectangular cabochons fashioned by Murray Thompson.

A Philips XL40 Controlled Pressure SEM fitted with an EDAX energy dispersive X-ray spectrometer (EDS) and a Robinson Back Scattered Electron (BSE) Detector, was used to identify gold and minerals associated with variscite.

X-ray fluorescence (XRF) for quantitative chemical analysis was performed on fused glass beads consisting of variscite mixed with lithium tetraborate and metaborate in the ratio 12:22 as flux. The beads were measured on a sequential PANalytical MagiX PRO XRF equipped with a 4.0 kW tube with fixed channels for Al and Si. Detection limits for most trace elements reported are ~10 ppm; major oxide report detection limits between 0.002% and 0.01%.

Reflectance spectra covered the visible to short-wave infrared wavelength range (400 to 2500 nm). Reflectance spectra of the unpolished and polished surface of each 20 mm square by 1–2 mm variscite slab were measured using an ASD Field Spec® Pro FR spectrometer (Analytical Spectral Devices, Boulder, U.S.A.), optimized and calibrated against a 100% reflectance Spectralon® white reference standard.

A mixed acid digest and the ICP-MS method of analysis was used for minor elements, the rare earths and Y, Th and U; Sc was analysed using ICP-optical emission spectroscopy.

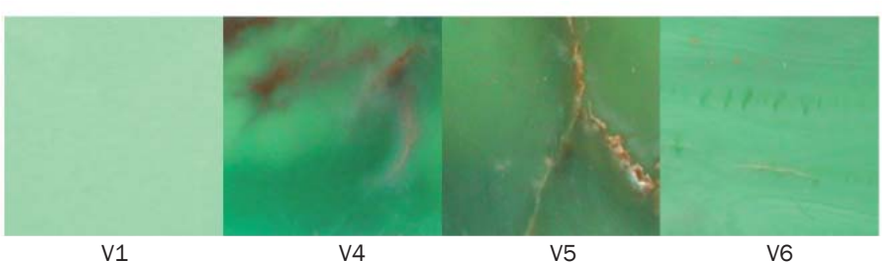

Figure 6a: Sections of four variscite specimens — V1,V4, V5 and V6 — used in this study.

Results

Optical mineralogy and petrology

Host rocks

Variscite is hosted within siltstones, where it commonly occurs in conformable seams, and in brecciated zones, where it may be accompanied by quartz. The light brown siltstones *(Figure 7a)* are very finely banded but non-fissile and may be locally silicified. The texture is accentuated by streaks and microlamellae of reddish-brown iron oxides that also occur as euhedral castes, probably pseudomorphs after iron pyrite. Siltstones in contact with variscite contain a high proportion of secondary minerals; including variscite, quartz, crandallite and jarosite *(Figures 7b, 7c)*. Within brecciated zones, rock fragments are commonly silicified and are distinctly harder than the siltstones. Many fragments have an ultrafine 'chert-like' texture and may appear red-brown and clouded white in reflected light; some fragments are cherts, others are probably silicified siltstones *(Figure 7d)*. Due to their fine-grained nature (1 μ), their mineralogy could not be confirmed by optical methods.

Figure 7a: Brown siltstone with stratabound variscite seam (20 mm thickness) in cross-fibre habit.

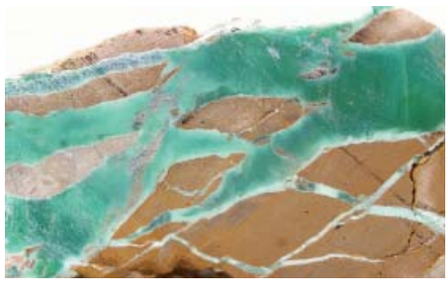

Figure 7b: Brown siltstone hosting veins of variscite and quartz lenses.

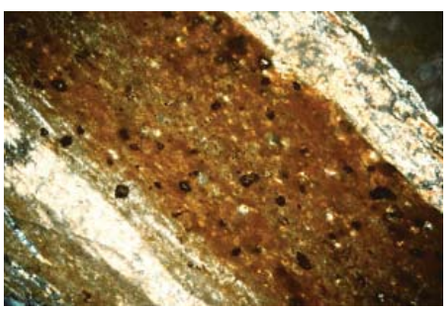

Figure 7c: Thin section of limonite-clouded siltstone, bordered by microlaminae of variscite and crandallite (colourless). The siltstone is speckled by granules of iron oxide-after-pyrite. Magnification 50x, cross polarized light.

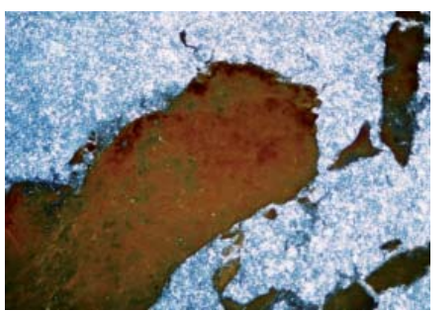

Figure 7d: Thin section of breccia showing oxidized and silicified siltstone fragments in a microcrystalline groundmass of variscite. Magnification 50x, cross polarized light.

Variscite and associated minerals

Variscite occurs in two distinct habits; equigranular *(Figure 7d)* and fibrous *(Figures 8b, 8c)*. Equigranular variscite with 'salt and pepper' 'chalcedonic-like' texture generally occurs within narrow veins and in zones bordering rock fragments within the brecciated zones. Fibrous variscite dominates in seam occurrences and characteristic reticulate patterns are developed in some places. These patterns have developed where bundles of variscite fibres, in elongate or pod-like forms, are closely packed with interstitial relict rock and brown-coloured matrix outlining their borders *(Figure 8a)*. Dimensions of pods vary; the longest measured 25 mm in the longest dimension. Pods often show variation in the green colour at their perimeters. Thin sections at greater magnification show the fibre patterns and concentric growth banding within individual pods *(Figures 8b, 8c)*. In longitudinal section pods show preferred fibre orientation and concentric banding *(Figure 8b)* with sweeping plumose extinction patterns when viewed between crossed polars. Variscite with these textures shows high translucency.

Especially well developed around pod borders is a distinctive pattern of polygonal brown patches *(Figure 8c)*. The pattern is clearly visible in plane polarized light (PPL) and is similar to a craquelure texture in the varnish of some old paintings and to that developed on the surfaces of septarian nodules. The texture may be the result of dehydration and shrinkage of pods, sometime after formation. Some pod borders are also lobed and finely fimbriated; these may

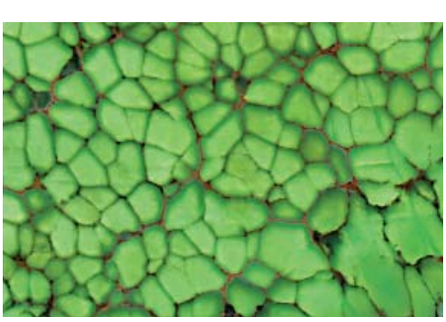

Figure 8a: Thin slice of variscite V6 viewed in transmitted light showing a reticulate pattern of variscite pods with interstitial matrix minerals. The variscite shows high translucency and green zones of different intensities are visible.

Figure 8b: Thin section of colloform variscite V5; fibres have aggregated to form elongated pods, with concentric growth patterns. Magnification 50x.

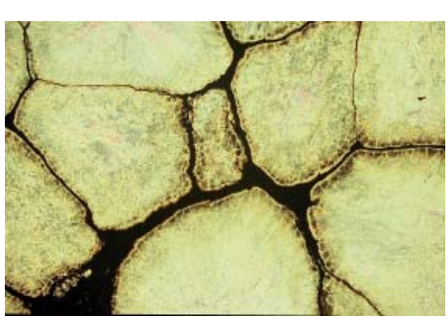

Figure 8c: Thin section of variscite V6 — transverse sections of pods, polygonal forms with reticulate pattern of interstitial remnant brown rock. Border zones of individual pods show desiccation textures. Magnified 50x.

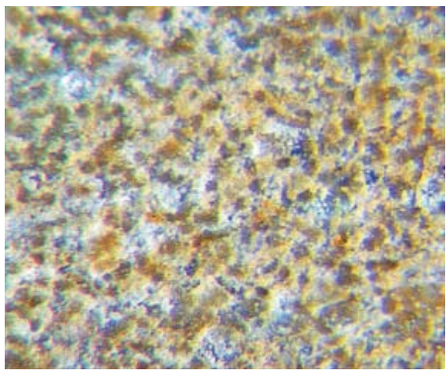

Figure 9a: The brown speckles on this host rock surface are crandallite.

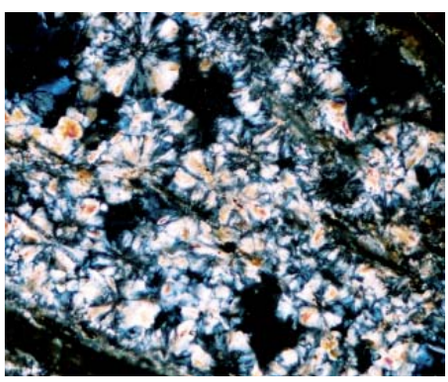

Figure 9b: Thin section showing crandallite microspheres in clouded siltstone. Magnification 50x, cross polarized light.

Table II: Summary of the gemmological properties of 'Woodlands' variscite

Colour	Light bluish-green
	Light to dark green
Diaphaneity	Opaque to translucent
Lustre	Waxy; takes a high polish
Hardness	~ 5
Fracture	Uneven
RI (range)	1.570 to 1.582
SG	2.49 to 2.55
UV fluorescence	Inert to both LW and SW
Chelsea colour filter	Grey to pale pink response
Absorption spectrum	Diffuse bands ~685 nm, 650 nm, 610 nm; absorption of the blue-violet
Microscopic features	Gold inclusions. Matrix: clay, quartz, iron oxides.

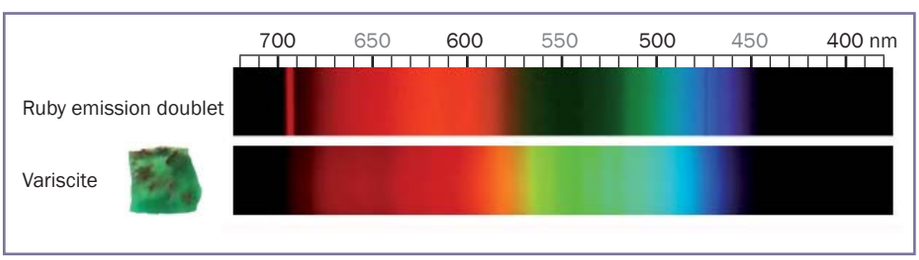

Figure 10: Absorption spectrum of variscite slab V4 ~2 mm thick, from a diffraction grating spectroscope, beneath a synthetic ruby spectrum showing its emission doublet as a calibration marker.

be deformational features caused by close packing and folding of the pods at the time of crystallization. The interstitial material between pods is dark coloured and interconnects, accentuating the reticulated overall pattern. It is optically semi-opaque and grey or brown in colour with red oxide grains. The presence of alunite, kaolinite and xenotime was confirmed using SEM; crandallite and quartz were identified as secondary fillings with layered growth banding; other substances could also be present.

Crandallite

Crandallite ($CaAl_3(PO_4)_2(OH)_5.H_2O$) occurs as a secondary mineral in fine bands (~2-3 mm) throughout some of the host rocks *(Figure 9a)*, especially common in those in contact with variscite. Grains display a range of habits: granules, fibrous sheaves and microspheroids ~25 µm in diameter *(Figure 9b)*. Crandallite in sheaf and spheroidal forms has commonly formed along open gashes and may show concentric growth and sweeping extinction patterns in thin section. In hand specimens some siltstones appear speckled due to the development of spherulitic crandallite.

Jarosite

Jarosite ($KFe_3(SO_4)_2(OH)_6$) is a minor component, occurring as encrustations on, and within, the siltstones as a late secondary mineral and is distinctly yellow or greenish yellow in colour. It is found in veinlets throughout rock fragments of the breccia as well as in fissures through zones of variscite. It occurs as lath-like grains and as fibrous fan-like sheaves. In thin section under crossed nicols it often displays anomalous interference colours of 'Berlin blue'

Quartz

Quartz is common in cross-cutting veins and lenses *(Figure 7b)* within the country rocks and brecciated horizons, and the associated variscite is often coarsely crystalline with hypidiomorphic granular textures. Well terminated quartz crystals occur in open veins and micro vugs where comb structures are also present.

Turquoise

Although not visible in specimens V1–V6, turquoise is reported occurring as thin conformable veins within the host rock (Nickel *et al.,* in press).

Gold

A rare and unique feature of the variscite is the occurrence of native gold as inclusions *(Figure 11a)*. In the group of specimens examined in this study, gold occurs in discrete grains, some as platelets, others as grains with spongy and pelletized surface textures. Grains range in diameter from 25 µ to 100 µ. Gold is most easily visible in the dark green variscite, although it is also reported to occur in massive and colloidal forms within the host rocks (Hancock, 2008). It occurs within the variscite as late syngenetic or epigenetic inclusions. The granules are reported to be of high purity containing no silver and may represent a

re-precipitation of primary gold that has been reported within the sedimentary sequences (Hancock, 2008).

Gemmological characteristics

Appearance

The selected cabochons and carvings fashioned from massive gem variscite *(Figure 6b),* exhibit light to intense green hues with some specimens showing a bluish-green. Most gem variscite is opaque, but portions of the dark green type show a marked degree of transparency. The brown matrix material provides the colour contrast in the characteristic web, cellular and reticulate patterns.

Optical and physical properties

The gemmological properties of the selected variscite cabochons and carvings are summarized in *Table II*. RIs, measured by the distant vision method on cabochons, range from 1.57 for the lighter material, to 1.58 for mid to darker green material. Small birefringence was evident on plane polished surfaces of translucent dark green variscite, and RI readings of 1.578 to 1.582, were recorded. The specific gravity of the variscite cabochons varies due to porosity and composition, from 2.49 to 2.55, the highest value being recorded from dark green material. The properties of this new 'Woodlands' variscite from Western Australia are within the ranges of published values in the gemmological literature (Webster, 1975).

The absorption spectrum of the predominantly translucent variscite V4 *(Figure 10)*, displays a Cr^{3+} spectrum with bands of diffuse absorption in the red at ~685 nm and ~650 nm, and an absorption cut-off below ~465 nm. A diffuse band at ~610 nm is unassigned. The Vis-NIR reflectance spectroscopy section gives a more detailed spectral analysis of the four variscite slabs (see below).

Inclusions

Microscopic examination of several polished specimens of gem quality variscite showed planes of yellowish-gold

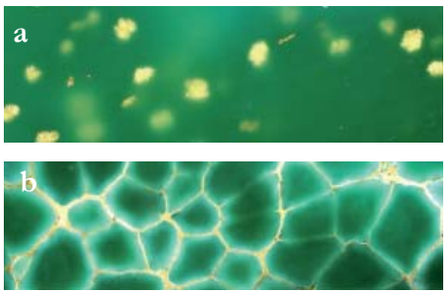

Figure 11: (a) Gold inclusions in variscite V6 between 30 and 100 µm across. Oblique illumination. (b) Reticulate patterning of matrix material outlining variscite pods. Oblique illumination 7x.

opaque inclusions *(Figure 11a)*. SEM-EDS analyses of surface-reaching inclusions confirmed their identity as elemental gold. SEM-EDS and XRD analyses of the brown matrix material, forming patterns within the variscite *(Figure 11b)*, confirm the presence of iron oxides, quartz, and traces of crandallite and alunite.

Mineral identification

Two X-ray diffraction patterns of 'Woodlands' massive gem-quality variscite samples V1and V5 *(Figure 12)* indicate that the dominant phase is variscite. Both patterns match 25-18, International Centre for Diffraction Data (ICDD) database for the 'Meßbach-type' variety of variscite (Salvador and Fayos, 1972). Minor amounts of metavariscite (Kniep and Mootz, 1973) are present in variscite sample V5, and crandallite and alunite are present as traces.

Table III: Chemical composition of 'Woodlands' variscite.

Oxide/ Element	Wt. %			
	V1	V4	V5	V6
Al_2O_3	31.6	32.10	30.6	31.5
SiO_2	0.47	1.04	0.50	1.46
P_2O_5	45.3	45.9	44.4	45.7
TiO_2	0.14	0.31	0.40	0.29
Fe_2O_3	1.37	1.08	1.86	1.27
CaO	bdl	bdl	0.19	0.05
Na_2O	0.08	0.10	0.19	0.12
K_2O	0.13	0.02	0.06	0.02
V_2O_3	0.35	0.32	0.46	0.50
Cr_2O_3	0.09	0.21	0.18	0.16
PbO	bdl	bdl	0.08	bdl
SO_3	0.43	0.09	0.31	0.11
F	0.05	0.10	0.11	0.07
LOI*	21.90	18.50	21.90	17.20
-O=2F	- 0.02	- 0.04	- 0.05	- 0.03
Total	101.89	99.73	101.19	98.42

bdl: below detection limit
* The loss on ignition value (LOI at 1050°C) was used to calculate total water in the formula for V1, V4-6.

V1 $(Al_{0.96}Fe_{0.03}V_{0.01})\Sigma_{1.00}$ $(P_{0.99}Si_{0.01}S_{0.01})\Sigma_{1.01}$ $O_4.1.91\ H_2O$
V4 $(Al_{0.96}Fe_{0.02}V_{0.01}Ti_{0.01})\Sigma_{1.00}$ $(P_{0.99}Si_{0.03})\Sigma_{1.02}$ $O_4.1.6\ H_2O$
V5 $(Al_{0.94}Fe_{0.04}V_{0.01})\Sigma_{0.99}$ $(P_{0.98}Si_{0.01}S_{0.01})\Sigma_{1.00}$ $O_4.1.91\ H_2O$
V6 $(Al_{0.96}Fe_{0.03}V_{0.01})\Sigma_{1.00}$ $(P_{1.00}Si_{0.04})\Sigma_{1.04}$ $O_4.1.6\ H_2O$

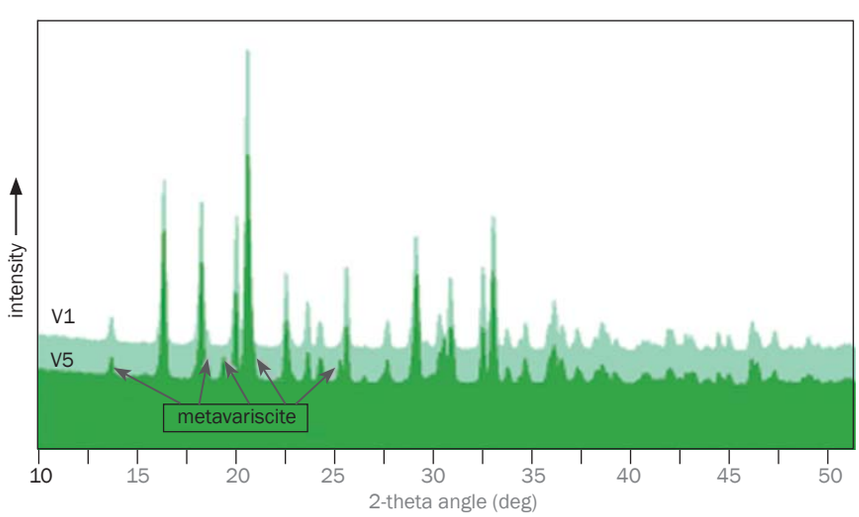

Figure 12: X-ray diffraction patterns of variscites V1 and V5. Patterns displaced vertically for clarity.

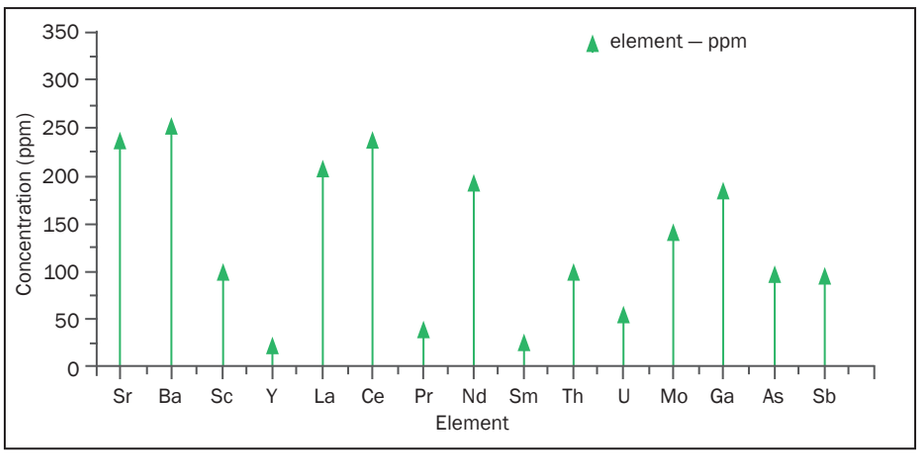

Figure 13: Minor element content of variscite V5.

Chemical composition

The ideal formula for variscite is $AlPO_4.2H_2O$. The results of quantitative x-ray fluorescence analyses of four gem grade 'Woodlands' variscite samples V1, V4-6 are summarized in *Table III*. In addition to the major detectable elements of Al, P and water in the ideal formula, minor amounts of Si, Ti, Fe, V, Cr and S are present. The elements Na, K and F are also present as traces. A separate analysis for the ferrous ion (Fe^{2+}) indicated that it was below the detection limit (bdl); consequently, all of the iron is assigned to the ferric (Fe^{3+}) state.

The vanadium and chromium contents of 'Woodlands' variscite *(Table III)* display a similar chemical fingerprint to the variscite deposits of El Bostal – Zamora (Spain) and Pannéce – Brittany (France), (Querre *et al.,* 2007, fig.1). The mean vanadium content of 2771 ppm and chromium content of 1094 ppm of the four 'Woodlands' variscites result in a vanadium to chromium ratio of 2.5:1, in comparison to ratios of 2.9:1 for El Bostal, and 2.2:1 for Pannéce.

The relatively high lead content of 750 ppm in variscite sample V5 *(Table III)* may signify selective enrichment of isotopes in the variscite and this specimen was also analysed using inductively coupled plasma mass spectrometry (ICP-MS). The results are summarized in *Figure 13* and show that the actinides, uranium (~50 ppm) and thorium (~100 ppm), are in high abundance, indicating the presence of active daughter nuclides and related gamma radioactivity, from the natural decays of U^{238} to Pb^{206}, U^{235} to Pb^{207} and from Th^{232} to Pb^{208} (Senior and Chadderton, 2007). This is consistent with the finding of anomalous radioactivity using a portable field scintillometer in the siltstone layer below seams of variscite (D.Vaughan, pers. comm., 2008).

Also of note is the scandium (Sc) content of 100 ppm, which equates to ~3oz per tonne and is similar to the variscite-Sc association in Utah. In 1942, several hundred pounds of variscite were found in the vicinity of the Utahlite mine, Utah, whilst the area was being prospected for scandium (Novak, 1982).

A sample of gem grade variscite analysed for elemental gold by neutron activation, contained 17.5 ppm gold.

Table IV: Absorption band centre wavelengths and band assignments in variscite.

Sample				Band assignment	Reference
V1	V4	V5	V6		
Band centre (nm)					
520	525	535	525	Transmission window	
-	-	-	424	Fe^{3+} ions	Calas *et al.,* 2005
-	451	-	-	Cr^{3+} v2 transition, $^4A_{2g}(F) \rightarrow {}^4T_{1g}(F)$	Calas *et al.,* 2005
631	630	629	631	Cr^{3+} v1 transition, $^4A_{2g}(F) \rightarrow {}^4T_{2g}(F)$	Calas *et al.,* 2005
655	656	656	655	Cr^{3+} spin forbidden transition, $^4A_{2g}(F) \rightarrow {}^2T_{1g}(G)$	Balan *et al.,* 2002 Calas *et al.,* 2005
690	690	690	690	Cr^{3+} spin forbidden transition, $^4A_{2g}(F) \rightarrow {}^2E_g(G)$	Balan *et al.,* 2002 Calas *et al.,* 2005
861	855	856?	857	Vanadyl, VO^{2+}, groups	Calas *et al.,* 2005
nd	886	888	887	Vanadyl, VO^{2+}, groups (?)	Calas *et al.,* 2005
1179	1177	1174	1175	OH overtone?	
1240	1239	1237	1239	V^{3+} spin forbidden transition, $^3T_{1g}(^3F) \rightarrow {}^1E_g(^1D),{}^1T_{2g}(^1D)$	Alda *et al.,* 2003
1281	1279	1280	1279	Unassigned	

NB: Band centre values are averaged from reflectance measurements for both the polished and unpolished surface of each variscite slab.
nd: not determined. The absorption band was too broad to accurately determine a centre position.

Vis-NIR reflectance spectroscopy

Colour properties: chromophores

Reflectance spectra for each unpolished surface of the four slabbed variscite samples V1, V4, V5 and V6 are presented in *(Figure 14a)*. The relatively greater overall reflectance ratio (albedo) of V1 is due to its opaque nature compared to the other variscite samples, which are near-translucent (i.e. gem-quality). The slabbed form allows transmission of some incident illumination with a corresponding reduction in the overall albedo, but the wavelengths of measured absorption bands are not affected.

The main absorption activity occurs in the visible to near-infrared wavelength range from 400 to ~1500 nm *(Figure 14b)*.

Ornamental variscite: A new gemstone resource from Western Australia

Absorption features in the shortwave infrared wavelength range, 1500 to 2500 nm, are generally weak, broad and poorly resolved. The broad band between 1460 and 1879 nm may be related to SO_4 groups of minor associated mineralogy (e.g., jarosite), whereas the sharp feature near 1430 nm can be assigned to OH vibration overtones of structural water within variscite. However, the main absorption activity occurs in the 400 to 1500 nm wavelength range, and it is this region that is the focus.

Wavelengths and band assignments of measured absorption features are listed in *Table IV*. The transmission window/maximum reflectance for variscite V1 is on the edge of the green at 520 nm, whereas transmission windows in samples V4–V6 shift towards the mid-green at ~528 nm. Two main absorption bands were detected at 520–750 nm (centre ~630 nm) and 750-1100 nm (centre ~865 nm); with the former band related to chromium and the latter feature due to vanadium. In octahedral co-ordination Cr^{3+} shows two absorption bands arising from the spin-allowed v1 and v2 transitions at 629 and 444 nm, respectively (Calas *et al.,* 2005). Whilst all measured variscite samples show a prominent Cr^{3+} spin-allowed v1 band, the v2 transition was not fully resolved in any of our variscite samples. Instrument noise at wavelengths <450 nm, together with the increasing absorption tail near 400 nm due to ligand-metal-charge-transfer (LMCT) from bands such as O-V in vanadyl and possibly O-Fe due to Fe^{3+} replacing Al in variscite, interfered and obscured the Cr^{3+} v2 transition at near-UV wavelengths.

The weak but sharp absorption features on the high wavelength side of the v1 transition at 655 nm and 689 nm (Figure 14b) are characteristic of Cr^{3+} in octahedral co-ordination (Calas *et al.,* 2005). Their detection confirms the presence of Cr^{3+}, rather than V, as the main chromophore in variscite (Calas *et al.,* 2005). Similarly, detection of these spin-forbidden transitions in spectra measured for dickite also confirmed the incorporation of Cr^{3+} within the structure of this clay mineral (Balan, *et al.,* 2002).

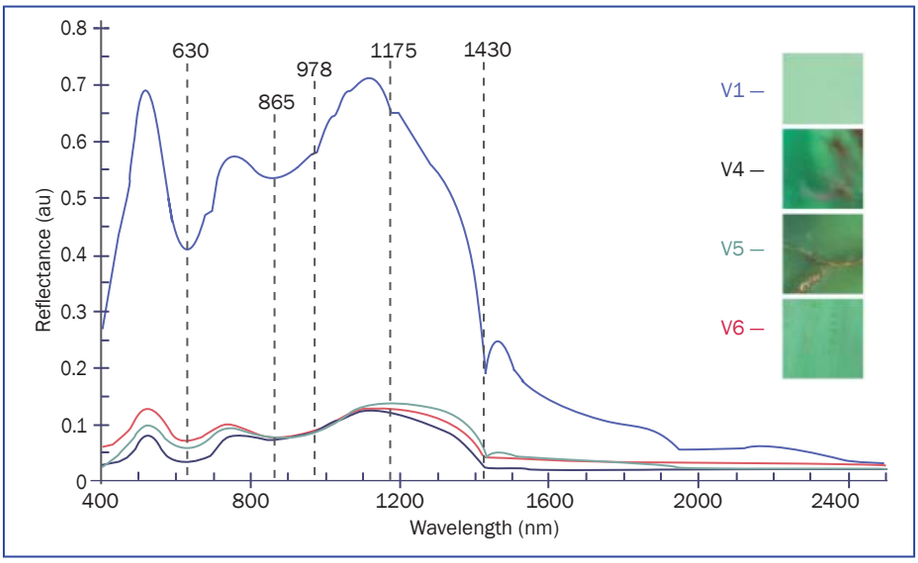

Figure 14a: Reflectance spectra for the unpolished surface of four slabbed variscite samples. The sharp features at approximately 978 and 1430 nm are overtones of OH vibrations from structural OH in variscite and are not listed in Table IV. Reflectance spectra have not been vertically offset.

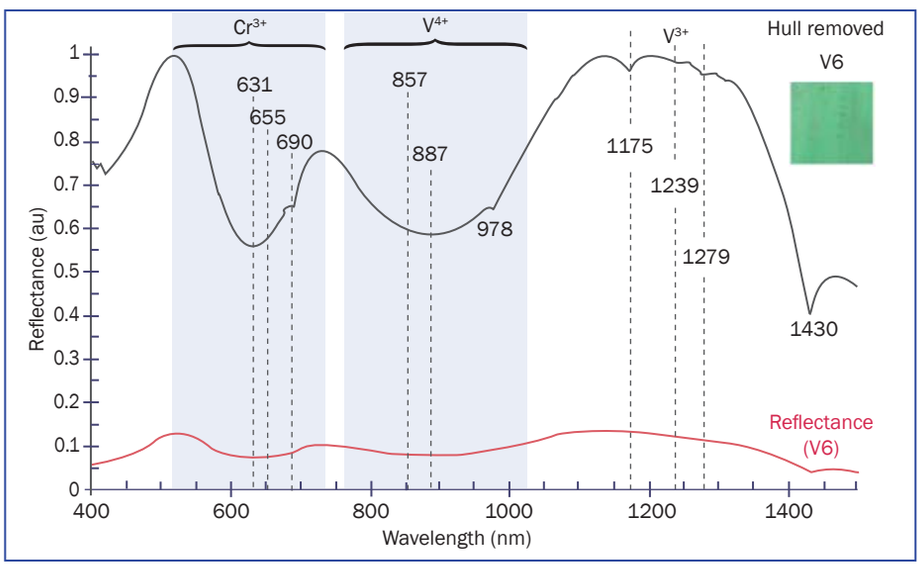

Figure 14b: Reflectance (red curve) and Hull removed spectra (black curve) for variscite V6, showing detail of absorption features in the 400 to 1500 nm wavelength range. The Hull removed spectra helps to emphasize small absorption features not easily resolved in the reflectance spectrum. Absorption features at 978 and 1430 nm are overtones of OH vibrations from structural OH in variscite and are not highlighted. The spectra have not been vertically offset.

The second main absorption band, centred at ~860 nm can be assigned to vanadyl, VO^{2+}, groups with V in the +4 oxidation state. Splitting of this band by an additional feature at 890 nm *(Table IV)* produced an asymmetric broadening to longer wavelengths. However, the smaller longer wavelength feature at 1240 nm, assigned to V^{3+} indicates that V in variscite may be in a mixed oxidation state. Vanadium can occur in either the +2, +3, +4 or +5 oxidation states, with transport of V^{4+} and V^{5+} in the fluid state being the most common (Schindler *et al.,* 2000). Recent optical absorption spectra recorded for variscite and metavariscite, detected only a very weak feature near 870 nm, which was interpreted by Calas (2005), supported by other data, as indicating little V^{4+} but substitution of PO_4 tetrahedra by V^{5+} as vanadate groups.

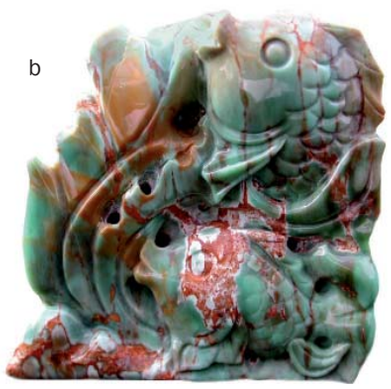

Figure 15: (a) Variscite carved in contemporary freeform style; height 11 cm. Carved by Dalan Hargrave, U.S.A.
(b) Chinese carving of variscite in traditional style; height 4.5 cm.

Discussion and summary

Variscite as an ornamental mineral is used in its microcrystalline and massive form and has adequate hardness for carved objects to take a good polish. Its attractive colour and appearance in complex textural patterns have contributed to its popularity *(Figures 15* and *16)*.

Although the exploitation of variscite has a long history, there have been few sources of ornamental quality material worldwide. Much of the variscite currently marketed is from stockpiled material from known and inactive occurrences principally from the states of Utah and Nevada, U.S.A. Some of this material has been collected on a casual basis from old workings, sites that are also visited by researchers and private mineral collectors. In contrast, non-gemmological low-grade variscite and microcrystals are not uncommon and are recorded from many countries.

Western Australia is now a source of ornamental quality material and deposits on the Woodlands sites have considerable economic potential. The deposits are situated within fine-grained dominantly argillaceous rocks of extensive occurrence, where gold is known to be present. The variscite occurs together with several minor minerals, notably crandallite, alunite, iron oxides and quartz; these minerals may be present within the ornamental grade material. Metavariscite was found to occur more commonly within pale coloured and partly altered variscite material. The presence of gold granules as co-genetic inclusions within the variscite is of great interest as a rare gemmological phenomenon and provides the prospects with added economic potential.

The variscite seams are generally <100 mm wide, limiting thickness of useable material and typical examples of carved, cut and polished variscite are illustrated. Larger objects can be worked from material using other directions and incorporating matrix material. The somewhat porous nature of variscite, due to its fibrous nature, may result in discoloration if in contact with certain liquids, and tests using refractive index oils, for example, resulted in yellowish staining.

The matrix material in the variscite with a reticulate pattern can be both friable and porous, and like turquoise, would need to be stabilized with wax or resins to avoid accidental damage and permanent

Figure 16: Variscite fish; dimensions 35 cm x 25 cm, ~4 kgs. Eyes fashioned from hessonite garnet. Carved by Robert Jüchem, Idar-Oberstein, Germany.

discoloration. Some cut material has been impregnated with cyanoacrylate, an acrylic resin, to stabilize the interstitial materials and obviate damage.

Reflectance spectra indicate that the chromium Cr^{3+} ion is the main chromophore responsible for the attractive green colour of 'Woodlands' variscite. Early indications show that variscite can incorporate vanadium (V) in a number of oxidation states. Reflectance spectroscopy may enable a quick assessment of V oxidation state(s) and this may provide an indicator of the conditions under which the formation of variscite occurred. X-ray adsorption spectroscopy (XAS) studies of the 'Woodlands' variscite are currently part of an investigation into the nature of and the potential relationship between gold mineralization and the oxidation state of V in variscite.

Acknowledgements

The authors wish to thank exploration licence holders David Vaughan and Glenn Archer, of Australian Outback Mining Pty. Ltd., for the generous supply of gem-grade variscite used in this study; David Vaughan for the preparation of plane plates of variscite, and loan of carvings and cut specimens for testing and photographing; Dr Michael Verrall for collection of the XRD and SEM data and assisting with data interpretation; Dr E. Nickel, Research Fellow, CSIRO (ARRC), is acknowledged for verification of 'Meßbach-type', crystals of variscite and wardite, and assisting with the empirical formula; John Harris for digital capture of the visible spectrum©; Dr Ian Robertson, CSIRO (ARRC), for use of the camera for photomicroscopy; Josep Bosch, Curator Neolithic Mines, Gavà, for loan of the image of the collar necklace; David Willing, for digital imaging; Francine Payette for sourcing some references; Dr Vernon Stocklmayer for critiquing the manuscript. We would also like to thank the Library staff at the CSIRO, Divisions of Floreat and Kensington (WA), and staff at the Geological Survey, Library WA.

Photo credits

Henri Oorjitham: 1a, 15a. Josep Bosch: 2a. Susan Stocklmayer: 1c, 2b, 3, 4, 7a, 7b, 8a. Margot Willing: 1b, 5a, 5b, 6b, 11a, 11b, 15b, 16. Ian Robertson: 5c, 8c, 9a. Ernest Nickel: 5d. Ian Pontifex: 7c, 7d, 8b, 9b. John Harris: V1, V4, V5, V6, 10.

References

Alda, E., Bazán, B., Mesa, J.L., Pizarro, J.L., Arriortua, M.I., and Rojo, T., 2003. A new vanadium (III) fluorophosphate with ferromagnetic interactions, (NH_4) $[V(PO_4)]$. *Journal of Solid State Chemistry,* **173,** 101-8

Arribas, A., Burg, J., and Nicolaou, J., 1970. New occurrence of precious variety of variscite in Spain. *Lapidary Journal,* **24**(5), 764

Balan, E., Allard, T., Morin, G., and Calas, G., 2002. Incorporation of Cr^{3+} in dickite: a spectroscopic study. *Physics and Chemistry of Minerals,* **29**, 273-9

Bauer, M., 1904. *Precious Stones*. Charles Griffin and Company Ltd., London. 403

Calas, G., Galoisy, L., and Kiratisin, A., 2005. The origin of the green colour of variscite. *American Mineralogist,* **90**, 984-90

Camprubi, A., Malgarejo, J.C., Proenza, J.A., Costa, F., Bosch, J., Estrada, A., Borell, F., Yushkin, N.P., and Andreichev, V.L., 2003. Mining and geological knowledge during the Neolithic: a geological study on the variscite mines at Gavà, Catalonia. *Episodes*, **26**(4), 295-301

Cassen, S., 1998. Parameters of the neolithisation in the west of France: From the circulation of prestige goods to the invention of symbols. 63rd Annual Meeting of the Society for American Archeology in the symposium: *Prehistoric communication: The first wheels, roads, metals, and monumental architecture*

Clark, A.M., 1993. *Hey's Mineral Index: Mineral Species, Varieties and Synonyms*. Chapman and Hall and The Natural History Museum, London

Crummy, N., 1983. The Roman small finds from excavations in Colchester 1971–1979. *Colchester Archaeological Report 2* (Colchester Archaeological Trust Ltd), 34

Dana, E.S., 1892. *The System of Mineralogy of James Dwight Dana*. 6th Edn. John Wiley & Sons, Inc., 824

Dickerson, P., 1971. New notes from Utah's treasure chest. *Lapidary Journal,* **25**(6), 830-41

Doelling, H. H., 1980. Geology and Mineral Resources of Box Elder County, Utah. *Utah Geological and Mineral Survey Bulletin,* **115**, 228-9

Dominguez–Bella, S., 2004. Variscite, a prestige mineral in the Neolithic-Aeneolithic Europe. Raw material sources and possible distribution routes. *Slovak Geol. Mag.,* **10**(1-2), 147-52

Forde, C.D., 1930. On the use of greenstone (jadeite, callais, etc.) in the Megalithic Culture of Brittany. *The Journal of the Royal Anthropological Institute of Great Britain and Ireland,* **60** (Jan-June), 211-34

Harrison, R.J., and Orozco Köhler, T., 2001. Beyond characterization. Polished stone exchange in the western Mediterranean 5500-2000 BC. *Oxford Journal of Archaeology,* **20**(2), 107-27

Hooley, D., 1988. General points from an accident of fortune. *Archaeology in York Interim,* **13**, 15-24

Kniep, R., and Mootz, D., 1973. Metavariscite — A redetermination of its crystal structure. *Acta. Crystallographica,* **B29**, 2292-4

Larsen, E.S., 1942. The mineralogy and paragenesis of the variscite nodules from near Fairfield, Utah. Part 3, *American Mineralogist,* **27**, 441-51

Laurs, B.M., Fritz, E.A., and Koivula, J. I., 2007. *Gems & Gemology,* **43**(1), 63-4

Meireles, C., Ferreira, N., and de Lourdes Reis, M., 1987. Variscite occurrence in Silurian Formations from Northern Portugal. *Comun. Serv. Geol. Portugal,* **73**(1/2), 21-7

Middleton, A., La Niece, S., Ambers, J., Hook, D., Hobbs, R., and Seddon, G., 2007. An elusive stone: the use of variscite as a semi-precious stone. *British Museum Technical Research Bulletin,* **1**, 29-34

Muhling, P.C., and Brakel, A.T., 1985. Geology of the Bangemall Group-the evolution of an intracratonic Proterozoic basin. *Western Australia Geological Survey Bulletin,* 128

Neal, D. S., 1974. *The excavation of the Roman Villa in Gadenbridge Park, Hemel Hempstead 1963-1968.* The Society of Antiquaries, London

Nickel, E.H., Hancock, E., Thorne A., Hough, R., Vaughan, D., and Verrall, M., 2008. *Woodlands variscite — gold occurrence in the North Gascoyne region of WA* (in press)

Novak, G.A., 1982. Verde web variscite from Lander County, Nevada. *Lapidary Journal,* **36**(3), 544-52

Querre, G., Herbault, F., and Calligaro, Th., 2007. Long distance transport of Neolithic variscite ornaments along the European Atlantic arc demonstrated by PIXE analysis. *Proceedings of the XI International Conference on PIXE and its Analytical Applications, Pueblo, Mexico, May 25-29,* 1-5

Salvador-Salvador, P., and Fayos, J., 1972. Some aspects of the structural relationship between 'Messbach-type' and 'Lucin-type' variscites. *American Mineralogist,* **57**, 36-44

Schindler, M., Hawthorne, F.C., and Baur, W. H., 2000. A crystal-chemical approach to the composition and occurrence of vanadium minerals. *The Canadian Mineralogist,* **38**, 1443-56

Senior, B.R., and Chadderton, L.T., 2007. Natural gamma radioactivity and exploration for precious opal in Australia. *The Australian Gemmologist,* **23**(4), 160-76

Simpson, E.S., 1952. *Minerals of Western Australia Vol. 3.* William H. Wyatt, Perth, 690–5

Thomssen, R.W., 1991. Forgotten phosphates of Fairfield. *Lapidary Journal,* **45**(4), 46-56

Webster, R., 1975. *Gems - Their Sources Descriptions and Identification*, third edn. Newnes-Butterworths, London, 322-3

Websites

Hancock, E., 2008. Gold-Variscite mineralization in the Bangemall Supergroup at Woodlands, Western Australia. http://www.wa.gsa.org.au/WAG/WAG_Feb-Mar_2008.pdf (p.13)

Mindat http://www.mindat.org/

Australian Outback Mining http://www.outbackmining.com/

Dietrich, R.V., http://www.cst.cmich.edu/users/dietr1rv/variscite.htm

The Authors

Margot Willing FGAA DipDT
Perth, Western Australia. email: margotwilling@iinet.net.au

Susan Stocklmayer FGA
Perth, Western Australia. email: nyanga@icenet.com.au

Dr Martin Wells
Perth, Western Australia. email: Martin.Wells@csiro.au

Visually distinguishing A-jadeite from B-jadeite

Li Jianjun, Liu Xiaowei, Zhang Zhiguo, Luo Yueping, Cheng Youfa and Liu Huafeng

Abstract: Jadeite grades A and B are described in the context of the Chinese gem trade. Visual distinction of the grades is described, illustrated and discussed in terms of surface lustre, distribution of colour, nature of inclusions, internal reflection of light, microfractures and features of the fashioning of various items. Development of these recognition skills is recommended but recourse to the laboratory should always be an option for difficult items.

Keywords: China, gem grading, jadeite, treated gems, visual skills

Introduction

The rapidly growing popularity of collectables has caused increasing interest in jadeite items, especially by ordinary Chinese citizens, and there is no reason to believe the enthusiasm will diminish in the future.

Determining the authenticity and values of jadeite items can be difficult problems. Their valuation involves many contentious issues but one of the most important is differentiating between A-jadeite, the natural and non-improved jade, and B-jadeite which is the clarity enhanced version of natural jadeite. This is especially important in commercial circumstances.

The ordinary dealer or collector is not generally familiar with professional gem identification instruments, and the absence of detailed technical knowledge about the production of B-jadeite, even amongst traders, means that evaluations made using basic instruments such as the magnifier may not be reliable. Being able to identify the different versions of jadeites simply by sight is, nevertheless, a highly desirable skill.

Definitions of A-jadeite and B-jadeite

The identifications of A-jadeite and of B-jadeite can only be undertaken when the precise definitions of these materials are understood. However, in China, there is no formal description in any Chinese National Standard and the distinction between them is yet to be established, especially for commercial use in this country.

It has been widely believed that A-jadeites have been only cut and polished without changing their appearance or durability, while B-jadeites have been acid treated and the developed cavities and pores have been filled with organic compounds (Fritsch *et al.,* 1992).

Organic compounds such as waxes, resins and epoxies can be difficult to identify when they have been applied as sealants and fillers. They are best detected and characterized using the infrared spectrometer but this instrument was not readily available in China until about 1996. Alternatively, a hot wire can be a useful preliminary means of detecting organic filling although it can be mildly destructive.

Jadeite carvers insist that a final sealing with wax is an essential completion step even for non-enhanced jadeite items. However, it is not really practical to attempt to distinguish between wax applied for polishing and that applied for filling cavities and pores produced by acid treatment. This resulted in wax-treatment for jadeites being listed as an enhancement in the 1996 edition of the Chinese National Standard (AQSIQ, 1996). In spite of this, it is currently widely accepted in the trade that such jadeite items treated with wax just for surface glazing can still be classed as A-jadeite, and therefore, the wax-filling does not need to be disclosed in sale notes or certificates.

Recently, it has been observed that some jadeite items had been excessively treated with wax or other sealants to well beyond that appropriate for finishing jadeite carvings. Gas bubbles are present in some of this material and can be seen with only the 10x loupe, sometimes even without a lens. Consequently, the 2003

©2008 Gemmological Association of Great Britain

edition of the Chinese National Standard (AQSIQ, 2003) listed such impregnation with wax or sealant as the commercially-defining treatment for B-jadeite.

Heat can also be used to turn some iron-pigmented jadeite red, and in the Chinese National Standard this colour-changing heat-treatment is also considered to be an enhancement (AQSIQ, 2003). However, such thermally treated jadeite still is considered to qualify as A-jadeite in a commercial sense.

Therefore, the definition of A-jadeite which is accepted in the Chinese gem trade is as follows. Type A-jadeite is jadeite that has only been treated by carving, polishing, or surface-filling with just a little wax to finalize the lustre development; additionally, heating to develop red colours and surface treatment with a mildly-bleaching acid such as oxalic acid or waxberry acid (but without damaging the structural integrity of the stone) are also considered to still qualify as A-jadeite (waxberry acid is derived from the China waxmyrtle or China bayberry of the family Myricaceae).

The accepted definition of B-jadeite is as follows. Type B-jadeite includes jadeite items which have been leached by strong acid and the resulting pores and cavities then filled with sealant such as a polymer (Fritsch *et al.*, 1992) or with wax, the latter of course being less durable or permanent than a thermoset polymer like an epoxy resin.

C-jadeite is generally understood to mean dyed jadeite, but without impregnation of sealant. This is not discussed in this paper.

B-jadeite production

In order to appreciate some of the more subtle differences between A and B-jadeite, the production process of B-jadeite is outlined below. Starting material appropriate for treatment is selected. Its grain size and structure should be coarse and conspicuous so that strong acid will easily attack and erode the undesirable components in the jadeite. Suitable material is generally of lower grade which enables a greater profit margin and it often contains numerous black inclusions of various kinds. The material is sliced and roughly formed. The thickness of the slices should not be significantly greater than that of the intended roughly formed items such as bracelets, because the time required for the acid to penetrate and affect depths of more than about a centimetre is excessive, which is unsatisfactory and expensive. The items are then treated with a solution of a strong mineral acid and controlled heating may also be beneficial to accelerate the action. After sufficient time in acid treatment the items are washed at least twice in aqueous solutions of alkali to neutralize any residual acid and are then rinsed. A second treatment with a much weaker solution of acid is generally conducted followed by a wash with a weak alkali solution and a final rinse in water prior to drying in the open air. Thus, the product is porous and chalky. (If the operator wants to produce B+C jadeite, porous and chalky zones on the items are selectively treated by hand with solutions of various dyes of appropriate colours which are readily absorbed to produce simulated patterning and colours resembling that of better quality untreated natural jadeite.) Finally the items are dried and then submerged into a melted or liquid sealant such as resin or uncured polymer and the air remaining in the pores and cavities in the jade is pumped out under vacuum. Releasing the vacuum then allows the atmospheric pressure to force the sealant to impregnate the voids. If necessary, the material is then cooled and is ready for carving.

Key points to be considered in visually identifying A and B-jadeite

Some of the rather subjective factors which can be used to distinguish A-jadeite from B-jadeite are listed and are then discussed in more detail below. Integration of these considerations can then usually result in a moderately reliable assessment of whether the item can be categorized as A-jadeite or B-jadeite:

1. surface lustre or comparative reflectance differences
2. distribution of coloration on the surface
3. nature of the internal inclusion patterns
4. internal reflection of light resembling the adularescence of moonstone
5. presence of micro-fractures
6. size of the item and the quality and intricacy of the carving

Visually identifying jadeite as type A or B requires careful and thorough examination with attention to all of these points in order to avoid erroneous conclusions.

Discussion of the key points

1. Authenticating jadeites based on differences in surface reflectance or lustre

When viewed under a suitable light source, larger polished items with substantial curved or comparatively flat surfaces may provide detectable differences in reflectance of A-jadeite surfaces *(Figure 1)* compared with those of B-jadeite. The more reflective glazed surface with a brighter vitreous gloss of A-jadeite contrasts with that of the generally less-reflective polymer-impregnated B-jadeite.

Localized zones (or belts) of surface area may also show distinct variations in the natures of the reflective highlights between A- and B-jadeites such that they are really more a difference of brightness than of colour. Imagining the view of the jadeite to be just a black and white image can improve comparative assessments of the relative intensities of these localized reflections.

2. Surface 'colour levels'

If A-jadeites with high transparency and an even texture are viewed with strong light, (for example, direct sunlight), the surface will appear to develop a 'cold' colour tone *(Figure 2)*. This effect can also occur on A-jadeites with an intrinsically 'warm' colour such as a yellow through brown to a red (see *Figure 3*). The appearance is probably a subjective mental evaluation of the sharpness of

Figure 1: Example of vitreous reflection which is sharply defined and three light belts with sharp boundary on the back leg of the carving, characteristic of A-jadeite.

Figure 2: 'Cold' colour sharp reflections on the surface of a green A-jadeite carving.

Figure 3: 'Cold' colour of well-defined reflections also observed on the surface of A-jadeite with a yellow-brown 'warm' body tone compared to the 'cool' green of the jadeite in Figure 2.

Figure 4: Clear colour boundaries and unaltered green core zones in partially weathered jadeite, characteristic of A-jadeite.

Figure 5: An exquisite 'qiao se' effect, which describes the use of different colour zones in the A-jadeite to artistically demonstrate the uniqueness of the piece.

the reflected images rather than any real difference in true colour perception, analogous to the 'hard' and 'cold' crisp brilliance of a well-faceted white diamond compared to the more 'soft' and 'gentle' appearance of most of its less refractive simulants. This elevated level of 'cold' contrast generally appears only on the surface of A-jadeite, presumably because the lower refraction of most of the organic sealants and impregnation agents used for B-jadeite leads to its lower reflectivity. Even most lay people who are usually uninformed in the intricacies of jadeite treatments can appreciate this distinction without difficulty, so that when two different polished glossy objects without much difference in body colour, although with distinct differences in reflectivity are compared, impressions of different 'colour tones' of 'cold' colour and 'warm' colour are perceived.

Sections of strong cold colour reflections which glisten with slight movement of the light source or specimen can be observed at different locations on the surface of A-jadeite pieces, but these crisper 'cold' colour reflections are less common on B-jadeite items with their contents of sealants and fillers.

3. Inclusions

Natural inclusions in jadeites can include brown or various alternatively coloured substances, black minerals and 'catkin' pellets. The externally oxidized and differently coloured weathering shell surface of rough jadeites is a common epigenetic alteration, and its deliberate retention in jadeite carvings to provide aesthetic colour contrasts generally indicates A-jadeite. However, false or simulated 'weathering shells' may also be encountered. Genuine weathering shells exhibit intense colour gradations and clear boundaries between the oxidized zone and the less affected interior. A genuine weathering shell gives the impression that the oxidation colours have diffused from outside to inside, but a dyed imitation or false weathering shell gives a contrary impression. A genuine weathering shell of a brown oxidized zone encapsulating an unaltered green core is illustrated in *Figure 4*.

Modern technology is now quite capable of imitating the brown component that earlier was considered to be evidence of untreated A-jadeite so that its presence is now less useful for differentiating A- from B-jadeites. However, there may be other evidence that can indicate A-jadeite rather then B-jadeite, such as a very fine quality of the carving technique, as well as 'qiao se' (a feature indicating the skill in exploiting the irregular distribution of the best natural colour to the best effect in the available material as shown in *Figure 5*).

Black oxide inclusions mainly consist of chromite, magnetite or franklinite (a zinc, manganese and iron spinel), apparent as opaque black dots and speckles. These black oxide particles commonly accompany the jadeite's brilliant green, lavender or grey body colours which are developed by naturally incorporated transition metal ions such as those of chromium, manganese and

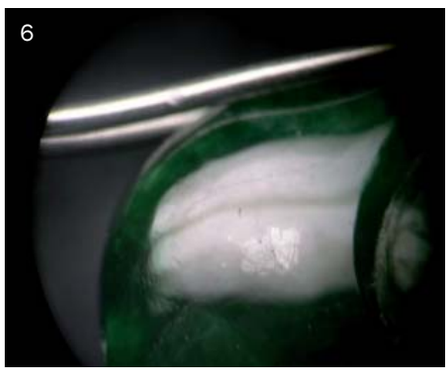

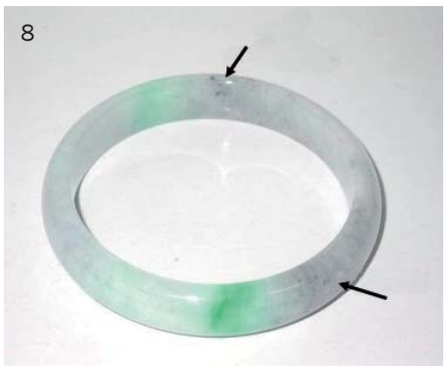

Figure 6: Reflective inclusion with metallic lustre exposed at the jadeite surface; diagnostic evidence of A-jadeite.
Figure 7: Black inclusion in a vivid green A-jadeite.
Figure 8: Black inclusion within a mottled grey and green jadeite, indicating that it is probably A-jadeite.
Figure 9: Greenish-blue epigenetic inclusion on a mesh-textured surface of an A-jadeite.
Figure 10: A-jadeite with greenish-blue inclusion when observed in transmitted light.

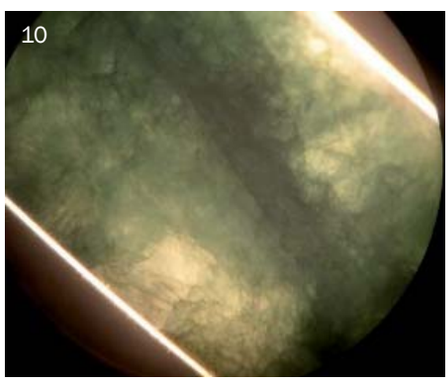

iron. Reflections produced by natural dark inclusions with a metallic lustre such as pyrite may indicate A-jadeite (see *Figures 6, 7* and *8*), but one should also be aware that small black particulate inclusions can equally be found in the B (and C) grades of jadeite. Sometime the man-made black spots in B- (and C-) jadeite will puzzle the dealer who thinks that they occur only in A-jadeite.

Surface characteristics caused by greenish-blue secondary inclusions (similar to dyed jadeite) in A-jadeite (as shown in *Figures 9* and *10*) can be similar to those in B-jadeite. Typically in A-jadeite, one usually sees brown epigenetic inclusions that are absent in dyed jadeite and, in terms of the Chinese jadeite trade, its appearance (as shown in *Figures 9* and *10*) is described as 'coarse ice dizi' ('dizi' being a description applied by Chinese jadeite specialists to specify texture of jadeites), which indicates a texture like granular ice. Compared with B-jadeite, A-jadeite can display orientation of crystal growth, partially radiated aggregates, and more often display longer prismatic crystals (as shown in *Figure 10*).

In A-jadeite with good 'shui tou' (transparency), there are commonly isolated centres of white cotton-like fibres which are roughly spherical as shown in *Figures 11* and *12*. They resemble the onset of flocculation in a solution, and such features can also be present in B-jadeite; however, in much B-jadeite polymer filling changes the appearance to tangled fibres or wisps as shown in *Figure 13*.

4. Internal behaviour of light resembling adularescence

The combination of reflection, refraction, scatter, interference and diffraction of light from many tiny crystal faces and fissures in jadeite commonly creates an effect resembling adularescence, commonly yellow.

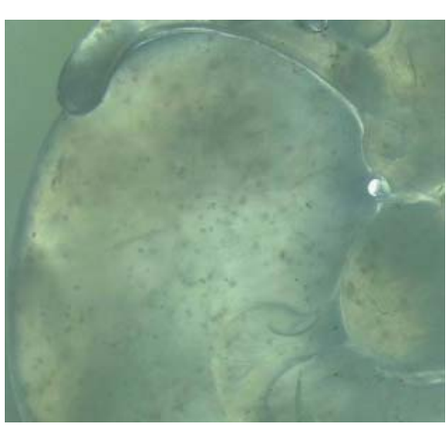

Figure 11: A-jadeite with roughly spherical separate centres of white cotton-like inclusions.

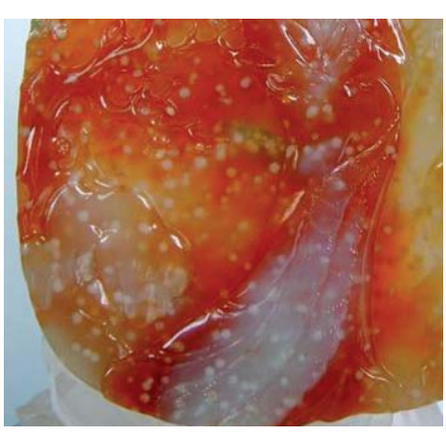

Figure 12: Isolated round cotton-like inclusion in A-jadeite.

Figure 13: Blurry irregular cotton-like inclusions in B-jadeite.

Figure 14: A-jadeite with good 'shui tou' showing yellow internal reflection.

A-jadeite has a distinctly 'cold' surface lustre but a 'warm' glow from internal reflected light, while B-jadeite does not have these features. Even on a blue background an A-jadeite with good 'shui tou' (transparency) shows a warm reflection from its interior in *Figures 14*, *15* and *16*.

In *Figure 15a* the halo around the Buddha's head shows a yellow glow typical of A-jadeite, while the B-jadeite in *Figure 15b* shows a white-blue tone in the halo. This latter effect is due to the treatment with polymer and some fluorescence.

It is worth noting the highly reflective area on the surface of the Buddha in *Figure 15a*, which suggests that the surface is very smooth, in contrast to that of the piece shown in *Figure 15b* which has poor lustre and probably a coarse surface microstructure.

Figure 15: Two Buddha carvings. The halo around the head in (a) exhibits a yellow glow characteristic of A-jadeite, while the halo in (b) exhibits a white-blue reflection, characteristic of B-jadeite.

Figure 16: A yellow glow is visible in the beads in the upper part of the A-jadeite carving.

This internal reflection resembling adularescence is a significant identification feature for A-jadeites because even in some jadeites with poor transparency, there can be small regions of nice transparency and even texture which generate this phenomenon.

Such an effect is absent in B-jadeite as the polymer (whose refractive index is closer to jadeite than that of air in micro-space) effectively reduces the odds of reflection (on the crystal faces and micro-fissures faces) and scatter (among the micro-crystals) of the transmitted light. Additionally the polymer's fluorescence is often blue-white. So it shows white in B-jadeite (in *Figure 15b*).

5. Authenticating jadeites based on tiny fissures:

In A-jadeite, especially jadeite with poor 'shui tou', fissures between crystals (probably stress-induced) can often be seen (*Figures 17, 18* and *19*). In B-jadeite, the filling of the interior fissures with modern polymers makes them less apparent.

The jadeite ring in *Figure 17* has a texture resembling broken ice and, in addition, in the upper part, when one observes it in transmitted light, it appears yellowish because of the scattered light (soft glow or effect resembling adularescence) which is also characteristic of A-jadeite.

Figure 17: The tiny fissures in this A-jadeite create an appearance like broken ice.

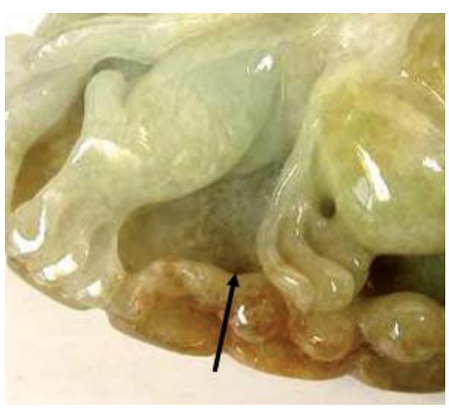

Figure 18: A-jadeite carving with a concave hollow in which fissures and crystal faces appear like broken ice.

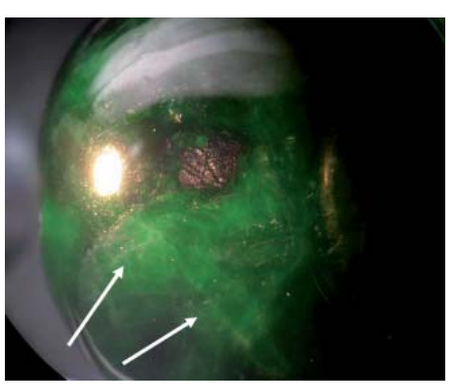

Figure 19: A-jadeite with white ridges, mid-left of picture, resulting from light reflected from linear fissures, characteristic of A-jadeite.

In *Figure 19*, the colour of the fissures on the left is whiter than the body colour of the jadeite; the white fissures are the sign of A-jadeite. Towards the centre of

the picture, and below the black metallic inclusion, is an array of fissures in a sinuous zone which also indicates that the jadeite is A-grade. In B-jadeite interior fissures are commonly difficult to see and at the surface they appear as veins like earthworm traces. However, ageing B-jadeites may also develop fissures on exposure to hot light, especially the lights in showcases.

In the A-jadeite carving in *Figure 20*, on the right of the picture, the ear of the pixiu (a legendary animal which can bring good luck) appears white. This is because the colour of the pixiu body or the green grain (called the 'colour root' in China) is blocked by a noticeable fissure just under the ear. This effect would not show in B-jadeite because the colour would not be blocked; the colour of the 'colour root' would diffuse through the fissures, a phenomenon which Chinese experts call 'colour drifting'.

The 'colour root' and 'colour drifting' are thus important concepts in identifying A- and B-jadeite in China.

There are two types of 'colour root', one with boundaries and one without. Disappearance of the colour of a jadeite at a big fissure indicates an A-grade stone, while the disappearance of colour where texture remains unchanged indicates B-jadeite.

'Colour drifting' is dependent on the texture and grain of the jadeite, and while common in B-grade stones, is not restricted to them. Imagine compacted snowballs on which a drop of ink is applied. The ink will migrate along grain boundaries and the whole mass will assume some colour. In the terms of the Chinese gem trade, 'dizi (texture) eats colours' and 'colours glorify dizi'.

6. The factors of size and quality of carving

Jadeite articles can be subjectively divided on the basis of size into two main groups: those carvings more than 3 cm across (about the size of an egg) and the rings, pendants and other jewellery items less than 3 cm thick (*Figures 21* and *22*).

Pieces more than 3 cm across are usually not filled with polymer, but jadeite jewellery made from slices (such as bracelets, two-dimensional ornaments with thickness less than 2 cm) should be examined carefully. Most B-jadeite comes from sliced material.

The degree of intricacy and skill of the carvings serves as more important evidence in identifying jadeites than their basic shape. For example, the large beautifully carved brush pot shown in *Figure 23* has a diameter larger than 3 cm and is A-jadeite.

Figure 20: One of the pixiu's ears appears white because there is a fissure immediately beneath it.
Figure 21: B-jadeite jade carving.
Figure 22: B- and C-jadeite jade bracelets and ring.
Figure 23: A-jadeite brush pot.
Figure 24: A-jadeite seal.
Figure 25: This jadeite with a sharp ridge is probably A-jadeite.

Figure 26: The points of these drop-shaped cabochons are a good indication of A-jadeite.

B-jadeite artefacts cannot be produced with very great intricacy of carving because their filling and sealing with polymers necessarily reduces their hardness. This restricts the shapes of B-jadeites to geometries without very sharp edges or points (*Figures 25* and *26*).

Conclusion

Mastering the skills described above would be of great benefit to dealers and ordinary consumers and is entirely possible with practice. However, because the visual skills still leave a margin for error in detecting frauds and such treatments as coating, reconstructing and dyeing, they should be used mainly for reference and only with caution at a commercial level. In some cases, turning to professionals in trade laboratories is the only way to reach accurate conclusions or get precise results.

References

Fritsch, E., Wu, S.-T., Moses, T., McClure, S.F., and Moon, M., 1992. Identification of bleached and polymer-impregnated jadeite. *Gems & Gemology,* **28**(3), 176-87

General Administration of Quality Supervision, Inspection and Quarantine of the People's Republic of China (AQSIQ), 1996. *National Standard of P.R. China: Gem-Nomenclature. (GB/T16552-1996).* Standards Press of China: Beijing, 10

General Administration of Quality Supervision, Inspection and Quarantine of the People's Republic of China (AQSIQ), 2003. *National Standard of P.R. China: Gem-Nomenclature. (GB/T16552-2003),* Standards Press of China: Beijing, 10

The Authors

Li Jianjun (geoli@vip.sina.com), Liu Xiaowei, Cheng Youfa and Liu Huafeng
National Gold & Diamond Testing Center of China (NGDTC), Jinan, P.R. China

Zhang Zhiguo
National Gem Testing Center of China (NGTC), Beijing, P.R. China

Luo Yueping
National Jewellery Quality Supervision and Inspection Center of China (NJQSIC), Beijing, P.R. China

Abstracts

Diamonds

Elements de caracterisation des diamants naturels et synthétiques colorés.

E. Eric. *Revue de gemmologie AFG,* 162, 2007, 4-13.

Summary with illustrations of natural and synthetic coloured diamonds. M.O'D.

Diamond integrated quantum photonics.

A.D. Greentree, B.A. Fairchild, F.M. Hossain and S. Prawer. *Materials Today,* **11**(9), 2008, 22-31.

Survey of the uses of diamond in the quantum computer industry. Particular coverage is given to the operation of colour centres in diamond. M.O'D.

Explosive maar-diatreme volcanism in unconsolidated water-saturated sediments and its relevance for diamondiferous pipes.

V. Lorenz. *Gemmologie. Z. Dt. Gemmol. Ges.*, **57**(1/2), 2008, 41-60. 5 photographs, 1 diagram, 3 maps.

Three examples of maar-diatreme volcanoes formed in soft sediment are discussed: one in the Saar-Nahe basin in southern Germany, one carboniferous midland valley basin in Scotland and the middle proterozoic diamondiferous diatremes of the Halls Creek Mobile belt in East Kimberley, Western Australia. E.S.

Formation of Archaean continental lithosphere and its diamonds: the root of the problem.

D.G. Pearson and N. Wittig. *Journal of the Geological Society*, **165**(5), 2008, 895-914.

The paper examines the formation of diamonds in the early evolution of the Earth; it is suggested that the presence of diamonds included in Hadean zircons may suggest that deep continental material may have existed as early as 4.2 Ga ago. M.O'D.

The use of laser and X-ray scanning to create a model of the historic Koh-i-Noor diamond.

S.D. Sucher and D.P. Carriere. *Gems & Gemology,* **44**(2), 2008, 124-41.

For centuries, the Koh-i-Noor was one of the world's largest diamonds. It was recut in 1852 to an oval of 105.60 ct. Using one of the two plaster casts now in the Natural History Museum, London, the present authors have captured the surface topology of the original Koh-i-Noor through photography plus laser and X-ray scanning methods. A crystallographic analysis of the major facets determined the diamond's orientation within a 'perfect' diamond crystal, which was used to refute the theory that this diamond had been cut from the Great Mogul. Computer modelling established the orientation of the recut diamond within the historic version. All this information was then used to create an accurate replica from cubic zirconia, offering a good approximation of the brilliance and optics of the original stone. R.A.H.

Gems and Minerals

Crystallization of biogenic Ca-carbonate within organo-mineral micro-domains. Structure of the calcite prisms of the *Pelecypod Pinctada margaritifera* (Mollusca) at the submicron to nanometre ranges.

A. Baronnet, J.P. Cuif, Y. Dauphin, B. Farre and J. Nouet. *Mineralogical Magazine,* **72**(2), 2008, 617-26.

Atomic force microscopy (AFM) and transmission electron microscopy (TEM) were used to investigate the fine structure of the calcite prisms from the pearl-oyster shell *Pinctada margaritifera*. The AFM analysis shows that the prisms are made of densely packed circular micro-domains (in the 0.1 µm range) surrounded by a dense cortex. The TEM images and diffraction patterns allow the internal structure of the micro-domains to be described. Each of them is enriched in Ca-carbonate. Hosted in distinct regions of each prism, some are fully amorphous, and some others fully crystallized as subunits of a large calcite single crystal. At the border separating the two regions, micro-domains display a crystallized core and an amorphous rim. Such a border probably marks out an arrested crystallization front having propagated through a previously bio-controlled architecture of the piling of amorphous micro-domains. Compared to recent data concerning the stepping mode of growth of the calcite prisms and the resulting layered organization at the µm-scale, these results give unexpected views regarding the modalities of biocrystallization. R.A.H.

L'Ambre Dominicain.

A.B. Costa. *Revue de gemmologie AFG,* 162, 2007, 15-16.

Short note on amber from the Dominican Republic. M.O'D.

About mineral collection. (Part 1 of 5.)

R. Currier. *The Mineralogical Record,* **39**(4), 2008, 305-13.

First part of a survey of the profession and hobby of mineral collecting with particular relevance to the United States. M.O'D.

Abstracts (continued)

Coloring of topaz by coating and diffusion processes: an X-ray photoemission study of what happens beneath the surface.

H. Gabasch, F. Klauser, E. Bertel and T. Rauch. *Gems & Gemology,* **44**(2), 2008, 148-54.

Surface-treated topaz has become a viable alternative to topaz coloured by irradiation, but unlike irradiation which affects the entire stone, coloration by chemical modification is limited to the near-surface region. The treatment techniques are well established, but less is known about how the processes involved create the desired appearance. X-ray photoemission spectroscopy, combined with sputter depth profiling, has allowed the characterization of two fundamentally different colouring mechanisms for chemically treated topaz: coloured coatings and diffusion-induced coloration. R.A.H.

Les gisements de corindons gemmes de Madagascar.

G. Giuliani, D. Ohnenstetter, A. Fety, M. Rakotondrazafy, A.E. Fallick and others. *Revue de gemmologie AFC,* 159, 2007, 14-28.

The geology and mineralogy of gem-quality corundum locations in Madagascar are discussed. A bibliography and map are included. M.O'D.

Le peuple Thrace en Bulgarie et les mines du Laurium.

E. Gonthier. *Revue de Gemmology AFG,* 162, 2007, 17-22.

Notes on the ancient lead slags of Laurium, Greece, and the possible use of the minerals found there by the people of Thrace, present-day Bulgaria. M.O'D.

Quelques variétes d'ambre animal et d'ambre vegétal.

E. Gonthier. *Revue de Gemmology AFG,* 163, 2008, 11-17.

Summary of ambers or amber-like substances of animal and vegetable origin. M.O'D.

Einige Gedanken zu Jadeit-Jade.

H. Hänni. *Gemmologie. Z. Dt. Gemmol. Ges.,* **57**(1/2), 2008, 5-12, 5 photographs, 1 graph, bibl.

Jadeite is a polycrystalline gemstone, the transparency of which is greatly influenced by grain size and homogeneity. The grain boundaries are opened by weathering of the jade blocks in the river. Transparency can be improved by cleaning with acid and filling of the pores. In green jadeite there is sometimes an isomorphous replacement of Al by Cr. A mixed crystal series from jadeite to kosmochlor produces colourless to green to black material with increasing RI and SG values. A new standard for jadeite definition is being introduced in Hong Kong, accepting small amounts of kosmochlor and omphacite; however, the the values must not exceed SG over 3.4 and RI over 1.688. Materials within this field are called Fei Cui jade in China. E.S.

Les granats andradites-demantoides d'Iran: zonage de couleur et inclusions.

S. Karampelas, E. Gallou, E. Fritsch and M. Douman. *Revue de Gemmology AFC*, 2007, 107, 14-20.

A recently-discovered deposit of demantoid garnet is described from Iran. A content of more than 0.7% up to 1.2% of chromium oxide is required to give the green colour. Inclusions of fibrous calcite are reported and specimens show marked colour zoning. M.O'D.

Gem News International.

B.M. Laurs. *Gems & Gemology,* **44**(2), 2008, 164-90.

Brief descriptions are given of a 2.41 ct cut diamond with a brownish-orange inclusion (possibly eclogitic garnet), under the table showing a strong resemblance to a bird in flight, and of a colourless diamond showing strong phosphorescence. Also mentioned are an orange-red labradorite from China, an orange beryl from India, a rare faceted Cr-rich clinochlore from Turkey, an orange danburite from Tanzania, faceted lawsonite form Marin County, California, and a green Cr/V-bearing paragonite from northern Pakistan. Faceted peridot extracted from a pallasite and rubies and sapphires from a new locality in eluvial soil at Winza in central Tanzania are illustrated. R.A.H.

The Königskrone topaz mine, Schneckenstein, Saxony, Germany.

H. Leithner. *The Mineralogical Record,* **39**(5), 2008, 355-67.

Wine-yellow crystals of gem-quality topaz have been mined from the Ebenstock granite in the Vögtland area in Upper Saxony, Germany. It is possible that crystals from this area were used in many European-made items of jewellery. Figures from *Goldschmidt, Atlas der Kristalformen* (1922) are reproduced. M.O'D.

Coated tanzanite.

S.F. McClure and A.H. Shen. *Gems & Gemology,* **44**(2), 2008, 142-7.

The examination of 23 tanzanites coated by an apparently new technique revealed that the smaller (4–5 mm) stones could be identified as coated, based on a combination of the unusually intense colour and microscopic examination which revealed surface iridescence as well as wear of facet junctions (small areas where the coating had been abraded away). Two larger (3+ ct) stones did not show iridescence or wear (unless examined at high magnification), and were thus much more difficult to identify. XRF and LA-ICP-MS analyses showed the presence of Co, Zn, Sn and Pd in the coating. R.A.H.

Le Nigeria. Source de pierres de couleur.

J-C. Michelou. *Revue de Gemmology AFG,* 159, 2007, 30-41.

The gem-producing potential of Migeria is discussed with particular reference to beryl and corundum mineral deposits and their geology. Nigeria is compared with other African countries. M.O'D.

Le retour de l'émeraude.

J-C. Michelou. *Revue de Gemmology AFG,* 163, 2008, 4-6.

General survey of emerald and its provenance. M.O'D.

Lab Notes.

T.M. Moses and S.F. McClure (Eds). *Gems & Gemology,* **44**(2), 2008, 156-63.

Items noted include a gem-quality fancy brown CVD synthetic diamond with traces of boron, crystals of a bluish-green plagioclase coloured by copper, and a

Abstracts (continued)

blue cut sapphire with an unusually high content of light rare earth elements. R.A.H.

Der Zonarbau des Alexandrits von Novello Claims, Simbabwe.

M. Okrusch, H. Brätz and U. Schüssler. *Gemmologie. Z. Dt. Gemmol. Ges.,* **57**(1/2), 2008, 13-22. 3 photographs 1 graph, 2 tables.

The optically visible zonation of an alexandrite twin from the Novello claim was investigated by EMP and LA-ICP-MS analysis. The colouring elements of this stone were chromium and iron-titanium; zinc, gallium, vanadium and scandium were found, the quantity varying with zonal distribution. E.S.

Rhodochrosit aus dem Blei/Zink-bergwerk Wudong bei Liubao, Guangxi, China.

A. Ottens. *Lapis,* **33**(10), 2008, 53-6.

Rhodochrosite of ornmanetal quality is described from the Wudong lead/zinc mine, Guangxi, China. M.O'D.

Nouvelles des travaux sur le beryllium et les saphirs bleus.

V. Pardieu. *Revue de Gemmology AFG,* 163, 2008, 7-9.

Review of beryllium-treated blue sapphires with illustrations of characteristic inclusions. M.O'D.

Les tourmalines cuprifères du Nigeria et du Mozambique.

B. Rondeau and A. Delaunay. *Revue de Gemmology AFC,* 107, 2007, 8-13

Paraíba-type bright blue tourmalines owing their colour to copper are reported from Nigeria and from Mozambique. Divalent copper, the origin of the colour, gives a broad absorption band at 690 nm. Some green and purple tourmalines show a similar band. Some green specimens also show a strong absorption of the blue to the ultra-violet and this has been attributed to trivalent manganese. Heat treatment up to 600–700°C has no effect on the green colour while dark blue stones lighten. Purple stones become light blue or colourless. Locality information can be gained from the composition of trace elements. There may be confusion between blue specimens from Brazil and Mozambique as trace element compositions can overlap. M.O'D.

Characterization of emeralds from a historical deposit: Byrud (Eidsvoll), Norway.

B. Rondeau, E. Fritsch, J.-J. Peucat, F.S. Nordrum and L. Groat. *Gems & Gemology,* **44**(2), 2008, 108-22.

An emerald deposit, mainly in small pegmatites intruding alum shales, at Byrud, southern Norway, yielded significant amounts of crystals and gem rough in the late nineteenth and early twentieth centures. Complex multiphase inclusions in the emeralds consist of water, gaseous methane, halite, sylvite, calcite and a sulphide assemblage (pyrrhotite, galena and sphalerite); this sulphide assemblage makes the Byrud emeralds easy to distinguish from those from elsewhere. They also have a characteristic chemical composition, being coloured mostly by vanadium (up to 1 wt % V_2O_3) and contain low Mg and Ma (≤ 0.1 wt % oxide). EPMA and LA-ICP-MS results are given. The relative amounts of Fe, Mg, Cr, Rb and Cs appear to be diagnostic. IR absorption spectra show that they contain little water. R.A.H.

Gruene Quartze – Farbursachen und Behandlung.

R. Schultz-Guettler, U. Henn and C.C. Milisenda. *Gemmologie. Z. Dt. Gemmol. Ges.,* **57**(1/2), 2008, 61-72. 10 photographs, 4 graphs, bibl.

Recently larger amounts of green faceted quartz have been observed in the trade. Most of these owe their colour to artificial irradiation. The original material is a colourless to light yellow quartz from Rio Grande do Sul in Brazil. In contrast to green prasolites obtained by heat treating amethysts, the colour will fade in strong sunlight or in temperatures above 150°C. The samples investigated showed a broad band in the absorption spectrum with a max of 592–620 nm. Prasolites have a broad absorption spectrum around 720 nm. Separation of heat treated and irradiated specimens is also possible with the Chelsea colour filter when illuminated with incandescent light: prasolites appear green, irradiated specimens red. Synthetic quartz has also appeared in the trade; the absorption spectrum shows broad bands at 740 nm and 930 nm as well as a band at 510 nm. E.S.

La Mine de Williamson.

S. Scolie, M. Philippe and D. Sirakian. *Revue de Gemmology AFC,* 107, 2007, 21-5.

History and updated geological survey of the Williamson diamond mine at Mwadui, Tanzania. M.O'D.

Bei den Demantoid – Väschern von Poldnevaja im Ural.

M. Sehrig. *Lapis,* **33**(11), 2008, 32-5.

Illustrated description of a significant deposit of demantoid garnet in the Urals, Russia. M.O'D.

Structural characterization and chemical composition of aragonite and vaterite in freshwater cultured pearls.

A.L. Soldati, D. E. Jacob, U. Wehrmeister and W. Hofmeister. *Mineralogical Magazine,* **72**(2), 2008, 579-92.

Vaterite and aragonite polymorphs in freshwater cultured pearls from mussels of the genus Hyriopsis (Unionidae) were structurally and compositionally characterized by Raman spectroscopy, micro computer tomography, high resolution field emission SEM, and LA-ICP-MS. The appearance of vaterite in pearls is related to the initial stages of biomineralization, but vaterite can not be a precursor to aragonite. Vaterite is not related to a particular crystal habit and therefore does not have a structural functional in the pearls. Larger contents of elements typically bound to organic molecules, such as P and S in vaterite, as well as larger total organic contents in vaterite as opposed to aragonite in conjunction with larger concentrations of Mn^{2+} and Mg^{2+}, imply a stabilizing role of organic macromolecules and X^{2+} ions for biological vaterite. Distribution coefficients between aragonite and vaterite for provenance-independent elements, such as Mn and Mg (0.27 and 0.04, respectively) agree very well with those observed in fish otoliths. R.A.H.

Nucleated cultured pearls: what is there inside.

M. Superchi, E. Castaman, A. Donini, E. Gambini and A. Marzola. *Gemmologie. Z.*

Abstracts (continued)

Dt. Gemmol. Ges., **57**(1/2), 2008, 33-40. Illustrated in black-and-white and in colour, bibl.

Discussions about nucleated cultured pearls are generally related to the nacre: surface, treatment and thickness. Productions using nuclei obtained from materials other than mother-of-pearl (established by classical rules) have started and are on the market without any specific declaration. This report publishes the results of a diffraction (Laue) testing system applied to nucleated cultured pearls, which allows the distinction between nuclei obtained from mother-of-pearl, from shells having crossed lamellar structure or from a composite artificial material called 'bironite'. E.S.

Infrared spectroscopic study of modern and ancient ivory from sites at Jinsha and Sanxingdui, China.

L. Wang , H. Fan, J. Liu, H. Dan, Q. Ye and M. Deng. *Mineralogical Magazine,* **71**(5), 2007, 509-18.

Ancient ivory, buried for several thousands of years at the Chengdu Jinsha and Guanghan Sanxingdui sites in China, has been compared with modern ivory, using IR spectroscopy in the 4000–400 cm^{-1} range. By combining these results with XRF data, the authors determined the crystallinity and crystal chemistry of the apatite component, as well as the structural characteristics of the ivories. The ancient ivory consisted almost entirely of hydroxyl-carbonate apatite. Compared to modern ivory, the PO^{3-}_4 and CO^{2-}_3 bands were stronger, the νPO_4 IR bands were clearly greater, and an extra OH^- band at 3569 cm^{-1} was observed. These results imply that there is a greater degree of crystallinity in the ancient apatite, and that there has been incorporation and recrystallization of CO^{2-}_3 in the apatite during burial. Positive correlations were found between apatite crystallinity, CO^{2-}_3 and OH^- contents, and burial time. The loss of organic matter from the ancient ivory may be the main reason why it is easily dehydrated and readily friable after being unearthed. R.A.H.

Rhodonit.

S. Weiss. *Lapis*, **33**(11), 2008, 36.

Illustrated summary of gem- and ornamental-quality rhodonite with some important sites included. M.O'D.

Herbert P. Obodda.

J.S. White. *The Mineralogical Record,* **39**(4), 2008, 315-31.

Gem-quality vayrynenite from Pakistan is featured as one of the very many rare gem-quality crystals which have passed through the hands of noted American mineral and gem dealer Herb P. Obodda whose illustrated biography is given. M.O'D.

New primary gem occurrences in Sri Lanka.

J.C. Zwaan and E.G. Zoysa. *Gemmologie. Z. Dt. Gemmol. Ges.,* **57**(1/2), 2008, 23-32. 9 photographs, 2 maps, bibl.

Primary pegmatitic and metamorphic gem deposits of commercial interest have recently been discovered in Sri Lanka. In the Opanayaka district about 25 km south of Ratnapura aquamarines have been found in pegmatites. Small hexagonal light- to grey-blue corundum crystals, some with more rounded outlines, were found in the eastern corner of the highlands at Wellawaya and at Kamburipitiya reddish-orange hessonite was found, 5–10% of fine gem quality, 20–30% medium quality. Properties were found to be similar to those of gems found in the rich alluvial deposits of Sri Lanka. E.S.

Synthetics and Simulants

Single-crystal polarised-light FTIR study of an historical synthetic water-poor emerald.

F. Bellatreccia, G. Della Ventura, M. Piccinini and O. Grubessi. *Neues Jahrbuch für Mineralogie – Abhandlungen,* **185**(1), 2008, 11-16

Re-examination of an emerald synthesized by Hautefeuille and Perry (1888) using a flux method has shown it to be very close to the stoichiometric composition and homogeneous except for a significant variation in Cr_2O_3 content (1.45–2.59 ct %); trace amounts of Ti, Mg, Fe, Zn, Na, K and F were also noted. It has *a* 9.2264, *c* 9.1904 Å. Despite the synthetic conditions, FTIR spectra in the OH-stretching region show the presence of weak but significant H_2O vibrations. The polarized FTIR spectra collected with E c consist of a unique sharp and intense band at 3463 cm^{-1}, whereas the E c spectra consist of two minor bands at 3643 and 3587 cm^{-1}. These bands are assigned to the ν3 antisymmetric stretching and ν1 symmetric stretching modes of type II water in the structural channels, respectively. These water molecules are probably associated with Li impurities in the mineral due to the flux used for the synthesis. Using the molar absorption coefficient of Libowitzky and Rossman (see *American Mineralogist*, **82**(11-12), 1997, 1111-15), a water content of ~ 30 ppm is derived for this emerald. R.A.H.

Abstractors

R.A. Howie – R.A.H. M. O'Donoghue – M.O'D. E. Stern – E.S.

Book reviews

Fleischer's Glossary of Mineral Species.
M.E. Back and J.A. Mandarino, 2008. The Mineralogical Record, Tucson. pp xiv, 345. Price on application.

The tenth edition of this most useful and convenient classic quick reference book follows its predecessors in its alphabetical list of validated species with reference to the most important citation in English, primarily *American Mineralogist* and *Mineralogical Magazine*. Group membership is indicated where appropriate and the groups themselves, with their constituent species, are described at the end of the main text. In this section the descriptions of some groups are expanded: this is particularly useful where the amphiboles are described and here some references are made to important studies.

The list of journals from which data have been obtained is impressive and covers six pages; non-English works are included.

To make up a reliable and quick trio of books for reference, Fleischer should be joined by the five volumes of Anthony *et al*. *Handbook of Mineralogy* (1990–2003) and the full-colour Bernard and Hyrsl *Minerals and their Localities* (2006). Gemmological laboratories and teaching establishments without at least two of these three should not be attracting customers! M.O'D.

Fluorite der Welt. Afrika, Amerika, Asien, Europa. extraLapis No. 35.
2008. Weise, Munich, Germany. pp 103, illus. in colour. €17.80.

The highly desirable extraLapis series continues with a beautifully illustrated overview of some of the world's most notable ornamental fluorite deposits. It is to be hoped that other deposits, for example the Blue John location in Derbyshire, England, will feature in a later issue. This would be worth waiting for. M.O'D.

Photoatlas of Inclusions in Gemstones, Volume 3.
E.J. Gübelin and J.I. Koivula, 2008. Opinio Publishers, Basel, Switzerland. pp 672, illus. in colour. ISBN 3-03999-047-4 €250.00.

Rarely has a gemmology book been so eagerly awaited and this, the third volume in the series of inclusions in gemstones by Eduard Gübelin (deceased 2005) and John Koivula, is excellent and exceeds expectations.

Volume 1, published in 1986, soon became a standard reference in the field of gemmology but it was not until 2005 that the second volume, which provided greater depth and scope, was published. The major commercial gemstones, diamond, ruby, sapphire and emerald, not covered in volume two, are the mainstay of volume three.

The book covers exactly what it says in the title and more. The 672 pages contain 1796 images and it is indeed a huge reference library of images and the practising gemmologist would be all the poorer for its absence.

The quality of production is excellent and the images are often of exceptional beauty. Anyone who has attempted photomicroscopy will feel humbled by the outstanding quality of the images which are a testament to the skill, knowledge and patience of the authors. I could find only one image that had been published previously (exsolved rutile in ruby from East Africa – Volume 1) but the difference in captions indicates that this feature had been re-evaluated. Thus the resource of images is cumulative for all three volumes. In this respect the user would benefit from the production of a DVD with search facilities rather than thumbing through three volumes.

As frequently stated or alluded to in the book, the basic premise of the study of microscopic features in gemstones is that similar processes will result in a range of similar features in gems of the same species. So whether these processes are geological, treatments or synthesis, significant information is stored within the gems that aid in their identification and separation.

Whilst Volume 1 was portrayed as a voyage of discovery and exploration into the world of inclusions in natural gemstones, their treatments, imitations and synthetics, this volume builds on the geological and process correlation established in Volume 2. This is a major strength of Volume 3 where, within individual species and varieties (including their synthetic counterparts and simulants) not only are they brigaded into geological settings but within that grouping arranged by locality or, in the case of synthetics and simulants, by manufacturing process. At the beginning of each of these groupings there is text that briefly, but succinctly, covers the topics that the images illustrate. At the end of the primary text that prefaces each gem material there is a useful list of additional reading references. Helpful, informative and often expansive captions that include illumination and magnification data complement the impressive photographs that beautifully illustrate the diagnostic features. The authors also discuss and illustrate the very latest discoveries of mineral and fluid inclusions in gems.

There is a very brief Introductory Section that outlines the basic premise of the role that inclusions play in the identification of gemstones and their treatments.

Section two, Inclusions in Major Commercial Gems, takes up 457 pages

Book reviews (continued)

and is the meat of Volume 3. It begins with inclusions in diamonds. The opening text covering mineral inclusions, peridotitic inclusions, eclogitic inclusions, inclusions from the deep mantle, cloud formations, the age of natural diamonds, diamond treatment, synthetic diamonds and diamond substitutes, gives an insight into the range of images that follow.

The diamond part of the section is followed by inclusions in corundum. These are conveniently arranged so that inclusions in rubies and sapphires from analogous petrological and geological settings can be compared. Thus, for example, rubies from Luc Yen and Quy Chau – Vietnam, rubies from Mogok and Mong Hsu – Myanmar (Burma), rubies from the Ganesh Himal area – Nepal, rubies from Azad and Hunza – Pakistan and rubies from Jagdalek – Afghanistan are presented sequentially as they are examples of rubies found in marbles. Inclusions indicative of treatment follow those typically found in natural corundum. Treatments illustrated are diffusion, heating, fillings, coating, and oiling and dying. The synthetic corundum inclusions illustrate the processes of flame fusion (Verneuil), Czochralski pulling, floating zone and flux growth. The latter is further subdivided in the text by manufacturer: Chatham, Kashan, Ramaura, Knischka and Douros. Unspecified Russian hydrothermal growth, and the images are annotated accordingly.

The third part of this section covers emeralds arranged according to their genetic types, followed by inclusions indicative of treatment and lastly inclusions in synthetics. It is here that the authors, looking to the future, give examples of repair through re-growth; an aspect considered only theoretical where gem rubies and sapphires are concerned.

The third and final section deals with Inclusions in Rare and Unusual Gems. Arranged alphabetically the gems are andalusite, apatite, axinite, benitoite, calcite, cordierite, danburite, diopside, ekanite, enstatite, fluorite, glass, gypsum, kornerupine, pezzottaite, sapphirine, scapolite, sillimanite, sinhalite, spodumene and taaffeite. Introductory text prefaces each of these.

Criticism, none of which will materially affect the gemmological user, is confined to the pernickety such as application of current mineralogical nomenclature (e.g. tantalite – (Mn) as opposed to manganotantalite, and the use of names that no longer have IMA-approved species status (e.g. biotite; which it is now recommended be used for a series such as the biotite-phlogopite series). One very minor irritation could be the presentation of descriptions on one page that pertain to images on a subsequent page such that some pages have no captions: this occurs but rarely. It would be wrong to give criticism because of omissions for as the authors state this is not a gemmological text book or gem identification manual.

In conclusion, these highly respected authors have produced an exceptional book drawing on decades of meticulous optical microscopic examination, research and highly specialized photomicrography. The greatest challenge facing the gemmologist is the need to recognize and separate natural gems from synthetics and untreated stones from those that have been treated. In facing up to this challenge this current work is an invaluable asset given that the gemstone industry has increasingly grown to depend on the interpretation of inclusions.

Collectively the Photoatlas volumes make an outstanding contribution to the field of gemmology. B. J.

Gems & Gemology in Review: Treated Diamonds.

J.E. Shigley, 2008. GIA, Carlsbad, California. pp 301. ISBN: 978-0-87311-054-9. £49.50.

Chapters in this excellently-produced book are adapted from papers already published in *Gems & Gemology* and like other compilations in the series cover the latest findings in a single subject area. The review could hardly have come at a more critical moment for the diamond trade and will certainly be widely distributed and used.

The chart in the back pocket illustrates the diagnostic features of filled diamonds and most usefully includes features of unfilled diamonds which could be mistaken for fillings.

This book is not just recommended – it is essential. M.O'D.

Working with Gemstones. A Bench Jeweler's Guide.

A.A. Skuratowicz and J. Nash, 2008. MISA/ASM Press, Providence RI. pp 128. ISBN 09713495-4-1. Price on application.

Pleasantly illustrated in colour, the book aims to present the major gemstones to the working jeweller, manufacturer and designer with practical advice on mounting, heat resistance and a number of other features that will assist both the wearer and the buyer. The photographs are high quality and the book design attractive. M.O'D.

Phenomenal Gems.

F. and C. Ward, 2008. Gem Book Publications, Malibu, California. pp 64. ISBN-13 978-1-887651-12-7. £10.95.

An especially attractive newcomer to the Fred Ward Gem Book series, this book describes gemstones exhibiting chatoyancy, asterism, play-of-colour, iridescence and other optical features. As always, Fred Ward's pictures are unmatchable and the book is a must. M.O'D.

Gem-A Bookshop

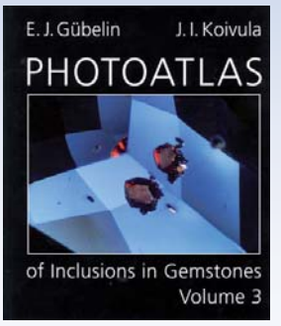

Photoatlas of Inclusions in Gemstones Volume 3
E.J. Gübelin and J.I. Koivula
£210.00

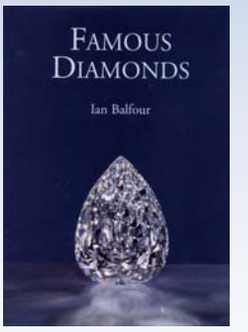

Famous Diamonds
5th edition
Ian Balfour
£50.00

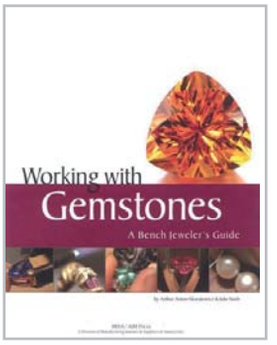

Working with Gemstones.
A Bench Jeweler's Guide
Arthur A. Skuratowicz and Julie Nash
£19.95

Phenomenal Gems
Fred and Charlotte Ward
£10.95

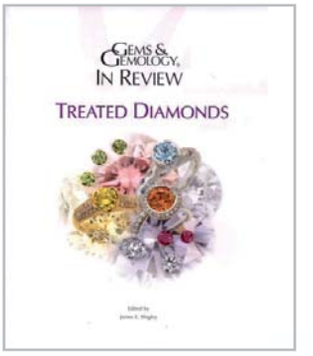

Gems & Gemology in Review: Treated Diamonds
Edited by J.E. Shigley
£49.50

Prices exclusive of postage and packing

To place an order or for further information contact:

The Gemmological Association of Great Britain
27 Greville Street, London EC1N 8TN, UK
t: +44 (0)20 7404 3334 f: +44 (0)20 7404 8843 e: shop@gem-a.com

Proceedings of the Gemmological Association of Great Britain and Notices

Educational Sponsorship

This year has been a resounding success for Gem-A, the effects of which have been felt globally by our students and members. As an educational charity, we are extremely grateful to our sponsors and supporters, who have helped us achieve many of our goals for 2008.

The 100 Club and the Educational Sponsorship initiatives were established in 2008 to invite members and supporters to donate a minimum of £1000 each, which would be used towards the expansion and updating of our courses worldwide. Thanks to our sponsors, The Gemmological Association of Great Britain has been able to create the new Foundation in Gemmology course notes which are now in use, containing up-to-date information and a new look. In addition, Gem-A has launched an online education resource centre for students which incorporates access to web-based assignments, a glossary of terms, past papers, student forums and a calendar of events. A member version of the site will be launched in 2009, so that members of Gem-A can also have access to online education resources. Our new Foundation in Gemmology Open Distance Learning course will provide students with a refractometer, twenty stones, a full gem testing kit, a gem reference guide and includes practical tuition within the UK. With all of these added benefits for our distance students, we are looking towards expanding internationally through our Open Distance Learning (ODL) Programme.

With the help of our sponsors, Gem-A has also launched a new website. With a clean look that is easy to navigate, prospective students are better able to find course information, and members and the trade are more easily able to find out about news and upcoming events. A members' area of the website will be launched in 2009, which will include exciting new features accessible to members-only, such as a searchable archives for *The Journal of Gemmology*.

Currently under development is a new short-term natural pearl course, leading to a certificate of completion, which will be taught in conjunction with the Dubai Pearl Exchange. The course will first be taught in Dubai in Autumn 2009, and is another step taken towards increasing worldwide accessibility of our courses.

Until we reach our target of 100 members for the 100 Club, the 100 Club initiative will continue. A plaque to commemorate those who have donated to the 100 Club will be placed in the lobby of the Gem-A headquarters. Educational Sponsorship is an on-going initiative, and we encourage 100 Club members and others dedicated to the Association to help us raise funds for 2009. As we enter the second century of gemmological education, our need for your help is still great. Next year we need funds to help us create course notes for a new Diploma in Gemmology course, set to begin in September 2009, as the follow-up to the new-style Foundation course. We are also looking to raise funds to purchase gem-testing equipment for our student teaching facilities, for research and for future supervised access for members. Donations in the form of gem testing equipment are also highly appreciated, and we would be delighted to receive a simple Raman, or a new UV/VIS spectrometer to have in-house for teaching.

For further information on sponsorship, or to see the list of sponsors on the web, visit http://www.gem-a.com/membership/sponsorship.aspx. If you would like to become a member of the 100 Club or become an Educational Sponsor for 2009, please email olga.gonzalez@gem-a.com.

Gem-A Awards

Gem-A Examinations were held worldwide in June 2008. In the Examinations in Gemmology 243 candidates sat for the Diploma Examination of whom 116 qualified, including 19 with Merit. In the Foundation in Gemmology Examination, 252 candidates sat of whom 176 qualified. In the Gem Diamond Examination 103 candidates sat of whom 50 qualified, including five with Distinction and five with Merit.

The **Christie's Prize for Gemmology** for the best candidate of the year in the Diploma Examination who derives their main income from activities essentially connected with the jewellery trade was awarded to **Antonia Ross** of Fleet, Hampshire.

The **Anderson Bank Prize** for the best non-trade candidate of the year in the Diploma in Gemmology examination was awarded to **Elizabeth Rasche** of London.

A new prize, the **Diploma Practical Prize** for excellence in the Diploma Practical Examination, was awarded for the first time, sponsored this year by Gwyn Green. The Diploma Practical Prize was awarded to **Antonia Underwood** of London.

In the Foundation Certificate in Gemmology examination, the **Anderson Medal** for the candidate who submitted the best set of answers which, in the opinion of the Examiners, were of sufficiently high standard, and the **Hirsh Foundation Award** for the best candidate of the year, were awarded to **Dr Pauline Jamieson** of Edinburgh.

The **Bruton Medal**, awarded for the best set of theory answer papers of the year in the Gem Diamond Diploma examination, was awarded to **Kundan Sarraf** from Kathmandu, Nepal. In addition to the medal, the winner received a copy of *Diamond Cuts in Historic Jewellery* by H. Tillander (donated by John Greatwood) and a Type II Diamond Spotter (donated by the SSEF Swiss Gemmological Institute, Basel).

The **Deeks Diamond Prize** for the best candidate of the year in The Gem Diamond Diploma examination, was awarded to **Jacqueline Larsson** of Amsterdam, The Netherlands.

The Tully Medal was not awarded.

The names of the successful candidates are listed below.

Gemmology Diploma

Qualified with Merit

Agarwal, Kamal Kishore, Jaipur, Rajasthan, India
Bai Feng, Beijing, P.R. China
Bigford, Julie Claire, Malvern Wells, Worcestershire
Gao Xiao Huan, Shanghai, P.R. China
Giertta, Maria, London
Harker, Catherine Anne, Birmingham, West Midlands
Huang Jinming, Guilin, Guangxi, P.R. China
Ji Qiusong, Guilin, Guangxi, P.R. China
Kui Nui, Reema, Yuen Long, Hong Kong
Lau Ho, Kowloon, Hong Kong
Lek Chin Kwang, Singapore
Luo Han, Guangzhou, P.R. China
Nwe, May Moe, Yangon, Myanmar
Peng, Hsiang Chieh, Taipei, Taiwan, R.O. China
Ross, Antonia, Fleet, Hampshire
Sharma, Anita, Haryana, India
Shaw, Heather Catherine, Barnsley, South Yorkshire
Skalwold, Elise Ann, Ithaca, New York, U.S.A.
Wu Dehe, Guangzhou, P.R. China

Qualified

Agu, Cecile, Le Cannet, France
Andersson, Joel, Umeå, Sweden
Au Chui Yee, Ada, Cascades, Homantin, Hong Kong
Baethe, Vanessa, Saint-Maur-Des-Fossés, France
Benson, Jillian Rose, Toronto, Ontario, Canada
Bhatia, Esha, Gujarat, India
Booth, Eveline Violet, Cheltenham, Gloucestershire
Brian, Jeremy, Marseille, France
Cai Qing, Wuhan, Hubei, P.R. China
Carre, Stephanie, Armées, France
Claydon, Louise, Morden, Surrey
Coppack, Flavia, London
Day, Helen Laura, Norwich, Norfolk
Dionne, Jean-Sebastien, Ste-Catherine-Jacques-Cartier, Quebec, Canada
Drai, Stephanie, Clamart, France
Dunn, Katherine Joanna, Toronto, Ontario, Canada
Fontaine, Josee, St-Basile-le-Grand, Quebec, Canada
Foran, Amelia Luetta, Toronto, Ontario, Canada
Freeman, Sarah, London
Gilli, Claude, Les Pennes Mirabeau, France

Goldman, Lucy, London
Hamren, Elisabeth, Ostersund, Sweden
Ho Siu Ming, Shaukiwan, Hong Kong
Hui Yuet Ming, Kowloon, Hong Kong
Jaugeat Blaise, Vanves, France
Kamoune Yannick, Ndemanga, Pierrefitte-sur-Seine, France
Keeffe, Veronica Cheryl, Oshawa, Ontario, Canada
Kim, Ji Eun, Busan, Korea
Kyaw Thu Min, Yangon, Myanmar
Lapsiwala, Foram Pravin, Gujarat, India
Larsson, Ylva, Vado, Sweden
Lee Hing Fan, New Territories, Hong Kong
Li Ying, Wuhan, Hubei, P.R. China
Liang, Jie, Birmingham, West Midlands
Liang Feng, Wuhan, Hubei, P.R. China
Liu, Huijing, Shanghai, P.R. China
Liu Yang, Wuhan, Hubei, P.R. China
Mao Li Hui, Wuhan, Hubei, P.R. China
Martins Molgard, Silvia, Colombo, Sri Lanka
Meraly, Afsana, Antananarivo, Madagascar
Mo, Zhuangguo, London
Ng Wai Hing, New Territories, Hong Kong
Nicolson, Louise Alexandra Patricia, London
Noronha Muthu, Sunita Karen, Gujarat, India
Pan Yang, Scarborough, Ontario, Canada
Pang Le, Wuhan, Hubei, P.R. China
Panicco, Fabio Michel, Antanavarivo, Madagascar
Perochon, Cyrielle, Castel-le-Lez, France
Piirto, Irmeli Anja Susanna, Espoo, Finland
Prendergast, Lorna, Great Missenden, Buckinghamshire
Pwint Phyu Win, Yangon, Myanmar
Pyrro, Riku Matti, Kirkkonummi, Finland
Qi Geng, Scarborough, Ontario, Canada
Qu Peng Cheng, Wuhan, Hubei, P.R. China
Rafferty, Frank, Ambrieres-les-Vallees, France
Ranorosoa, Nadine Joelle, Antananarivo, Madagascar
Razanadimby, Lalanirina, Antananarivo, Madagascar
Rufus, Simon, London
Samaratunge, Punyadevi, Horana, Sri Lanka
Shah, Prachi Hirenbhai, Surat, India
Siriwardena, Henarath H. D. Ajith Lal, Raddolugama, Sri Lanka
So Lai Yin, Shau Kei Wan, Hong Kong
Soh Shi Hong, Johor Bahru, Johor, Malaysia
Soumaré, Myriam, Paris, France
Spauwen, Timotheus A. P., Geleen, The Netherlands
Spencer, Jason, Birmingham, West Midlands
Tan Kiat Choo, June, Johor Bahru, Malaysia
Teng, Ying, Shanghai, P.R. China
Teng Yongqing, Guilin, Guangxi, P.R. China
Valerio Sa', Helena, Mississauga, Ontario, Canada
Valley, Aurelie, Amberieu-en-Bugey, France
Veenhoven, Taletta W., Amsterdam, The Netherlands
Wang Fang, Wuhan, Hubei, P.R. China
Wang Hongmei, Guilin, Guangxi, P.R. China
Wang Hui, Guilin, Guangxi, P.R. China
Wang Li Geng, Hubei, P.R. China
Wang Liling, Guangxi, P.R. China
Wang Weny-I, Tainan City, Taiwan, R.O. China
Wang Youran, Hubei, P.R. China
Watrelos, Celine, Paris, France
Win, Thein Thein, Cricklewood, London
Win, San San, Singapore
Wong Ka Yee, New Territories, Hong Kong
Woo Ka Yin, Kowloon Bay, Hong Kong
Wu, Dandan, Guangzhou, P.R. China
Yang Jing, Wuhan, Hubei, P.R. China
Ye Ying, Singapore
Yu Xiaoyan, Beijing, P.R. China
Yu Xuan, Wuhan, Hubei, P.R. China
Yuang Hongqing, Wuhan, Hubei, P.R. China
Zaleszczyk, Alicja, London
Zhang Jieqin, Guilin, Guangxi, P.R. China
Zhang Qian, Wuhan, Hubei, P.R. China
Zhang Wukun, Wuhan, Hubei, P.R. China
Zhao Bo, Wuhan, Hubei, P.R. China
Zhong Xiangtao, Guilin, Guangxi, P.R. China
Zhu Ye, Shanghai, P.R. China

Foundation in Gemmology

Qualified

Akmeemana, G.G.N., Kandy, Sri Lanka
Asakawa, Masako, Johetsu-City, Niigata, Japan
Ayabe, Hiroko, Nishinomiya City, Hyogo Pref., Japan
Bahadur, Seema, London
Bahri, Sebastien, Feucherolles, France
Beer, Jasmin, Birmingham, West Midlands
Bezant, Laura, Chelmsford, Essex
Boele, Georgette, Les Acacias, Switzerland
Bright, David, The Hague, The Netherlands
Brom, Jean-Baptiste, London
Brown, Claire E., Perth, Scotland
Brutsch, Sonia, Lucinges, France
Campbell-Jones, Amy V., Sheffield, South Yorkshire
Cao Juan, Shanghai, P.R. China
Cao Weifeng, Guilin, Guangxi, P.R. China
Cartier, Laurent E., Basel, Switzerland
Chang Cheng, Taipei, Taiwan, R.O. China
Chang Hsuan Ming, Taipei, Taiwan, R.O. China
Chatzipanagiotou, Ioannis Tzannis, Attiki, Greece
Chen Shaofeng, Guangzhou, P.R. China
Chen Jing, Guangzhou, P.R. China

Chen Wei, Guangzhou, P.R. China
Cheng Wing Yan, New Territories, Hong Kong
Cheung Mei Yee, Agnes, Repulse Bay, Hong Kong
Cheung Sau Yee, New Territories, Hong Kong
Chok Yee Quin, Selangor Darul Ehsan, Malaysia
Chou Mei-Lien, Taipei, Taiwan, R.O. China
Cox, Rebecca Jane, York
De Souza, Mary-Anne, Carshalton, Surrey
Deng, Baosheng, Guangzhou, P.R. China
Dimitrakopoulos, Charalabos, Athens, Greece
Do Mi Sun, Daegu, Korea
Duboeuf, Olivier, Nancy, France
Eastwood, Layla, Gerrards Cross, Buckinghamshire
Eronen, Evelina, Lannavaara, Sweden
Falah, Jamal, Blacktown, New South Wales, Australia
Fellows, Nicola, Birmingham, West Midlands
Feng Xi, Guilin, Guangxi, P.R. China
Fraissinet, Laurent, Antananarivo, Madagascar
Fu Kangyu, Guilin, Guangxi, P.R. China
Gang Seo Hui, Jeollanam-do, Korea
Gough, Hannah Jane, Telford, Shropshire
Grounds, Camilla Sara, London
Guenin, Nathalie, Sainte Foy, Quebec, Canada
Guo Yunrong, Shanghai, P.R. China
Guo Haifeng, Shanghai, P.R. China
Guo Hao, Guilin, Guangxi, P.R. China
Guo Yengli, Guilin, Guangxi, P.R. China
Guy, Tracy-Anne, London
Hanson, Lindsay, London
Hayry, Tiia, Helsinki, Finland
Hell, Martine Svitlana, Lannavaara, Sweden
Hiipakka, Janica Elisabet, Lappeenranta, Finland
Ho Ming Yan, Hong Kong Island
Holland, Nancy, Fuquay-Varina, North Carolina, U.S.A.
Horler, Rebecca Anne, Tunbridge Wells, Kent
Hovi, Maria, Hyvinkaa, Finland
Huang, Yuan, Shanghai, P.R. China
Huby, Melanie, Liège, Belgium
Hyvatti, Jaakko, Helsinki, Finland
Iggstrom, Per-Hakan, Rosersberg, Sweden
Ikeda, Tomoka, Imari Coty, Saga Pref., Japan
Jang Ae Ji, Daegu, Korea
Ji Kaijie, Shanghai, P.R. China
Kagia, Georgia, Nikea, Greece
Kamal, Mohamed Azhar Ilham, Colombo, Sri Lanka
Kamoune Yannick, Ndemanga, Pierrefitte-sur-Seine, France
Kim Chan Ju, Daejeon, Korea
Kim, Ji Eun, Busan, Korea
Ko Yum Sum, Iris, Kowloon, Hong Kong
Lai Yuen Wan, Eva, Stanley, Hong Kong
Lam Shun, Kowloon, Hong Kong
Landale, Natalie, Wormshill, Kent
Lau Shuk Ping, New Territories, Hong Kong
Lee Hae Jung, Daegu, Korea
Lee Wai Yin, Kitty, New Territories, Hong Kong
Lepage, Anick, Mont Saint Hilaire, Quebec, Canada
Li Ah-Yun, South Croydon, Surrey
Li Wenhui, Guangzhou, P.R. China
Li Li Lin, Guilin, Guangxi, P.R. China
Li Jiaxuan, Guilin, Guangxi, P.R. China
Li Yi, Guilin, Guangxi, P.R. China
Liang Huan, Guilin, Guangxi, P.R. China
Lilley, Heather Jane, Newcastle-under-Lyme, Staffordshire
Lindquist, Mia Caroline, Solna, Sweden
Liu, Xianfeng, Shanghai, P.R. China
Lo Wai Sze, Causeway Bay, Hong Kong
Lo Wai Yee Bibian, Tsing Yi, Hong Kong
Loke Hui Ying, Singapore
Ma, March Yu, Birmingham, West Midlands
Ma Pui Man, Kowloon, Hong Kong
Ma Xu, Guilin, Guangxi, P.R. China
Ma Yan Ting, Tsim Sha Tsui, Hong Kong
Maccaferri, Arianna, London
McKenna-Venne, Doreen, Laval, Quebec, Canada
Maltais, Paege, West Ealing, London
Matsuk, Daria, Maida Vale, London
Meraly Afsana, Antananarivo, Madagascar
Micatkova, Michaela, London
Mikkola, Samuli, Oulu, Finland
Ming Yan, Guilin, Guangxi, P.R. China
Mithaiwala, Priyanka M., London
Mizukami, Yusuke, Saitama City, Saitama Pref., Japan
Nandwani, Shailja, Gujarat, India
Naylor, Peter D., Birmingham, West Midlands
Ng Yuk Yu, New Territories, Hong Kong
Ngan Yin Ying, Kowloon, Hong Kong
Ngao Mei Wan, New Territories, Hong Kong
Nishikawa, Takamichi, Nomura Kusatsu City, Shiga Pref., Japan
Nishimura, Fumiko, Kofu City, Japan
Oike, Akane, Tokyo, Japan
Olofsson, Marcus, Gothenburg, Sweden
Oncina, Christelle, Aix-en-Provence, France
Ouchene, Linda, Paris, France
Oxberry, Hannah Clare, Kings Lynn, Norfolk
Panicco, Fabio Michel, Antanavarivo, Madagascar
Parvela-Sade, Anu, Espoo, Finland
Perochon, Cyrielle, Sainte-Therese, Quebec, Canada
Petit, Gregory, Moraugis, France
Petropoulou, Alexia, Athens, Greece
Petropoulou, Eleni, Nea Smyrni, Athens, Greece
Plant, Grace, Stone, Staffordshire

Platis, George, Athens, Greece
Pulecio, Gabriel, Bogota, Colombia
Pulver, Caroline M.L., Nairobi, Kenya
Qi Ming, Guilin, Guangxi, P.R. China
Qin Qing, Guilin, Guangxi, P.R. China
Qureshi, Erum Ali, Thane, India
Rabetaliana, Andoniaina Harijaona, Antananarivo, Madagascar
Rajaffand, Guy, Pantin, France
Rakotomalala, Cedric Anthony, Antananarivo, Madagascar
Ribarevic, Ivanka, Montreal, Quebec, Canada
Sahni, Harcharan Singh, Stourbridge, West Midlands
Seo, Jung Yeon, Daegu, Korea
Share, Rebecca Louise, Kingswinford, West Midlands
Shen Huanqun, Shanghai, P.R. China
Sigihara, Toshiyuka, Osaka City, Osaka, Japan
Sim Tam Yuk, North Point, Hong Kong
Sun Norton, Central, Hong Kong
Sung, Sophia, Taipei, Taiwan, R.O. China
Szvath, Gabriella, Laukaa, Finland
Tang, Michelle, Shanghai, P.R. China
Tay Kunming, Singapore
Tian Mi, Guilin, Guangxi, P.R. China
Tissa, V.G. Samith Madhawa, Colombo, Sri Lanka
Tosun, Rachel Megan, Bo'Ness, West Lothian, Scotland
Trolle, Natascha, Copenhagen, Denmark
Ueda, Kenji, Abeno-ku, Osaka, Japan
Vajanto, Leena Maaria, Helsinki, Finland
Valley, Aurelie, Montreal, Quebec, Canada
Wakita, Yoko, Osaka City, Osaka, Japan
Walvius, Peter, Nijmegen, The Netherlands
Wan Ho Shun, Tuen Mun, Hong Kong
Wang, Cong, Fulham, London
Wang, Songfang, Kofu-City, Yamanashi Pref., Japan
Wang Junyi, Guilin, Guangxi, P.R. China
Wetherall, Alan, Hitchin, Hertfordshire
Wiguna, Aland, Bangkok, Thailand
Wilkinson, Catherine E.P., Blockley, Gloucestershire
Williams, Richard Marcus Andrew, Porthcawl, Mid Glamorgan
Williams, Laura, London
Wingate, Simon James, Tiverton, Devon
Wong Nga Yin, Chaiwan, Hong Kong
Wong Siu Yin, New Territories, Hong Kong
Wong Wai Lam, Anita, New Territories, Hong Kong
Wu Na, Guilin, Guangxi, P.R. China
Yamaguchi, Nao, Shikonawate City, Osaka, Japan
Yan Yaying, Guilin, Guangxi, P.R. China
Yeung On Na, Kowloon, Hong Kong
Yeung Yick Sin, New Territories, Hong Kong
Young, Chun Yin Stewart, North Point, Hong Kong
Yu Zhiwei, Shanghai, P.R. China
Zarandi, Annabel, London
Zhang Xiaohu, Guilin, Guangxi, P.R. China
Zhao Chunji, Shanghai, P.R. China
Zhou Mengji, Shanghai, P.R. China

Gem Diamond Examinations

Gem Diamond Diploma

Qualified with Distinction
Gill, Julia Mary, Dudley, West Midlands
Larsson, Jacqueline, Amsterdam, The Netherlands
Sarraf, Kundan, Kathmandu, Nepal
Wootton, Sophie Louise, London
Yung Wai Lam, Hung Hom, Hong Kong

Qualified with Merit
Henning, Sarah Alexandra, Edgbaston, West Midlands
Naylor, Peter D., Birmingham, West Midlands
Russell, Marie, Worcester
Tidd, Lauren Elizabeth, Churchdown, Gloucester
Tsantoulas, Apostolos, Athens, Greece

Qualified
Bracey, Anne Christine, Birmingham, West Midlands
Chen Wenlong, Beijing, P.R. China
Chen Xi, Beijing, P.R. China
Corser, Elizabeth, Wellington, Shropshire
Craddock, Natalie, Bridport, Dorset
Cui, Xianzhong, London
Cui Xue, Wuhan, Hubei, P.R. China
de Fere, Susannah, London
Dessypri, Eleni, Athens, Greece
Ding, Hui, Surbiton, Surrey
Ewington, Craig A., London
Fraser, Brenna Heather, Kingston-upon-Thames, Surrey
Gallant, Victoria, London
Hsien Pui Ling, Tsuen Wan, Hong Kong
Humphreys, Stephen J., Beckenham, Kent
Iwamoto, Akiko, London
Kettle, Georgina Elizabeth, Birmingham, West Midlands
Kirk, Kelly Hope, Birmingham, West Midlands
Lam Cheuk Hei, Kowloon, Hong Kong
Lee Ching Wah, Shatin, Hong Kong
Lui Fong, New Territories, Hong Kong
Lung Mei Ting, May, Shatin, Hong Kong
Moroz, Magdalena, London
Noble, Frances, Wendover, Buckinghamshire

Nordgren, Pia Yu, Vallingby, Sweden
Rajbanshi, Niren Man, Kathmandu, Nepal
Richardson-Jefferies, Phillipa, London
Russell-Stoneham, Alexandra, London
Smith, Mark, Richmond, Surrey
Smith, Laura Sian, Oxford
Tai, Caroline, Tseung Kwan O, Hong Kong
Tsoi Mei Yu, New Territories, Hong Kong
Vaughan, Angela, Limerick, Ireland
Vikatos, Ilias, Patras, Greece
Wan Bresson, Wuhan, Hubei, P.R. China
Watson, Sarah Louise, Rowley Regis, West Midlands
Wong Yin Tak, Tony, Kowloon, Hong Kong
Wratten, Nicholas William, Notting Hill, London
Yang, Yiwei, London
Yau Cho Kwan, Chai Wan, Hong Kong
Yip Wing Man Kennis, Kowloon, Hong Kong

Gem-A Events

Gem-A Centenary Conference and Second European Gemmological Symposium

During the weekend of 25 and 26 October at the Hilton London Kensington Hotel Gem-A hosted the Second European Gemmological Symposium in conjunction with our centenary celebrations. The dynamic two-day conference covered both the history of gemmology and the jewellery trade, and new techniques that are relevant to today's gemmologists. The speakers included Sandra Brauns, Rui Galopim de Carvalho, Emmanuel Fritsch, Al Gilbertson, Henry Hänni, Ulrich Henn, Alan Hodgkinson, John Koivula, Michael Krzemnicki, Yvonne Markowitz, Jack Ogden, Duncan Parker and Brad Wilson.

A programme of events arranged to coincide with the Conference held on Monday 27 and Tuesday 28 October included the Graduation Ceremony at Goldsmiths' Hall (see below), a guided tour of the Crown Jewels at the Tower of London with David Thomas, and a private viewing of the new William and Judith Bollinger Jewellery Gallery at the Victoria and Albert Museum. In addition two workshops were held, one on a new approach to the use of the refractometer with Darko Sturman and Duncan Parker, and the second on precious metal clay with Helen O'Neill. The final event was a Gem Discovery Club Specialist Evening when Antoinette Matlins demonstrated the value of small, simple gem testing tools (a report of this Specialist Evening is given on page 147).

A report of the Conference will be published in the December 2008 issue of *Gems & Jewellery*.

Conference Sponsors and Supporters:

The Association is most grateful to the following for their support:

Major Sponsors

Marcus McCallum FGA, London
Benjamin Zucker, Precious Stones Company, New York, U.S.A.

Supporters

Apsara, Tadworth, Surrey
Bear Essentials, Stone Group Labs, Jefferson City, Missouri, U.S.A.
Marcia Lanyon Ltd, London
Maggie Campbell Pedersen FGA, London
dg3 Diversified Global Graphics Group for sponsoring the folders and delegate badge

Graduation Ceremony

On Monday 27 October the Graduation Ceremony and Presentation of Awards was held at Goldsmiths' Hall in the City of London. Professor Alan Collins, Chairman of the Gem-A Council, presided and Gem-A President Professor Andy Rankin presented the awards.

Michael O'Donoghue and Terry Davidson who had retired from the Council during the year, were presented with certificates honouring their contribution to the work of the Association.

The Prize Winners at Goldsmiths' Hall (from left): Antonia Underwood (Diploma Practical Prize), Kundan Sarraf (the Bruton Medal), Elizabeth Rasche (Anderson Bank Prize), Jacqueline Larsson (the Deeks Diamond Prize), Dr Pauline Jamieson (the Anderson Medal and the Hirsh Foundation Award) and Antonia Ross (The Christie's Prize for Gemmology). Photo courtesy of Photoshot.

We were particularly pleased to welcome a number of Fellows and Diamond members who had graduated in Gem-A examinations in past years. To mark the celebration of One Hundred Years of Gemmological Education, those who had been unable to be present at the Graduation Ceremony in the year in which they qualified, were invited to attend the 2008 event for the formal presentation of their Diplomas.

In his address Professor Rankin referred to the international status of our examinations saying to the graduates: "Your Gem-A qualifications are recognized throughout the world as the gold standard in training and education of professional gemmologists for the gem and jewellery industry. This recognition is in part due to long-standing traditions of excellence over 100 years, and in part due to the a hard work and commitment you have put into achieving your awards. You can be justifiably proud of your achievements which are being celebrated here today ."

Professor Rankin finished by again congratulating the graduates on their achievement and wishing them every success for the future.

The ceremony was followed by a reception for graduates and guests.

A report of the Graduation Ceremony will be published in the December issue of *Gems & Jewellery*.

Pearl evening at Christie's

On 29 September Christie's King Street kindly hosted a champagne reception and pearl evening for the benefit of Gem-A's educational initiatives. Presentations included 'Pearls: a perspective on size and value' by David Warren, Head of the Jewellery Department at Christie's Dubai, 'Pearl Fishing in Scotland' by Kenneth Scarratt, Director of Research at GIA (Thailand), and 'The Romance and History of Pearls' by Gem-A CEO Dr Jack Ogden.

A report of the event was published in the October issue of *Gems & Jewellery*.

Centenary Dinner

A dinner was held on 3 July at Goldsmiths' Hall in the City of London to celebrate one hundred years of gemmological education. The evening commenced with a champagne reception in the setting of the Goldsmiths' Company's exhibition 'Treasures of the English Church' followed by a livery-style dinner. Those attending included representatives of international gem laboratories and institutes, and members of the British gem trade auction houses. After dinner a speech was given by John Benjamin FGA DGA, valuer and jewellery consultant with considerable experience of the gem and auction trade both in the UK and overseas.

A report of the event was published in the August issue of *Gems & Jewellery*.

Centenary Dinner Sponsors

The Association is most grateful to the following for their support:

Major Sponsors

Venue: **The Goldsmiths' Company,** London
Champagne Reception: **SSEF, Swiss Gemmological Institute,** Basel, Switzerland
Table Gifts: **Fellows & Sons Auctioneers & Valuers,** Birmingham, West Midlands
Candlelit Chandeliers: **Hazlems Fenton,** Chartered Accountants, London
Flowers: **QVC,** London
Stationery: **dg3 Diversified Global Graphics Group,** London, and **Peter G. Read FGA DGA,** Bournemouth, Dorset

Programme Sponsors

Backes & Strauss, London
Chatham Created Diamond, San Francisco, California, U.S.A.
David Gann, London
Reed Exhibitions, London
Theo Fennell, London

Raffle Sponsors

Christie's, London
Designs from Memory, Bromsgrove, Worcestershire
John Greatwood FGA, Mitcham, Surrey
The Hilton London Kensington, London
Marcus McCallum FGA, London
Organic Gems, London
Zultanite Gems LLC, Fort Lauderdale, Florida, U.S.A.

Hong Kong Graduation and Awards Dinner

A special dinner and graduation ceremony was held in Hong Kong on 16 September at the Royal Palace Restaurant, Tsimshatsui, Kowloon, in celebration of One Hundred Years of Gemmological Education. The event was organized in conjunction with Gem-A's teaching centres in Hong Kong, the Asian Gemmological Institute and Laboratory Ltd (AGIL) and the Hong Kong Institute of Gemmology (HKIG). The guest speaker was Charles Chan, President of the Hong Kong Jewellery and Jade

Manufacturers' Association. Speeches were also given by Gem-A CEO Dr Jack Ogden, Prof. Mimi Ou Yang Chiu Mei of HKIG and Dominic W.K. Mok of AGIL.

A report of the event was published in the October issue of *Gems & Jewellery*.

Hong Kong Graduation and Awards Dinner Sponsors and Supporters

Gem-A is indebted to the many sponsors, donors and volunteers listed below who made the event possible.

Major Sponsor

Feng Hsiu-Yun FGA DGA, Taiwan Earth Gemmological Inc. ATC, Taichung, Taiwan R.O. China

Sponsors

Dr Ellen Lau GG FGA, Hong Kong
Gemmological Association of All Japan, Tokyo, Japan

Dinner Supporters

Rosamund Clayton FGA DGA, London
Qiu Zhi-Li FGA, Zhongshan University ATC, Guangzhou, P.R. China
Prof. Mimi Ou Yang Chiu Mei FGA, Hong Kong Institute of Gemmology, Hong Kong

Dinner Prize draws, Table Prizes and special donations

Luk Fook Jewellery
Prof. Mimi Ou Yang Chiu Mei FGA
Eddie Fan
3-D Gold
Hong Kong Jewellery & Jade Manufacturers' Association
Louis Lo FGA, Sunning Holdings Ltd
Mercury in X
Johnson Li
AGIL, Asian Gemmological Institute and Laboratory Limited
HKIG, Hong Kong Institute of Gemmology
GAHK, Gemmological Association of Hong Kong
J. H. Berry & Company, Goldsmiths
Jewellery News Asia
China Gems Magazine
Kim Robinson
Sun Po Gold Jewellery Ltd
Appellation Limited
Victoria Dispensary
Lu Coral
Wu Chao-Ming FGA DGA
Charles & Colvard Ltd.
Kafa Coffee
Action Design and Production Ltd
Prof. Yan Weixuan FGA DGA

Guest of Honour Charles Chan, President of the Hong Kong Jewellery and Jade Manufacturers' Association, speaking at the Hong Kong Graduation and Awards Dinner.

Nature's Treasures: Minerals and Gems

On 7 December at the Flett Lecture Theatre, Natural History Museum, London SW7, a seminar was held which had been arranged jointly between Gem-A, The Mineralogical Society and The Russell Society.

Short talks on a wide range of topics including diamonds, inclusions, ancient gems, agates, mineral luminescence, environmental aspects and many more were enjoyed by an audience of nearly 100.

After lunch, there were displays and demonstrations on various aspects of gems and minerals.

Members' Meetings

London

Annual General Meeting

The Gem-A Annual General Meeting was held at the National Liberal Club, Whitehall Place, London SW1, on 30 June. Professor Alan Collins chaired the meeting and welcomed members. The Annual Report and Accounts were approved. Professor Andrew Rankin was elected President for the period 2008-2010. Michael O'Donoghue

and Evelyne Stern retired from the Council in rotation and being eligible Evelyne Stern was re-elected to the Council. Michael O'Donoghue did not seek re-election. Jim Collingwood and John Greatwood retired from the Members' Audit Committee by rotation and being eligible John Greatwood was re-elected to the Committee. Jim Collingwood did not seek re-election. Hazlems Fenton were re-appointed as auditors for the year.

The AGM was followed by a presentation by David Warren, Jewellery Department head of Christie's London King Street and Dubai. He shared anecdotes and tales from his exciting 30 years of experience working with the firm. Having been based in London, Glasgow, Hong Kong and other areas, he specializes in developing the jewellery departments of different regions and had just completed his third successful sale for Christie's in Dubai.

Gem Discovery Club Specialist Evenings

The Gem Discovery Club meets every Tuesday evening at the Gem-A London headquarters when members have the opportunity to examine a wide variety of stones. Once a month, a guest specialist speaker is invited to give a presentation.

On 13 May the guest speaker was Dennis Allen, whose presentation focused on synthetic moissanite. Well known in the industry, Dennis Allen was a founder of Emagold UK and was appointed President of the group for three years. He was also Chairman of the BJA in the early 1990s. He is now an industry consultant, a role that includes acting as technical director for a diamond sight holder and an advisor for TPS for the jewellery section of the International Spring Fair. In his presentation, Dennis Allen gave a background to synthetic moissanite since its introduction ten years ago, and explained what moissanite is and how it was discovered. He then focused on the growth in self-purchasing and how this has repositioned synthetic moissanite, concluding with the current position on sales and growth in the UK and customer comments on the product.

On 9 July the guest speaker was Branko Deljanin, Director, EGL Canada, who gave a presentation on the Identification of Small, Colourless and Fancy Colour HPHT-grown and CVD-grown Diamonds. Branko discussed both standard and advanced gemmological methods, including microscopy, UV, FTIR spectroscopy, XRF chemistry and PL Imaging and also problems in identification of small laboratory diamonds, diamond screening and testing, grading, certification and the CIS Fluorescence system. At the beginning of the evening, the speaker signed copies of his new 85-page book *Laboratory-grown Diamonds: Information Guide for HPHT-grown and CVD-grown diamonds* (2nd edition).

On 28 October the specialist speaker was Antoinette Matlins, a respected gemmologist and well-known author and lecturer. Often seen on several television networks offering important consumer information, Antoinette devotes much of her work to education and consulting within the trade. Antoinette has an unusual ability to translate complex material into relevant, practical, and — most important — useful information, and she conducts product knowledge training for some of the most prestigious retailers and industry groups in the USA. Many gemmologists today overlook basic tools and techniques that can be important aids to gem identification and treatment detection; Antoinette's specialist evening was a fresh and invigorating look at the simple side of gemmology. Her hands-on presentation demonstrated the value of small, simple tools and gave the audience a new appreciation for their value in this high-tech world, whether checking for treatments, checking parcels for 'salting,' or guarding against HPHT enhanced diamonds. At the end of the evening, the speaker signed copies of her new book *Gem Identification Made Easy* (4th edn).

Two Gem Discovery Club Specialist Evenings were held in November. On 4 November the guest speaker was Thomas Dailing. With nearly 50 professional designing

Gifts and Donations to the Association

The Association is most grateful to the following for their gifts and donations for research and teaching purposes:

Chao-Ming Wu FGA DGA, Taipei, R.O. China, for a selection of polished jadeite slabs and rough sapphire crystals

John R. Fuhrbach FGA BSc GG, JONZ Fine Jewels, Las Cruces, USA, for a collection of rough and cut, natural and synthetic stones

Keecha Narayanamurthy FGA, Ipoh Perak, Malaysia, for a selection of rough black tourmaline and white topaz

C.W. Sellors Fine Jewellery, Ashbourne, Derbyshire, for a selection of cut gems

Prof. Weixuan Yan FGA DGA, Beijing, P.R. China, for a collection of 100 pieces of animal carvings, books and photos, in memory of Prof. Zhonghui Chen

The 100 Club (£1000)

Joerg Baudendistel, Obertshausen, Germany
Helen L. Plumb FGA DGA, Aberdeen, Scotland

awards, Thomas has become one of North America's most recognized jewellery designers. Thomas Dailing Designs are contemporary classics, delicately balanced with dramatic artistry and a strong sense of engineering. His creations typically showcase concave faceted gems by Richard Homer. By continually pioneering new techniques, Thomas Dailing brings his unique vision to the jewellery world. Thomas's presentation with images of his creations focused on his history and progression as a jewellery designer and on his interaction with the legendary gem cutter Richard Homer.

On 11 November was a meeting with challenges designed to assess the skills necessary for any successful stone dealer. There were many tests, such as parcel paper folding, gemstone weight estimation and valuing parcels of stones and during the evening participants had the opportunity to try their hand at 'being a dealer' themselves. The gem dealer and guest speaker was Jason Williams of G.F. Williams, London. Jason is on the Board of Trustees of Gem-A; in order to source the best stones for his stock Jason travels extensively, bargaining hard and exercising strict quality control, resulting in a fantastic range of coloured stones.

Midlands Branch

The Branch held their annual summer luncheon party on 16 June at Barnt Green. On 26 September a monthly meeting was held at the Earth Sciences Department, Birmingham University, Edgbaston, where Branch Vice Chairman Doug Morgan talked on the early development of gem cutting, the practical problems in dealing with various gem materials, modern equipment and methods for carrying out complex gem cutting as an art form.

On 31 October, also at the Earth Sciences Department, Dr Sally Baggott, Curator at the Birmingham Assay office, gave an illustrated talk on Birmingham Silver and the Influence of Matthew Boulton.

On 28 November John Benjamin, an independent jewellery valuer, historian and author, traced jewellery design from the grim iconography of 1700s memento mori to neo-classicism and the era of sentimental jewellery in the 1800s. Topics included how diamonds and gems were cut and set, pastes, cut steel, Berlin ironwork, romanticism and much more.

The Midlands Branch Anniversary Dinner and Centenary Conference were held on Saturday and Sunday, 29 and 30 November at Menzies Strathallan Hotel, Edgbaston. Speakers included Doug Garrod, Gwyn Green, Henry Hänni, Alan Jobbins, Shena Mason and Vanessa Paterson.

North East Branch

At a Branch meeting held on Thursday 23 October at the Ramada Jarvis Hotel, Wetherby, West Yorkshire, Gwyn Green, a Gem-A examiner and tutor, gave a presentation and a practical session on the identification of colourless gems in jewellery. Gwyn's presentation and practical session appealed not only to students and valuers but also to the working jeweller.

North West Branch

Meetings held at the YHA Liverpool International, off Wapping, Liverpool, included a practical evening on 19 June when participants had the opportunity to examine a variety of rubies (synthetic and treated), diamonds (glass infill, and laser treated) and sapphires (synthetics). On 18 September Andrew Spicer of Bonhams of Chester gave a talk entitled 'Fakes and Forgeries in the Silver Markets'.

At the Branch Annual General Meeting held on 16 October James Riley was elected Chairman, Secretary and Treasurer. The AGM was followed by a talk by Jo Jones, an archaeologist and expert witness, entitled 'Gem Archaeology'.

Scottish Branch

Monthly meetings held at the British Geological Survey, Edinburgh, included a presentation and practical session on 11 June on the identification of colourless stones in jewellery by Gwyn Green, a Gem-A examiner and tutor. On 17 September Andrew Ross, Principal Curator of Invertebrate Palaeontology and Palaeobotany at the National Museums Scotland, gave a presentation on his observations on amber stability and properties. Dr Cigdem Lule spoke on 16 October on the reasons why it is important to have an understanding of gemmology in the jewellery business, citing zultanite from Turkey as an example.

On 11 November jewellery appraiser and expert witness Peter Buckie gave a talk entitled 'The challenge of valuing one of the world's largest diamonds: appraiser's dream or nightmare?'; this highlighted a faceted diamond weighing over 200 carats, D-colour, internally flawless, with excellent symmetry and polish; that he had recently been asked to value.

A joint meeting with the Scottish Mineral and Lapidary Club was held on 23 October at the Club's headquarters in Maritime Lane, Edinburgh. The speaker was Brad Wilson, Vice President and Fellow of the Canadian Gemmological Association, who gave a presentation entitled 'Coloured gemstone discoveries in Canada'.

South East Branch

On 14 June members had the opportunity to view a collection of African gems and minerals, which were beautifully presented in a small private museum near Sevenoaks, Kent. Most of the specimens had been collected at source by our host over many years during the course of his work in Africa.

On 22 October at the Queen Elizabeth Room, Portland Place, London W1, Marcus McCallum gave a presentation entitled 'An Informal Chat with a Travelling Gem Dealer'. Marcus, a well known and respected gem dealer based in Hatton Garden, focused on how he got into the trade, how things have changed over the years and shared some interesting anecdotes. Participants had the opportunity to examine a variety of unusual specimens Marcus had brought along.

On 19 November members of the Branch had the opportunity to visit the new William and Judith Bollinger Jewellery Gallery at the Victoria and Albert Museum. The visit included an introduction to the gallery, which displayed more than 3500 pieces telling the story of European Jewellery during the last 800 years, by members of the curatorial team, Richard Edgcumbe, Jo Whalley and Clare Phillips.

South West Branch

Branch members were challenged by Jason Williams of G.F. Williams of London to 'Beat the Dealer' at a meeting held at BRLSI Building, Queen Square, Bath, on 9 November. This was an afternoon designed to assess the skills which are necessary for any successful stone dealer. Time is money to a stone dealer; the faster you are the more stones you can buy, sort and ultimately sell. However, you must also be accurate. Tests included spotting the rogue CZ in a parcel of diamonds, quickly and accurately sorting a matching set of stones from a parcel, parcel paper folding, gemstone weight estimation and valuing parcels of stones. He is on the Council of Gem-A and regularly speaks at branch meetings and London's Gem Club. In order to source the best stones for his stock Jason travels extensively, bargaining hard and exercising strict quality control. This results in a fantastic range of coloured stones, from small jobbing stones to exquisite neon Paraiba tourmaline, colour-changing alexandrite and lush green tsavorite. During the afternoon, participants had the opportunity to see a range of Jason's stones.

Membership

Between 1 June and 30 November 2008 the Council approved the election to members of the following:

Fellowship and Diamond Membership (FGA DGA)

Chiu Wai Yu Yuki, Sheung Shui, Hong Kong. 2005; 2006
Lai Sau Han, Winnie, Hong Kong. 2008, 2006
Peers, Sofia, London. 2005, 2006

Fellowship (FGA)

Agu, Cecile, Le Cannet, France. 2008
Baethe, Vanessa, The Hague, The Netherlands. 2008
Bigford, Julie Claire, Malvern Wells, Worcestershire.2008
Booth, Eveline, Cheltenham, Gloucestershire.2008
Chan Wing Kwok, Tai Po, Hong Kong. 2008
Chien Lien-Chin, Taichung City, Taiwan, R.O. China. 2008
De Alwis Dissanayake, M.D., Colombo, Sri Lanka. 2008
Ding Hui, Surbiton, Surrey. 2008
Driscoll, Brian John, New York, U.S.A. 2008
Dunn, Katherine Johanna, Toronto, Ontario, Canada. 2008
Ellis, Trevor Edward, Birmingham, West Midlands. 1985
Hamrén, Elisabeth, Ostersund, Sweden. 2008
Hon Wai Ching, Kowloon, Hong Kong. 2008
Hsu Chia Jung, Taichung City, Taiwan, R.O. China. 2007
Hui Yuet Ming, Kowloon, Hong Kong. 2008
Jensen, Annalisa, London. 2006
Keeffe, Veronica Cheryl, Oshawa, Ontario, Canada. 2008
Kui Nui, Reema, Yuen Long, Hong Kong. 2008
Kyaw Swar Htun, Yangon, Myanmar. 2008
Lau Yuen Yee, Simmy, Kowloon, Hong Kong. 2008
Lin Chun Hsien, Taipei, Taiwan, R.O. China. 2007
Maclellan, Kiki, London. 2008
Mak Bing Lan, New Territories, Hong Kong. 2008
Martins Molgard, Silvia, Colombo, Sri Lanka. 2008
Mathur, Chetna, Indore, India. 2003
Ng Wai Hing, New Territories, Hong Kong. 2008
Nicolson, Louise Alexandra Patricia, London. 2008
Overton, Thomas William, Carlsbad, California, U.S.A. 2008
Pan Yang, Scarborough, Ontario, Canada. 2008
Partridge, Jennifer Anne, Cambridge. 2008
Piirto, Irmeli Anja Susanna, Espoo, Finland. 2008
Pyrro, Riku Matti, Kirkkonummi, Finland. 2008
Qi Geng, Scarborough, Ontario, Canada. 2008
Rufus, Simon, London. 2008
Shaw, Heather Catherine, Barnsley, South Yorkshire. 2008
Sikkema, Ariane, Almelo, The Netherlands. 2008
Siriwardena, Henarath H.D. Ajith Lal, Raddolugama, Sri Lanka. 2008
Skalwold, Elise Ann, Ithaca, New York, U.S.A. 2008

Soh Shi Hong, Johor Bahru, Malaysia. 2008
Soumaré, Myriam, Paris, France. 2008
Spagnoletti Zeuli, Lavinia, London. 2007
Spauwen, Timotheus A. P., Geleen, The Netherlands. 2008
Spencer, Jason, Birmingham, West Midlands. 2008
Strafti, Kalliopi-Maria, Athens, Greece.2008
Tan Kiat Choo, June, Johor Bahru, Malaysia. 2008
Thomas, Caan, Chesham, Buckinghamshire. 1998
Tsang Wai Ming, Causeway Bay, Hong Kong. 2008
Valerio Sa', Helena, Mississauga, Ontario, Canada. 2008
Vildiridis, Athanasios, Athens, Greece. 1989
Wang Weny-I, Tainan City, Taiwan, R.O. China. 2008

Diamond Membership (DGA)

de Fere, Susannah, London. 2008
Ng Che Keung, New Territories, Hong Kong. 2008
Nordgren, Pia Yu, Vallingby, Sweden. 2008
Richardson-Jefferies, Phillipa, London. 2008
Russell-Stoneham, Alexandra, London. 2008
Smith, Mark, Richmond, Surrey. 2008
Tai, Caroline, Tseung Kwan O, Hong Kong. 2008
Vikatos, Ilias, Patras , Greece. 2008
Wong Kin Ching, New Territories, Hong Kong. 2006
Yau Cho Kwan, Chai Wan, Hong Kong. 2008

Associate Membership

Agrawal, Preeti, Kathmandu, Nepal
Alawathage Don, Rohana Priyantha, Avissawewella, Sri Lanka
An, Ran, London
Boele, Georgette, Les Acacias, Switzerland
Cargill, Jan, Arbroath, Scotland
Crossley, Ursula, Augsburg, Germany
Daughters, Paul, London
Eastwood, Layla, Gerrards Cross, Buckinghamshire
Ekai, Richard Titus, Bangkok, Thailand
Evans, Charles, London
Evans, Daniel Raymond, Brisbane, Queensland, Australia
Evans, Eibhlin Ide, Skelmersdale, Lancashire
Ferracuti, Letizia, London
Fox, Karen, Waterloo, Ontario, Canada
Hammond, Ross, London
Harding, Jan, London
Häyry, Tiia Marjiut, Hinthaara/Porroo, Finland
Hell, Martine Svetlana, Stjørdal, Norway
Huang, Shih-Jung, London
Jeans, Jane E., Healesville, Victoria, Australia
Johnstone, Isobel Phoebe, St Lucia, Queensland, Australia
Khan, Irfan Younas, South Shields, Tyne and Wear
Kovanovic, Milena, London
Lajtha, Jessica, Loxwood, East Sussex
Leavey, Hariet, Yelverton, Devon
Lepage, Anick, Mont St Hilaire, Quebec, Canada
Lomas, John Proctor, London
Mclachlan, David, Woking, Surrey
Michaelides, Emma, Enfield, Middlesex
Miller, Terrie Lynn, Tenby, Dyfed, Wales
Murakami, Akiko, London
Naylor, Peter D., Birmingham, West Midlands
Nazari, Yasin, London
Neslen, Lewis, London
Parvela-Säde, Anu, Espoo, Finland
Patel, Maulika, London
Patel, Priti, Harrow, Middlesex
Premchamd, Purushothaman, Billericay, Essex
Ramasamy, Sonia Kala, Selangor, Malaysia
Rowe Rawlence, Emily, London
Salah, Ismail Jama, London
Samuh, Elizabeth, London
Seubert, Michael, Munich, Germany
Sheikh, Adnan, Luton, Bedfordshire
Stöt, Linda, Stockholm, Sweden
Szymaniak, Peter Jerzy, Watford, Hertfordshire
Thum Fu-Tsing (Leon), Penang, Malaysia
Ward, Neil, Reighton Gap, North Yorkshire
Waugh, Andrew Donald, Braintree, Essex
Williams, Richard Marcus Andrew, Porthcawl, Mid Glamorgan, Wales
Yambala, Benoit Odimula, London
Young, Stephanie, Chalfont St. Peter, Buckinghamshire

Transfers

Fellowship to Fellowship and Diamond membership (FGA DGA)

Bracey, Anne Christine, Birmingham, West Midlands. 2008
Corser, Elizabeth, Wellington, Shropshire. 2008
Cui, Xianzhong, London. 2008
Ding, Hui, Surbiton, Surrey. 2008
Rajbanshi, Niren Man, Kathmandu, Nepal, .2008
Sarraf, Kundan, Kathmandu, Nepal.2008
Wootton, Sophie Louise, London. 2008

Diamond membership to Fellowship and Diamond membership (FGA DGA)

Harker, Catherine Anne, Birmingham, West Midlands. 2008
Ho Siu Ming, Shaukiwan, Hong Kong. 2008
Lee Hing Fan, New Territories, Hong Kong. 2008

Associate membership to Fellowship (FGA)

Coppack, Flavia, London. 2008
Freeman, Sarah, London. 2008
Giertta, Maria, London. 2008

Mo, Zhuangguo, London. 2008
Prendergast, Lorna, Great Missenden, Buckinghamshire. 2008
Rafferty, Frank, Ambrieres-les-Vallees, France. 2008
Ross, Antonia, Fleet, Hampshire. 2008
Win, Thein Thein, Cricklewood, London. 2008
Woo Ka Yin, Kowloon Bay, Hong Kong. 2008

Associate membership to Diamond membership (DGA)

Moroz, Magdalena, London. 2008
Naylor, Peter D., Birmingham, West Midlands. 2008
Yang Yiwei, London. 2008

Subscriptions 2009

It has been arranged that membership subscriptions will remain unchanged for 2009 at £72.50 for UK members, £80.00 for those in Europe and £85.00 for overseas.

The Journal of Gemmology

We are pleased to announce that as from 2009, The Journal will go online. We will be using a state-of-the-art interface for this, providing full search facilities. Access will be via our website and will require membership log-in. The articles will be peer reviewed as now and will be placed online as soon as they are ready.

All online Journal articles will have a detailed summary in our magazine *Gems & Jewellery,* explaining the interest, relevance and importance of the article, the science, if necessary, and, of course, pointing to the online article where the full text, charts, tables and so on will published. These summaries will be readable and interesting brief articles, not to be confused with the succinct abstracts that will continue to be provided online.

All the Journal articles placed online in 2009 will be also published in 'hard copy' as a single issue in similar format to the present Journal and sent to all paid-up Gem-A members as part of their 2009 subscription.

Editorship of the Journal

As the advertisement on this page shows, Gem-A is seeking a new editor for *The Journal*. Dr Roger Harding is retiring as editor of after 15 years. Roger was Director of Gemmology for the Gemmological Association from 1990 to 2003 and became Editor of *The Journal* in 1994. As Editor, Roger has worked tirelessly to keep *The Journal* to its renowned high standards, working closely with an international editorial panel and Mary Burland, the production editor.

His retirement comes at a time when *The Journal* is about to move online as an adjunct to the printed version and this change will provide new challenges and opportunities for the next editor.

The Council of the Gemmological Association are extremely grateful to Roger for all his hard work and dedication over the years, and take this opportunity to thank him and to wish him well for the future.

Gem-A is seeking a new

HONORARY EDITOR

for *The Journal of Gemmology*

The Gem-A Board is seeking an Honorary Editor for *The Journal of Gemmology*, to work from home with occasional meetings at Gem-A, London.

Responsibilities will include proactively soliciting suitable papers, managing peer review, copy editing, proof reading and working closely with the production editor.

Applicants, whose first language will be English, should be current Fellows of the Association and possess:

- a demonstrable high level of mineralogical and/or geological knowledge and understanding
- editing skills and editorial experience
- a suitable computer, broadband internet connection and a reasonable level of IT skills, including knowledge of Word and Adobe Acrobat.

The Editor will receive an honorarium and some expenses.

For further information contact Dr Jack Ogden at **jack.ogden@gem-a.com**.

Gem-A Events 2009

Wednesday 21 January	**SCOTTISH BRANCH** **An evening with gems with Alan Hodgkinson** *Venue:* British Geological Survey, Edinburgh
Friday 30 January	**MIDLANDS BRANCH** **Annual General Meeting followed by the annual Bring and Buy and Team Quiz** *Venue:* Earth Sciences Department, Birmingham University, Edgbaston
Friday 27 February	**MIDLANDS BRANCH** **The Cheapside Hoard by James Gosling** *Venue:* Earth Sciences Department, Birmingham University, Edgbaston
Sunday 15 March	**MIDLANDS BRANCH** **Practical Training Day: Identification of Gemstones Mounted in Jewellery** *Venue:* Barnt Green, Worcestershire
Wednesday 25 March	**SCOTTISH BRANCH** **Scottish Pearl Evening at Cairncross of Perth**
Friday 27 March	**MIDLANDS BRANCH** **An Exploration into the World of Pearls by Gwyn Green** *Venue:* Earth Sciences Department, Birmingham University, Edgbaston
Friday 24 April	**MIDLANDS BRANCH** **Cometh the Day, Cometh the Jewel by David Callaghan** *Venue:* Earth Sciences Department, Birmingham University, Edgbaston
Friday 1 to Monday 4 May	**SCOTTISH BRANCH CONFERENCE** *Venue:* The Queen's Hotel, Perth (Further details given on page 90)
Sunday 21 June	**MIDLANDS BRANCH** **Summer Luncheon Party**
Saturday 17 and Sunday 18 October	**GEM-A ANNUAL CONFERENCE** *Venue:* Hilton London Kensington
Monday 19 October	**GEM-A GRADUATION AND PRESENTATION OF AWARDS** *Venue:* Goldsmiths' Hall, Foster Lane, London EC2

Contact details

Gem-A Headquarters:	Olga Gonzalez on 020 7404 3334 email olga.gonzalez@gem-a.com
Midlands Branch:	Paul Phillips on 02476 758940 email pp.bscfgadga@ntlworld.com
North East Branch:	Mark Houghton on 01904 639761 email sara_e_north@hotmail.com
North West Branch:	James Riley on 01565 734184 or 07931 744139 email jameshriley@btinternet.com
Scottish Branch:	Catriona McInnes on 0131 667 2199 email scotgem@blueyonder.co.uk
South East Branch:	Veronica Wetten on 020 8577 9074 email veronica@wetten.co.uk
South West Branch:	Richard Slater on 07810 097408 email RichardS@fellows.co.uk

For up-to-the minute information on Gem-A Events visit our website at **www.gem-a.com**

Gem-A

THE GEMMOLOGICAL ASSOCIATION
OF GREAT BRITAIN

Be committed to your career

Pursue a Gem-A Education.

Whether you choose to study in the fast-paced City of London, or within the comfort of your home, studying with the world's longest established and leading educator in gemmology is an investment in your future. Our new London daytime course leading to a Diploma in Gemmology and FGA membership status commences in March 2009, along with our newly revised open distance learning programme.

For further information on our courses, email information@gem-a.com call +44 (0) 20 7404 3334 or visit www.gem-a.com.

Make sure to register now, so you are better prepared for the future.

The Journal of
Gemmology
2008 / Volume 31 / Nos. 3/4

Contents

73 A fancy reddish brown diamond with new optical absorption features
Taijin Lu, T. Odaki, K. Yasunaga and H. Uesugi

77 A place for CZ masters in diamond colour grading
M. D. Cowing

85 The geological context of gems in the Velasco Pegmatitic District, Argentina
F. Guillermo Sardi

91 Magnetic susceptibility, a better approach to defining garnets
D. B. Hoover, C. Williams, B. Williams and C. Mitchell

105 The refraction of light by garnet depends on both composition and structure
D. K. Teertstra

111 Ornamental variscite: A new gemstone resource from Western Australia
M. Willing, S. Stöcklmayer and M. Wells

125 Visually distinguishing A-jadeite from B-jadeite
Li Jianjun, Liu Xiaowei, Zhang Zhiguo, Luo Yueping, Cheng Youfa and Liu Huafeng

132 Abstracts

136 Book Reviews

139 Proceedings of The Gemmological Association of Great Britain and Notices

152 Gem-A Events 2009

Cover Picture: Variscite set in 18ct yellow gold, containing Australian champagne, cognac and colourless diamonds, suspended from a diamond bead strand. Variscite fashioned by Murray Thompson; jewellery designed and crafted by Thomas Meihofer, Stacey Illman and Kristian Fraurud. Photo by Jurgen Lunsmann. (See Ornamental variscite: a new gemstone resource from Western Australia, page 111.)

The Gemmological Association of Great Britain

27 Greville Street, London EC1N 8TN
T: +44 (0)20 7404 3334 **F**: +44 (0)20 7404 8843
E: information@gem-a.com **W**: www.gem-a.com

FSC Mixed Sources
Product group from well-managed forests and other controlled sources
www.fsc.org Cert no. TT-COC-002454
© 1996 Forest Stewardship Council

Copyright © 2008
Designed and printed by DG3 (Europe) Ltd
ISSN: 1355-4565